Title

Analysis of M. tuberculosis-mediated phagosome maturation arrest and a role for Esx-1 secretion

Permalink

https://escholarship.org/uc/item/0ss1f75k

Author

MacGurn, Jason Andrew

Publication Date

2007-03-16

Peer reviewed|Thesis/dissertation

Analysis of *M. tuberculosis*-mediated phagosome maturation arrest
and a role for Esx-1 secretion

by

Jason MacGurn

DISSERTATION

Submitted in partial satisfaction of the requirements for the degree of

DOCTOR OF PHILOSOPHY

in

Program Name

in the

GRADUATE DIVISION

of the

UNIVERSITY OF CALIFORNIA, SAN FRANCISCO

ACKNOWLEDGEMENTS

A great deal of work in Chapter 4 of this thesis would not have been possible without the help and guidance of Andrew Krutchinsky and Justin Blethrow. Over the past year, these two individuals have facilitated all of my mass spectrometry experiments, teaching me much about sample preparation, instrumentation, and data analysis. From them, I have learned important lessons that I hope to apply throughout my career in science.

I am grateful to everyone who has been a part of the Cox Lab since its inception. Individual members of the lab have always been a great source of technical expertise and support. In particular, I am deeply grateful to Scott Converse, Sarah Stanley, Sridharan Raghavan, and Madhulika Jain. These four individuals have been colleagues and friends throughout my graduate career, and I have benefited greatly from my interactions with them.

My development as a graduate student was facilitated by financial support from the NSF Graduate Student Fellowship and the NIH Microbial Pathogenesis Training Grant. I am very grateful for these programs and I'm proud to have participated in them.

I thank my parents, Bruce and Janice MacGurn, for fostering my development as a person, as a student, and as a scientist. I thank my Grandparents Jones and my Grandparents MacGurn for a lifetime of love and support and for continuing interest in my professional development. I thank my aunts Joyce and Denise for their guidance and encouragement over the years. I am grateful to my brother, Jeff, for his continued interest in all of my endeavors.

I am eternally grateful to my wife, Elena, who has been an important part of my life for 11 years. She is my pillar of support and my ocean of inspiration. Words cannot express how much I love her and how grateful I am for all her support, patience, and sacrifice over the years. I am also very grateful to my daughter, Margaret MacGurn. Although she is only 7 months old, she has already taught me more about the world than I can hope to teach her in a lifetime. She is my sunshine and I love her very much.

The text of Chapter 2 is largely a reprint of the material as it appears in "A genetic screen for *M. tuberculosis* mutants defective for phagosome maturation arrest identifies components of the ESX-1 secretion system" MacGurn, J.A., Cox, J.S. Infection and Immunity, in press.

The text of Chapter 3 is largely a reprint of the material as it appears in "A non-RD1 gene cluster is required for Snm secretion in *Mycobacterium tuberculosis*" MacGurn, J.A., Raghavan S., Stanley S.A., Cox, J.S. Molecular Microbiology, September 2005; 57(6): 1653-63.

ABSTRACT

Analysis of *M. tuberculosis*-mediated phagosome
maturation arrest and a role for Esx-1 secretion
Jason MacGurn

Mycobacterium tuberculosis, an acid-fast bacillus, is a highly successful intracellular pathogen that is estimated to infect approximately one third of the world population. A keystone feature of *M. tuberculosis* pathogenesis is the parasitism of host macrophages following phagocytic entry, which is thought to be facilitated by the bacteria's ability to prevent the maturation of the phagosome into an acidic, hydrolytic compartment. While *M. tuberculosis*-mediated phagosome maturation arrest (PMA) is a well-documented phenomenon, bacterial factors responsible for altering phagosome trafficking are not well understood. The overall goal of the work presented here is to decipher the molecular mechanisms employed by *M. tuberculosis* to mediate PMA during macrophage infection. The first part of this thesis describes a genetic screen that identified several *M. tuberculosis* mutants defective for PMA. Contrary to the proposal that *M. tuberculosis* growth in macrophages requires PMA, we identified two mutants that grew with wildtype kinetics in macrophages despite localizing to lysosomal compartments. Our results support the alternative suggestion that *M. tuberculosis*-mediated PMA may be important for isolating the bacteria from host antigen presenting compartments, thereby altering the immune response to infection. Interestingly, a subset of the trafficking mutants were also defective for Esx-1 secretion, establishing a role for this specialized protein secretion system in mediating PMA. We show that mutants for two known substrates of the Esx-1 pathway did not exhibit trafficking defects, leading us to hypothesize that other effectors of the system may be involved in mediating PMA. These studies reveal a previously unappreciated phenotype of Esx-1 mutants and suggest a novel pathogenic function for this secretion pathway. The second part of this thesis describes our efforts to characterize one of the genes required for PMA, *espC*, which we show is required for Esx-1 secretion. We demonstrate that, in addition to being required for Esx-1

secretion, *espC* encodes a substrate of the system, consistent with the mutually-dependent

secretion observed with all characterized Esx-1 substrates. We show that secreted EspC

associates in a high molecular weight complex that exhibits sphingomyelinase activity. We

propose that a protein complex containing EspC may be involved in targeting a sphingomyelinase

activity to phagosomal membranes during host infection. By generating ceramide on host

membranes, such a sphingomyelinase activity represents an intriguing host-pathogen interaction

with the potential to modulate the host response to infection.

TABLE OF CONTENTS

LIST OF FIGURES AND TABLES

Chapter 1

Introduction

Infection by *Mycobacterium tuberculosis* leads to more deaths worldwide than any other single bacterial species. The success of this human pathogen is highlighted by the fact that over two million people die of tuberculosis annually, and it is estimated that roughly one third of the world population is currently infected with *M. tuberculosis*. Although some antibiotics are effective for treating tuberculosis infection, the emergence of multi-drug resistant strains and the increase in co-infection with human immunodeficiency virus has created the need to develop new drugs and treatments. By deciphering the molecular mechanisms of *M. tuberculosis* pathogenesis, we hope that improved understanding of the host-pathogen interaction will inspire novel strategies for treatment and prevention of this devastating disease.

M. tuberculosis mediates phagosome maturation arrest (PMA)

Macrophages are host immune cells designed to kill invading microbes. Normally, when a non-pathogenic microbe or an inert particle like a bead is encountered, the particle will be internalized by phagocytosis. The nascent phagosome then undergoes a process of maturation, taking place over the course of 30-60 minutes, during which the phagosomal lumen is acidified and various proteolytic and lipolytic activities are acquired. This process of phagosome maturation subjects microbes to a very inhospitable environment which in many cases leads to microbial demise. It is therefore paradoxical that macrophage – the very cell designed to phagocytose and kill invading microbes – is a favored niche of *M. tuberculosis*.

Once an *M. tuberculosis* bacillus encounters an alveolar macrophage in the host lung, it can be internalized by several different phagocytic mechanisms (Aderem et al., 1999) but the route of entry does not affect the outcome of infection (Zimmerli et al., 1996). Following internalization, *M. tuberculosis*-containing phagosomes (MCPs) have the intriguing ability to prevent phagosome maturation into an acidic, hydrolytic compartment. This phenomenon of phagosome maturation arrest (PMA) was first described over 3 decades ago in classic electron microscopy studies showing that during macrophage infection, MCPs were able to resist fusion with lysosomal compartments even at very late time points post-infection (Armstrong et al., 1971). Since then, many studies have contributed to our understanding of the phagosome in which *M. tuberculosis* resides(Deretic et al., 1999; Russell, 2001; Deretic et al., 2006). Even at very late time points post-infection, MCPs maintain many characteristics and properties of early endosomal compartments, including enrichment for early endosomal markers like Rab5 (Via et al., 1997), transferrin accessibility (Clemens et al., 1996), and a relatively neutral pH (~pH 6.5) (Sturgill-Koszycki et al., 1994; Pethe et al., 2004). Additionally, MCPs do not acquire the properties associated with the maturation of phagosomes containing latex beads or killed *M. tuberculosis* bacilli, such as enrichment for lysosomal protein markers like Rab7 and LAMP-2, enrichment for multivesicular body lipids like LBPA, and lumenal acidification associated with acquisition of the vacuolar ATPase (Sturgill-Koszycki et al., 1994). It is presumed that *M. tuberculosis*-mediated PMA directly contributes to the pathogen's ability to survive and grow inside the host macrophage. However, it has also been proposed that PMA could benefit *M. tuberculosis* pathogenesis by sequestering the bacteria away from antigen presenting compartments, thereby

altering the host immune response (Ramachandra et al., 2001) (Singh et al., 2006) (Ullrich et al., 2000; Flynn et al., 2003).

Although the molecular mechanisms of phagosome maturation are still poorly understood, the small GTPase Rab5 appears central to the process. Rab5 is known to regulate SNARE assembly on endosomal/phagosomal membranes and plays a crucial role in specifying fusion with other endocytic compartments (Woodman, 2000). Conditions that affect Rab5 activity or association with endosomal/phagosomal membranes also affect maturation. For instance, stress-induced activation of p38 signaling directly activates the Rab5 GDI, leading to rapid cycling of Rab5 from its inactive GDP-bound form to its active GTP-bound form and thus increasing the rate of endocytosis and endosome maturation(Cavalli et al., 2001). This is consistent with observations that cytokine stimulation, which can activate p38 signalling, tends to increase rates of phagosome maturation, even in mycobacteria-containing phagosomes (Schaible et al., 1998). Several Rab5-associated proteins are also known to be important regulators of maturation. EEA1, for instance, is an important SNARE tethering protein that is recruited to early endosomal/phagosomal membranes by phosphatidylinositol-3-phosphate (PI3P) and subsequently associates with Rab5. Treatment of cells with wortmannin, a PI3P kinase inhibitor, blocks association of EEA1 with early endosomal/phagosomal membranes and inhibits maturation (Mills et al., 1999). Although Rab5 and its effector proteins have been implicated as key players in early fusion events that determine phagosome maturation, many molecular details regarding the specification and regulation of fusion events remain to be elucidated. We believe that

a molecular understanding of *M. tuberculosis*-medatied PMA will contribute to our understanding of the molecular mechanisms that dictate normal phagosome maturation.

Previous studies have linked *M. tuberculosis* lipids and proteins to PMA in the macrophage. Early studies suggested that when applied to macrophages, mycobacterial sulfolipid-1 blocked maturation of phagosomes *in trans* (Goren et al., 1976), but these results were later shown to be the result of artifacts (Goren et al., 1987) and a rigorous genetic study subsequently refuted the idea that sulfolipid affects phagosomal trafficking (Rousseau et al., 2003). More recently, one study showed that coating beads with mycobacterial lipoarabinomannan (LAM) can reduce the rate of PMA (Fratti et al., 2003) but the effect was slight and does not account for the full activity of *M. tuberculosis*-mediated PMA. Furthermore, genetic evidence demonstrating that LAM interferes with phagosomal trafficking during *M. tuberculosis* infection is lacking. Another recent study showed that a *Mycobacterium bovis BCG* mutant in *pknG*, a serine/threonine protein kinase thought to be secreted, was defective for PMA in macrophages (Walburger et al., 2004). However, it was subsequently shown that *pknG* mutants have *in vitro* growth defects and defects in regulating glutamate/glutamine levels, perhaps leading to auxotrophy during starvation conditions (Cowley et al., 2004). These results suggest that *pknG* is not involved in mediating PMA directly but rather mediates metabolic adaptation to living inside the host phagosome. While these efforts have contributed to our overall understanding of *M. tuberculosis* pathogenesis and survival in host macrophages, they also highlight the need for genetic screens to identify *M. tuberculosis* factors involved in mediating PMA during macrophage infection.

In the first part of this thesis, I took advantage of recent advances in *M. tuberculosis* genetics to identify several genes required for PMA. Contrary to the idea that PMA is crucial to survival in the macrophage, we identified mutants of *M. tuberculosis* that trafficked to lysosomes without consequence to intracellular growth. These results support the proposal that PMA may be important for isolation of *M. tuberculosis* from antigen presenting compartments, thus altering the host immune response to infection. We also show that mutants defective for Esx-1 protein secretion traffic to lysosomal compartments, but two known substrates of the pathway are dispensable for PMA. We propose that novel Esx-1 substrates may be important mediators of PMA during *M. tuberculosis* infection.

Identification of novel components of the Esx-1 secretion system

Mycobacterium tuberculosis is known to utilize at least four secretion systems: the SecYEG pathway, the twin arginine translocation (TAT) pathway, the SecA2 pathway, and the Esx pathway. The SecYEG and TAT pathways are both essential for *in vitro* growth(Sassetti et al., 2003; Saint-Joanis et al., 2006) and thought to secrete largely housekeeping proteins, although substrates of both pathways have been implicated in pathogenesis(Berthet et al., 1998; Saint-Joanis et al., 2006). The SecA2 and Esx secretion pathways are both non-essential for growth *in vitro* but required for full virulence in mice(Braunstein et al., 2003; Hsu et al., 2003; Stanley et al., 2003; Guinn et al., 2004). Our finding that several Esx-1 mutants of *M. tuberculosis* were also PMA mutants led us to consider that a novel Esx-1 effector may mediate PMA.

In *M. tuberculosis*, the two most abundantly secreted proteins in culture are ESAT-6 and CFP-10, two small proteins that lack SecYEG signal sequences and interact to form a dimer(Renshaw et al., 2002; Lightbody et al., 2004; Renshaw et al., 2005). ESAT-6 and CFP-10, encoded by *esxA* and *esxB* genes, respectively, are part of a large family of 23 (strain H37Rv) or 25 (strain CDC1551) genes, known as the Esx family(Pallen, 2002). These Esx family members are small proteins (~100 amino acids), typically encoded in pairs, many of which are known to be secreted despite lacking SecYEG signal sequences. In the case of ESAT-6 and CFP-10, secretion is dependent on several genes encoded at the same genetic locus (*Rv3870*, *Rv3871*, *Rv3876*, *Rv3877*) (Hsu et al., 2003; Stanley et al., 2003; Guinn et al., 2004), called the Esx-1 locus. In the case of six other Esx family operons, the surrounding genes are conserved, containing many proteins similar to those observed at the Esx-1 locus(Gey Van Pittius et al., 2001). Thus, there are seven conserved Esx loci. While only Esx-1 and Esx-5 (Abdallah et al., 2006) have been shown to encode specialized secretion systems, it is tempting to speculate that each locus could encode related yet distinct secretion pathways.

Several recent studies focusing on Esx-1 secretion have begun to elucidate potential roles during host infection. Mutants defective for Esx-1 secretion exhibit a range of diverse phenotypes, including defects in immune modulation, *in vivo* growth, phagosome trafficking, and growth in macrophages (Stanley et al., 2003) (Guinn et al., 2004) (Hsu et al., 2003) (Tan et al., 2006). Despite the plethora of virulence phenotypes exhibited in Esx-1 mutants, a direct role for ESAT-6 / CFP-10 dimers in the molecular pathogenesis of mycobacteria has not been demonstrated. One hypothesis is that the various phenotypes exhibited in Esx-1 mutants could reflect the possibility that multiple

substrates are secreted by the pathway, each with a separate pathogenic function. Ultimately, deciphering the complex pleiotropy of the Esx-1 mutants will require knowledge of all the substrates of this secretion system.

In the second part of this thesis, I selected one of the PMA mutants for further study and discovered that mutant gene, called *espC* (*Rv3615c*, *snm9*), is required for Esx-1 secretion. We show that the EspC protein is secreted in an Esx-1 dependent manner and associates in a high molecular weight complex that exhibits sphingomyelinase activity. We propose that the EspC protein complex may be involved in targeting sphingomyelinase activity to host phagosomal membranes and that this may be a crucial mechanism by which *M. tuberculosis* interferes with the host response to infection. This study highlights a potentially crucial host-pathogen interaction and has implications for tuberculosis vaccine development.

Chapter 2

A Genetic Screen for *M. tuberculosis* Mutants Defective for Phagosome Maturation

Arrest Identifies Components of the ESX-1 Secretion System

Abstract

Following phagocytosis, the intracellular pathogen *Mycobacterium tuberculosis* arrests the progression of the nascent phagosome into a phagolysosome, allowing for replication in a compartment that resembles early endosomes. To better understand the molecular mechanisms that govern phagosome maturation arrest, we performed a visual screen on a set of *M. tuberculosis* mutants specifically attenuated for growth in mice to identify strains which failed to arrest phagosome maturation and trafficked to late phagosomal compartments. We identified 10 such mutants that partitioned into two classes based on the kinetics of trafficking. Importantly, four of these mutants harbor mutations in genes that encode components of the ESX-1 secretion system, a pathway critical for *M .tuberculosis* virulence. Although ESX-1 is required, the known ESX-1 secreted proteins are dispensable for phagosome maturation arrest suggesting a novel effector required for phagosome maturation arrest is secreted by ESX-1. Other mutants identified in this screen had mutations in genes involved in lipid synthesis and secretion, molybdopterin biosynthesis, as well as genes with unknown function. Most of these trafficking mutants exhibited a corresponding growth defect during macrophage infection, but two mutants grew like wildtype *M. tuberculosis* during macrophage infection. Our results support the emerging consensus that multiple factors from *M. tuberculosis*, including the ESX-1 secretion system, are involved in modulating trafficking within the host.

Introduction

        Following phagocytosis by a host macrophage, *M. tuberculosis*, the causative

agent of tuberculosis disease, resides in a phagosomal compartment that resists

maturation into to an acidic phagolysosome and maintains many characteristics of early

endosomes (Deretic et al., 1997; Russell, 2001; Deretic et al., 2006). This phenomenon,

termed phagosome maturation arrest (PMA), was first observed over three decades ago in

landmark studies demonstrating that most (~70%) *M. tuberculosis*-containing

phagosomes (MCPs) failed to mix with lysosomal tracers (Armstrong et al., 1971). Since

then, the phenomenon of PMA during *M. tuberculosis* infection has been well

characterized. During infection of the macrophage, *M. tuberculosis* bacilli reside in

transferrin accessible (Clemens et al., 1996), mildly acidic (pH 6.5) (Sturgill-Koszycki et

al., 1994) (Pethe et al., 2004) early phagosomal compartments even at very late time

points post-infection. In contrast, phagosomes containing inert particles such as latex

beads or killed *M. tuberculosis* gradually mature, usually within an hour of phagocytosis,

into more acidic late phagosomal compartments that are enriched for late

endosomal/lysosomal markers (Clemens et al., 1995). These observed trafficking

differences between live and killed *M. tuberculosis* suggests that there is a labile activity

associated with live bacteria. Although the precise molecular details remain to be

elucidated, evidence is mounting that multiple *M. tuberculosis* factors, including lipids

(Fratti et al., 2001) (Fratti et al., 2003) and proteins (Walburger et al., 2004), may be

involved in arresting the maturation of the phagosome.

        There are several reasons why PMA might benefit the pathogenesis of *M.*

tuberculosis. Trafficking to the acidic and hydrolytic lysosomal environment could

decrease intracellular viability. One study supporting this notion showed that co-infection with *Coxiella burnetii* resulted in acidification of MCPs, which coincided with inhibited intracellular growth of *M. tuberculosis* (Gomes et al., 1999). In contrast, a recent study identified two mutants of *M. tuberculosis* that trafficked to late compartments without suffering a decrease in intracellular survival (Pethe et al., 2004). Additionally, it has been proposed that PMA could benefit *M. tuberculosis* pathogenesis by sequestering the bacteria away from antigen-presenting compartments, thereby altering the host immune response (Ramachandra et al., 2001; Flynn et al., 2003; Singh et al., 2006). Although the potential benefits of PMA to *M. tuberculosis* pathogenesis are numerous, understanding its precise virulence function has been complicated, since any strain with increased susceptibility to killing by the macrophage will traffic to late compartments as a secondary consequence of decreased viability (Ng et al., 2004) (Darwin et al., 2003) (Rousseau et al., 2004).

Microbial pathogens often use specialized secretion pathways to export virulence factors that subvert host defense functions. *Legionella pneumophila,* for example, uses the Dot/Icm specialized secretion system to export effector proteins into host cells, some of which interfere with normal phagosome trafficking (Vogel et al., 1999; Shohdy et al., 2005). Likewise, the recently-discovered ESX-1 protein secretion pathway in *M. tuberculosis* secretes effector proteins important for host interaction and pathogenesis. In addition to being attenuated for virulence in mice (Stanley et al., 2003; Guinn et al., 2004) (Hsu et al., 2003), mutants of the ESX-1 secretion pathway in *M. tuberculosis* exhibit a range of pathogenic defects, including attenuation of intracellular growth in macrophages (Guinn et al., 2004) (Stanley et al., 2003), altered immune modulation of

host cells, and a diminished ability to lyse pneumocytes (Hsu et al., 2003). While several of the genes required for ESX-1 secretion in *M. tuberculosis* have been described (Stanley et al., 2003; Guinn et al., 2004) (Hsu et al., 2003), only a few proteins that require ESX-1 for export have been reported. These include ESAT-6 and CFP-10, two highly abundant culture filtrate proteins which interact to form a dimer (Berthet et al., 1998; Renshaw et al., 2002), and EspA (Fortune et al., 2005). Currently, the function of these proteins is not known.

Interestingly, the live attenuated vaccine strain *Mycobacterium bovis* bacilli Calmette-Guerin (BCG), a species related to *M. tuberculosis*, arrests the maturation of the phagosome during macrophage infection (Deretic et al., 1997) despite lacking a functional ESX-1 secretion system (Mahairas et al., 1996; Cole et al., 1998; Behr et al., 1999). This has led to the assumption that the ESX-1 pathway is dispensable for phagosome maturation arrest. In contrast, a recent study reported that ESX-1 secretion is required for phagosome maturation arrest during macrophage infection by *Mycobacterium marinum* (Tan et al., 2006), another species closely related to *M. tuberculosis* that causes similar disease in poikilothermic hosts. Currently, rigorous evidence defining the requirement of ESX-1 secretion in *M. tuberculosis*-mediated phagosome maturation arrest during macrophage infection is lacking.

Recently, two studies used forward genetics to identify mutants which fail to arrest phagosome maturation. One study used a magnetic selection methodology to identify mutants of *M. tuberculosis* that failed to arrest phagosome maturation, many of which were severely impaired for survival in macrophages (Pethe et al., 2004). Another study identified trafficking mutants of BCG using flow cytometry to sort acidified MCPs

and determined mutant representation by transposon hybridization to microarrays
(Stewart et al., 2005). These two studies identified mutually exclusive sets of genes with
a range of predicted functions, including lipid synthesis and transport, metabolic
enzymes, cell wall components, and genes of unknown function.

We adopted a different strategy to identify mutants of *M. tuberculosis* that fail to
arrest phagosome maturation. Starting with a collection of 67 *M. tuberculosis* mutants
specifically attenuated for growth during mouse infection, we employed a fluorescence
microscopy methodology to identify mutants with aberrant trafficking phenotypes. We
reasoned that if PMA is required for growth during *M. tuberculosis* infection, a subset of
these 67 mutants might exhibit trafficking defects. This visual screen identified 10
mutants that trafficked to late phagosomal compartments with varying kinetics. Genes
required for PMA encode proteins with a range of functions, including ESX-1 secretion.
We show that while ESX-1 is required for PMA, known substrates of the pathway are
dispensable for PMA suggesting that novel ESX-1 effectors could play a role in
modulating phagosome traffic in the host.

Results

Identification of *M. tuberculosis* strains that fail to mediate PMA

To assess the ability of *M. tuberculosis* to mediate PMA, we infected naïve
murine bone marrow-derived macrophages with live or heat-killed *M. tuberculosis* at a
low multiplicity of infection (MOI = 1) for two hours. After inoculation, monolayers
were washed extensively to remove extracellular bacilli and the infection was allowed to
proceed for 24 or 72 hours post-inoculation. At these time points, infected monolayers

were pulsed for 10 minutes with fluorescent dextran to label early endosomes immediately prior to fixation. Fixed monolayers were processed using a modified acid-fast procedure to stain the bacteria, and fluorescence deconvolution microscopy was used to collect three-dimensional images and quantify the fraction of *M. tuberculosis*-containing phagosomes (MCPs) that co-localized with the fluorescent dextran. At both 24 and 72 hours post-infection, ~65% of live MCPs, but only ~30% of heat-killed MCPs, co-localized with the short pulse of dextran (Fig. 1A, 1C, Table 2). This is consistent with previously reported quantitation of PMA during *M. tuberculosis* infection (Armstrong et al., 1971) (Clemens et al., 1996) (Xu et al., 1994).

Using this experimental approach, we screened 67 mutant strains that were previously identified in a genetic screen for attenuated virulence in mice (Cox et al., 1999). For primary characterization, >70 phagosomes were scored using deconvolution microscopy at both 24 hours and 72 hours post-infection for each strain. 57 of the mutant strains tested, including several PDIM mutants which are severely attenuated for growth *in vivo* (Cox et al., 1999), showed intracellular trafficking that was indistinguishable from wildtype bacteria (data not shown). The remaining 10 mutants exhibited aberrant co-localization patterns (Fig. 1B). These 10 mutants were then characterized more extensively by scoring >200 phagosomes from at least three experiments to quantify the trafficking defects. We grouped these mutants into two kinetic classes: Class I mutants (Fig. 1C), which exhibited aberrant dextran co-localization at both 24 and 72 hours post-infection, and Class II mutants (Fig. 1D), which appeared like wild-type at 24 hours post-infection but aberrant by 72 hours post-infection.

To confirm trafficking defects in these 10 mutants, we performed similar co-localization experiments using a different marker of early compartments, fluorescent transferrin (Fig. 2A). Similar to the short dextran pulse, ~62% of live MCPs but only ~40% of heat-killed MCPs co-localized with the fluorescent transferrin. Mutants defective for co-localization with the short dextran pulse were similarly defective for co-localization with the fluorescent transferrin (Table 2). Together, the dextran and transferrin co-localization data strongly suggest that these mutants are defective for arresting phagosome maturation.

Of the 10 genes required for PMA during macrophage infection, 6 genes (*Rv3870*, *Rv3871*, *Rv3877*, *Rv3615c, mmpL9*, and *pcaA*) have been reported to be required for full virulence in mice (Stanley et al., 2003) (Domenech et al., 2005) (Glickman et al., 2000) (MacGurn et al., 2005). For the remaining 4 genes (*Rv2206*, *Rv2693c*, *moeB1*, and *Rv3887c*), analysis of results from the signature-tagged mutagenesis screen indicated that growth *in vivo* defects of these mutants range from mild (*Rv2693c::Tn*) to severe (*Rv2206::Tn*) (Fig 3A, 3B).

PMA mutants traffic to late phagosomal compartments

To further characterize the trafficking defects of these mutants, we analyzed infected macrophage monolayers for localization of MCPs to late phagosomal compartments using immunofluorescence microscopy. As expected, co-localization with late compartment markers such as lysobisphosphatidic acid (LBPA) (Fig. 2B) and Lamp-2 (Fig. 2C) was greater for heat-killed MCPs (~60-70%) than live wild-type MCPs (~35-45%) at both 24 hours and 72 hours post-infection (Table 2). Similar analysis of the

trafficking mutants revealed that failure to mediate PMA correlated with increased co-localization with late compartment markers (Fig 2B, Fig 2C, Table 2). In summary, these data indicate that the mutants isolated in this study fail to arrest phagosome maturation during macrophage infection, and instead traffic to late phagosomal compartments by either 24 hours (Class I) or 72 hours (Class II) post-infection.

Intracellular survival of trafficking mutants

It is well-documented that killed *M. tuberculosis* are unable to mediate PMA and instead traffic to late phagosomal compartments (Clemens et al., 1995; Clemens et al., 1996; Malik et al., 2003). Thus, there are two potential reasons that a mutant would traffic to late compartments: the mutant is killed by the macrophage and subsequently traffics to late compartments, or the mutant is defective for a mechanism that specifically mediates phagosome maturation arrest. To attempt to distinguish between these possibilities for the mutants identified in this study, we assessed the ability of each mutant to grow during macrophage infection.

The Class I mutant *Rv2206::Tn* (Fig. 4a) and the Class II mutants *pcaA::Tn* (Fig. 4d) and *moeB1::Tn* (Fig. 4e) had growth defects in macrophages that corresponded to the observed trafficking defects. The same is true for all ESX-1 secretion mutants tested, which exhibited trafficking defects that correlated with growth defects during macrophage infection (Guinn et al., 2004) (Stanley et al., 2003) (MacGurn et al., 2005). In these cases, it is possible that the mutants trafficked to late compartments as a secondary consequence of loss of viability.

In contrast, both *Rv2693c::Tn* (Fig. 4b) and Δ*mmpL9* (Fig. 4c) mutants grew at approximately wild-type levels in macrophages despite trafficking to late compartments. These results indicate that trafficking to late compartments does not inherently attenuate the growth of *M. tuberculosis* at the level of the infected macrophage.

ESX-1 components, but not known substrates, are required for PMA

Having isolated multiple ESX-1 mutants in our screen, we further investigated the role of ESX-1 secretion in modulating phagosome trafficking during infection. To confirm that loss of ESX-1 secretion was responsible for the mutant trafficking defect, we performed complementation analysis of the *Rv3877::Tn* mutant since *Rv3877* is absolutely required for secretion of all known ESX-1 substrates. Introduction of a wildtype copy of *Rv3877* which partially rescues ESX-1 secretion (Stanley et al., 2003) similarly rescued the trafficking defect observed in the mutant (Fig. 5). We therefore attribute the trafficking defect in these mutants to the loss of ESX-1 secretion.

The correlation between ESX-1 secretion and phagosome maturation arrest led us to hypothesize that substrates of the system, such as ESAT-6, CFP-10, or EspA, could be required for phagosome maturation arrest. To test this, we analyzed an Δ*esxA* mutant, which does not express ESAT-6 and CFP-10 (Stanley et al., 2003) (Guinn et al., 2004) and fails to secrete EspA (Fortune et al., 2005), for the ability to arrest phagosome maturation. In contrast to the other ESX-1 secretion mutants, the Δ*esxA* strain showed wild-type co-localization patterns with each marker tested, significantly co-localizing with the short pulse of dextran (Fig. 5A) and transferrin (Fig. 6A, 6B) while exhibiting limited co-localization with the late markers LBPA (Fig 6C, 5C,) and Lamp-2 (Fig. 5D).

To confirm this difference and to rule out any possibility of artifacts associated with the modified acid-fast stain, we tested GFP-expressing *Rv3877::Tn* and *ΔesxA* mutants for co-localization with LBPA (Fig. 6D). Again, the data suggest that the *ΔesxA* mutant arrests the maturation of the phagosome while the *Rv3877::Tn* mutant traffics to late phagosomal compartments. Thus, we conclude that essential components of the ESX-1 secretion system are required for normal trafficking in the host cell while three known substrates of the system, ESAT-6, CFP-10 and EspA, are dispensable for arresting the maturation of the phagosome.

Discussion

We screened a set of *M. tuberculosis* mutants attenuated for virulence in mice and identified 10 mutants (representing about 15% of the strains tested) defective for PMA. These mutants were classified into two kinetically distinct groups: six strains were Class I mutants, trafficking to late compartments by 24 hours post-infection, while four strains were Class II mutants, trafficking to late compartments by 72 hours. There is no overlap between our mutants and mutants identified in previous studies (Pethe et al., 2004; Stewart et al., 2005), which could be due to differences in experimental design. While other screens were unbiased, our screen was based on the assumption that PMA mutants would be represented in a set of mutants attenuated for virulence. Additionally, while previous screens for PMA mutants focused on isolation of mutants with trafficking defects several hours post-infection, we focused on defects apparent on the order of days post-infection. Indeed, the isolation of Class II mutants from our screen demonstrates that we were able to isolate mutants with trafficking defects at much later time points.

Overall, there was not a strong correlation between degree of attenuation *in vivo* and defects in PMA: mutants with comparable trafficking defects exhibited a range of *in vivo* growth defects from mild (*Rv2693c::Tn*) to severe (*Rv2206::Tn*), while other strains like those defective for PDIM synthesis are severely attenuated for growth *in vivo* (Cox et al., 1999) without consequence to PMA or growth in macrophages (data not shown, (Rousseau et al., 2004)). Likewise, these mutants exhibited varying growth phenotypes in a macrophage infection model: six had severe growth defects in macrophages, two showed moderate growth defects at late time points post-infection, and two grew with wildtype kinetics in macrophages. Since we did not perform complementation on any mutants outside the ESX-1 locus, we cannot exclude the possibility that the observed trafficking defects are due to unlinked mutations or polar effects on surrounding genes.

Interestingly, four of the 10 mutants identified in the screen were defective for ESX-1 secretion (Stanley et al., 2003). Isolation of multiple ESX-1 secretion mutants with trafficking defects in the host, coupled with our complementation of the trafficking defect associated with mutation at the ESX-1 locus, lead us to conclude that this secretion pathway is important for *M. tuberculosis*-mediated PMA. *Rv3877::Tn* and *Rv3615c::Tn* were Class I mutants, while *Rv3870::Tn* and *Rv3871::Tn* were Class II mutants. It is unclear why these mutants have similar secretion defects yet kinetically distinct trafficking defects. One possible explanation is that a putative ESX-1-dependent PMA mediator may be only partially affected by mutations in *Rv3870* and *Rv3871* but completely nullified by mutations in *Rv3877* and *Rv3615c*. The observation that the ESX-1 pathway is required for phagosome maturation arrest is consistent with a recent study in *M. marinum* (Tan et al., 2006), but raises several questions about the trafficking

phenotype of the attenuated vaccine strain, BCG. Although BCG lacks a functional

ESX-1 secretion system, it still mediates PMA during macrophage infection (Deretic et

al., 1997). It is possible that BCG's ability to mediate PMA hinges largely on conserved

lipid factors (Chua et al., 2004), while *M. tuberculosis* also employs protein factors

secreted by ESX-1. It is also possible that, having lost the ESX-1 secretion system, BCG

compensates by utilizing one or more of the ESX-1 paralogs (Gey Van Pittius et al.,

2001) to arrest phagosome maturation during infection. More studies comparing PMA in

M. tuberculosis- versus BCG-infected macrophages will be required to decipher this

phenotypic puzzle.

Unexpectedly, the *ΔesxA* mutant was not required for phagosome maturation

arrest, suggesting that expression of ESAT-6, CFP-10 and secretion of EspA are

dispensable for wild-type trafficking in the host. It is possible that other substrates of the

ESX-1 pathway could mediate PMA in an *esxA*-independent manner. Discovery of

additional ESX-1 substrates will be critical to resolve this issue.

The remaining six mutants identified in the screen exhibited wild-type levels of

ESAT-6 and CFP-10 secretion (data not shown), indicating that they are not defective for

ESX-1 secretion. The *Rv3887c* gene is an integral membrane protein homologous to

Rv3877, a component of the ESX-1 secretion system, and is situated downstream of an

esx pair (*esxC* and *esxD*), suggesting that it might also be involved in the secretion of

other Esx family member proteins. The *Rv3887c::Tn* mutant is attenuated for growth in

macrophages at early time points (A. Lau and J. Cox, unpublished results) corresponding

to the trafficking defects observed in this study. Likewise, mutation of *Rv2206*, which

encodes a conserved transmembrane protein with unknown function, resulted in a

trafficking defect by 24 hours post-infection. This mutant was severely attenuated for growth during macrophage infection and may be sensitive to early macrophage effector mechanisms.

The Class II mutant *pcaA::Tn* is defective for cyclopropyl modification of mycolic acids, a lipid species crucial to mycobacteria cell envelope structure. The mutant was reported to have a growth defect in macrophages by 48 hours post-infection but not at 24 hours post-infection (Rao et al., 2005), which is consistent with our results. Similarly, the Class II mutant *moeB1::Tn* was attenuated for growth at later time points corresponding to the observed trafficking defect. The *moeB1* gene encodes an enzyme involved in synthesis of molybdopterin, a cofactor used in many enzymatic reactions including nitrate reduction (Schwarz, 2005). Based on the moderate growth defects of the *pcaA::Tn* and *moeB1::Tn* mutants during macrophage infection, we hypothesize that these mutants are sensitive to macrophage effector mechanisms and thus are killed and traffic to late phagosomal compartments at later time points post-infection.

The *Rv2693c::Tn* and *ΔmmpL9* mutants were interesting because they failed to arrest the maturation of the phagosome without consequence to survival during macrophage infection. Interestingly, the trafficking defects observed in the *Rv2693c::Tn* and *ΔmmpL9* mutants at 24 hours post-infection were slightly less severe than other mutants described in this study (Fig 1C, Table 2). It is possible that these mutants have a moderate trafficking defect that does not critically affect growth in macrophages. However, the *ΔmmpL9* mutant, which by 72 hours post-infection exhibits a more severe trafficking defect, grew with wildtype growth kinetics even at very late time points post-infection. *MmpL9* encodes a membrane protein that is part of a large family of homologs

22

known to be involved in the secretion of lipids (Cox et al., 1999) (Converse et al., 2003) (Domenech et al., 2005). Although a lipid substrate for *MmpL9* has not yet been identified, this is consistent with previous observations that lipids play an important role in *M. tuberculosis*-mediated PMA (Chua et al., 2004) (Pethe et al., 2004) (Stewart et al., 2005). Interestingly, Pethe et al. isolated a mutant with a similar phenotype in their screen (*Rv2930::Tn*) which resided in an acidified phagosome but grew at wild-type levels in macrophages (Pethe et al., 2004). Given the possibility of artifacts inherent to the macrophage infection model, we cannot rule out the possibility that trafficking or growth phenotypes in macrophages *ex vivo* might not mimic cellular pathogenesis *in vivo*. However, taken at face value, these results suggest that phagosome maturation arrest, while likely important for *M. tuberculosis* pathogenesis, is not directly required for growth or survival in naïve macrophages. Instead, PMA may benefit *M. tuberculosis* during infection by sequestering the bacteria away from important immune response elements, such as the MHCII antigen presentation machinery or pathogen recognition receptors. It is also possible that phagosome maturation arrest, while dispensable for growth in naïve macrophages, is critical for survival in harsher, more acidified and oxidative phagosomes of activated macrophages. Indeed, macrophage activation could explain the results of the previous study linking phagosome maturation to loss of *M. tuberculosis* viability in the context of co-infection with *Coxiella burnetii* (Gomes et al., 1999), given the complexities of host response to multiple invading pathogens.

Materials and Methods

Bacterial Strains and Culture Conditions. Strains of *Mycobacterium tuberculosis* (Erdman) used in this study are listed in Table 1. All strains were grown as previously described (Cox et al., 1999). Briefly, cultures for macrophage infection were grown to mid-logarithmic phase in 7H9 media supplemented with 10% Middlebrook OADC (BD Biosciences), 0.5% glycerol and 0.05% Tween 80. Heat-killed *M. tuberculosis* were prepared by boiling for 20 minutes.

Antibodies and Reagents. Fixable 10,000 MW Alexa488-conjugated dextran and Alexa488-conjugated human transferrin were purchased from Molecular Probes. Mouse monoclonal LBPA antibody was a generous gift from Dr. Jean Gruenberg. Rat polyclonal LAMP-2 antibody (ABL-93) was purchased from the Developmental Studies Hybridoma Bank (NICHID, University of Iowa). Alexa488-conjugated anti-mouse and anti-rat secondary antibodies were purchased from Molecular Probes.

Macrophage Infection for Co-localization. Macrophages used in all experiments were derived from bone marrow cells isolated from C57BL/6 mice and differentiated for 6 days in BMM media (DMEM with 30% L-cell supernatants, 20% FCS, 2mM glutamine, 0.11mg/mL sodium pyruvate). 24 hours prior to infection, 5×10^6 macrophages were seeded onto 10cm tissue culture dishes containing sterile glass coverslips. For infection, mid-log phase *M. tuberculosis* cultures were washed three times in PBS, centrifuged at low speed to remove large clumps, and sonicated briefly to generate a single-cell

24

suspension. Inocula were prepared by diluting bacteria to an MOI of 5 in DMEM containing 10% horse serum. Macrophage monolayers were inoculated for 2 hours, washed three times in warm PBS, covered in warm BMM media and returned to the incubator.

At the indicated time points post-infection, coverslips were removed from tissue culture dishes and fixed in freshly prepared fixative (4% paraformaldehyde in PBS, pH 7.4). For dextran or transferrin labeled samples, coverslips were incubated in BMM media containing fluorescent dextran (0.25 mg/mL) or fluorescent transferrin (0.05 mg/mL) for 10 minutes and washed in PBS immediately prior to fixation.

Immunofluorescence Labeling of Infected Macrophages. Fixed monolayers were permeabilized by incubation in fresh blocking solution (0.1% BSA, 0.05% saponin in PBS) for 20 minutes at room temperature. Lamp-2 immunofluorescence was performed by incubating coverslips in primary antibody (1:100 in blocking solution), washing three times in PBS, and incubating in Alexa488-conjugated anti-rat secondary antibody (1:200 in blocking solution). LBPA immunofluorescense was performed as previously described (Matsuo et al., 2004).

Modified Acid-Fast Stain. To visualize mycobacteria in infected macrophages, we modified traditional acid-fast staining protocols to improve compatibility with multi-color fluorescence imaging. Fixed, infected monolayers were stained with a solution of dye (0.55% Rhodamine B, 55% glycerol, 7.5% phenol) diluted 1:5000 in PBS for 5

25

minutes then washed extensively in PBS. Stained monolayers were then mounted and analyzed immediately following preparation.

Fluorescence Microscopy. Coverslips were mounted onto slides with SlowFade antifade reagent (Molecular Probes) and imaged using a DeltaVision DV3 Restoration Microscope (Applied Precision) using a MicroMax 5 MHz cooled CCD camera (Roper Scientific). For each infected monolayer, 5μm z-stacks, centered at the mycobacteria bacillus, were collected for roughly 70 infected macrophages. Each stack was deconvolved and analyzed using SoftWoRx software (Applied Precision).

For each strain and marker used in this study, fraction co-localization was quantified from at least three separate infections totaling over 200 individual phagosomes. Student's t-test was used to determine statistical significance compared to wildtype.

Growth Determination in vivo and in cultured macrophages. Signature-tagged mutagenesis, mutant isolation, tag representation and insertion determination were performed as previously described (Cox et al., 1999). Briefly, pools of 48 signature-tagged transposon mutants were pooled, cultured, and used to inoculate two C56B6 mice by tail vein injection. At 3 weeks post-infection, signature DNA tags from mutant mycobacteria harvested from innoculum pools or the lungs of two mice were amplified, radiolabelled and hybridized to array filters. Tag representation was determined by measuring mean pixel intensity using Image J software (http://rsbweb.nih.gov/ij/).

CFUs from macrophages infected with *M. tuberculosis* were determined as previously described (MacGurn et al., 2005). Briefly, three separate monolayers were inoculated at an MOI of 1 for 2 hours. Infected monolayers were washed and lysed at 0, 24, 72, 120 and 168 hours post infection. Lysates were diluted and plated on 7H10 media. Growth curves shown are representative from at least two independent experiments.

**Figure 1. Identification of trafficking mutants in _M. tuberculosis._**

Bone-marrow derived macrophages were infected with strains of _M. tuberculosis_ and, at 24 and 72 hours post-infection, pulsed for 10 minutes with fluorescent dextran immediately prior to fixation. Fixed monolayers were imaged using fluorescence deconvolution microscopy. Fluorescent dextran is green while bacilli were stained red. White arrows point to individual bacilli. **(A)** Live and heat-killed _M. tuberculosis_ were used as controls. **(B)** The screen identified several mutants exhibiting aberrant dextran co-localization. **(C and D)** For each strain, fraction co-localization at 24 hours (black bars) and 72 hours (gray bars) post-infection was averaged over at least three separate infections totaling > 200 phagosomes. A total of 10 mutants with co-localization defects were identified. Scale bars = 10μm. ** indicates p value < 0.001.

Fig. 1

A

Dextran Pulse (green)
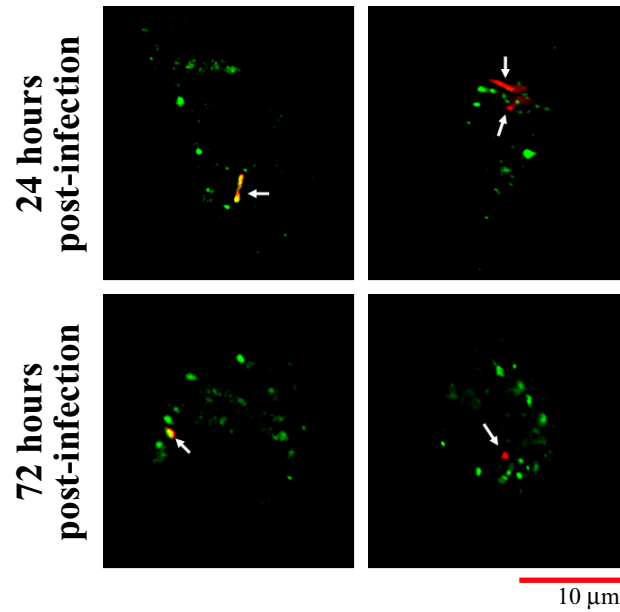
B

Dextran Pulse (green)

Fig. 1 (cont.)

C

Class I Mutants

D

Class II Mutants
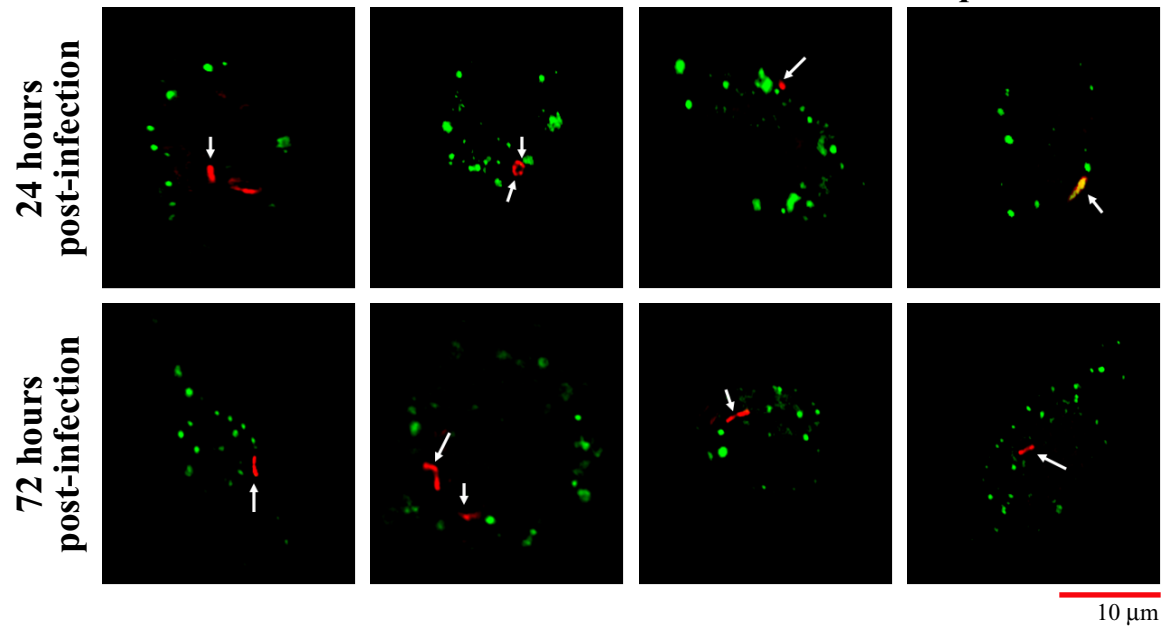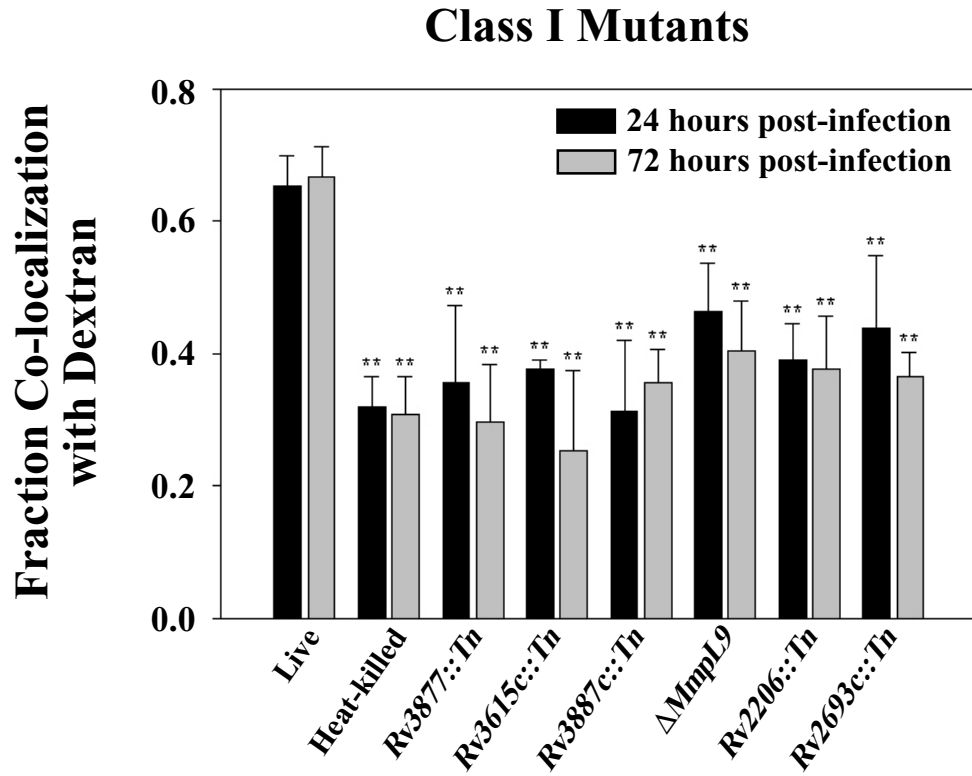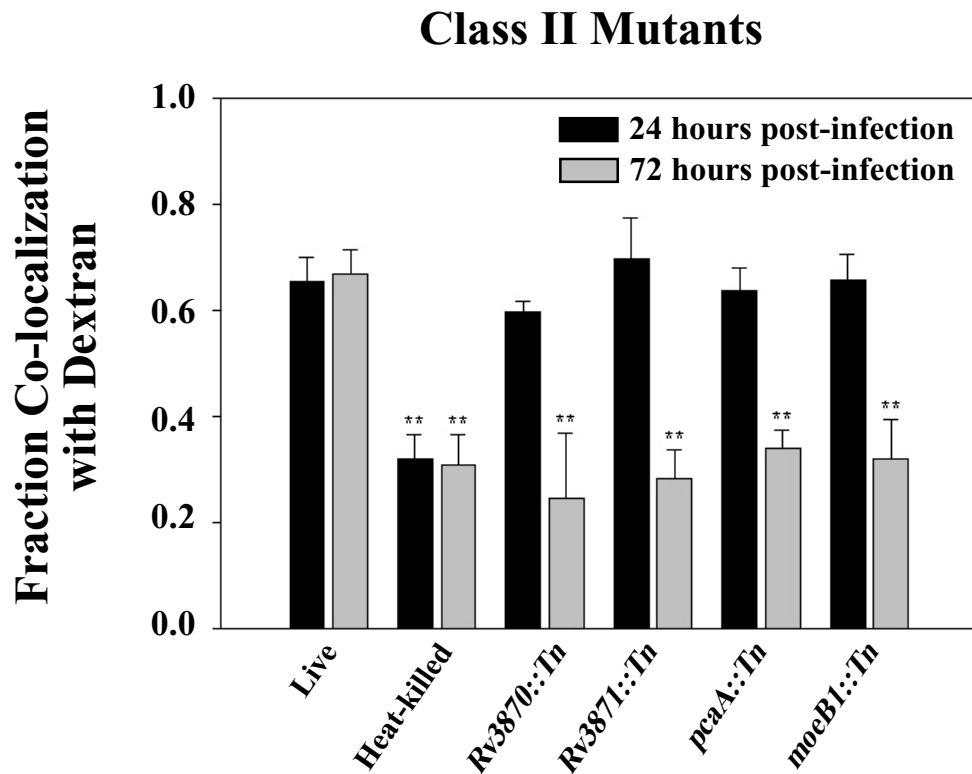
Figure 2. Co-localization of _M. tuberculosis_ strains with different maturation markers.
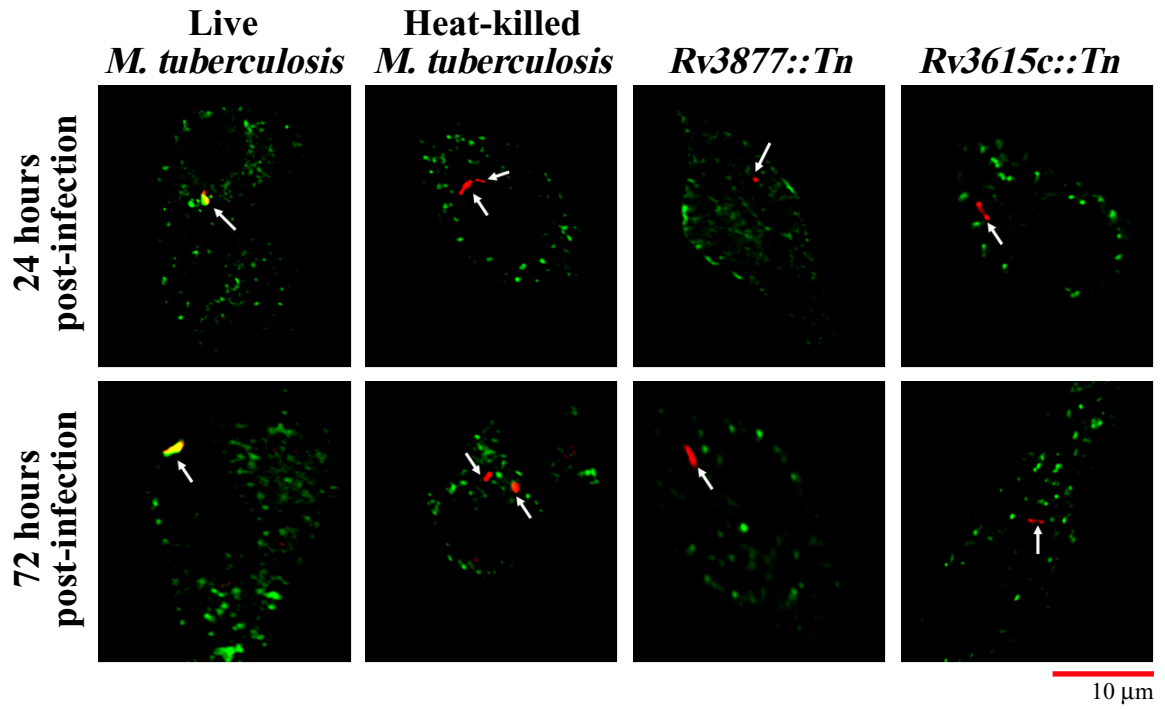
Infections were performed and imaged as in Fig. 1. Representative images for 24 hours and 72 hours post-infection are shown from macrophages infected with live and heat-killed _M. tuberculosis_, as well as _Rv3877::Tn_ and _Rv3615c::Tn_ mutant strains. Maturation markers are green while bacilli were stained red. White arrows point to individual bacilli. **(A)** For fluorescent transferrin co-localization, infected monolayers were pulsed with fluorescent transferrin for 10 minutes immediately prior to fixation. **(B and C)** Fixed monolayers were stained for late compartment markers LBPA and Lamp-2 using indirect immunofluorescence. Scale bars = 10μm.

Fig. 2

A

Transferrin (green)

| | Live *M. tuberculosis* | Heat-killed *M. tuberculosis* | *Rv3877::Tn* | *Rv3615c::Tn* |

24 hours post-infection

72 hours post-infection

10 μm

B

LBPA (green)

| | Live *M. tuberculosis* | Heat-killed *M. tuberculosis* | *Rv3877::Tn* | *Rv3615c::Tn* |

24 hours post-infection

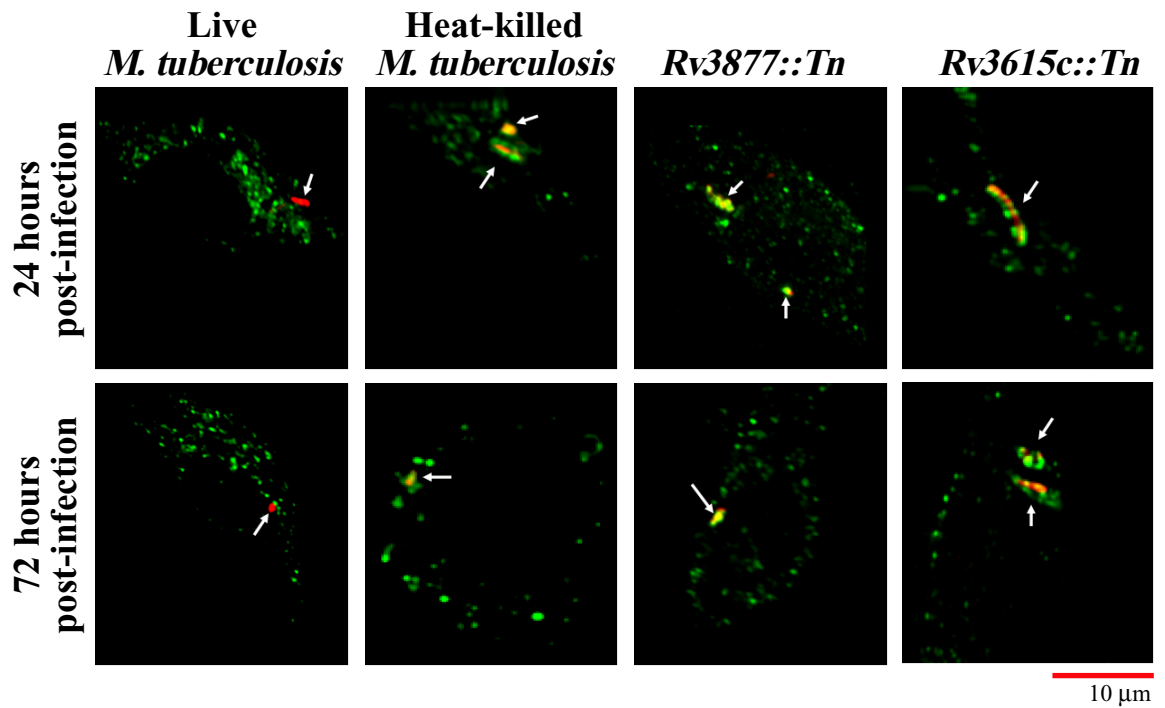72 hours post-infection

10 μm

32

Fig. 2 (cont.)
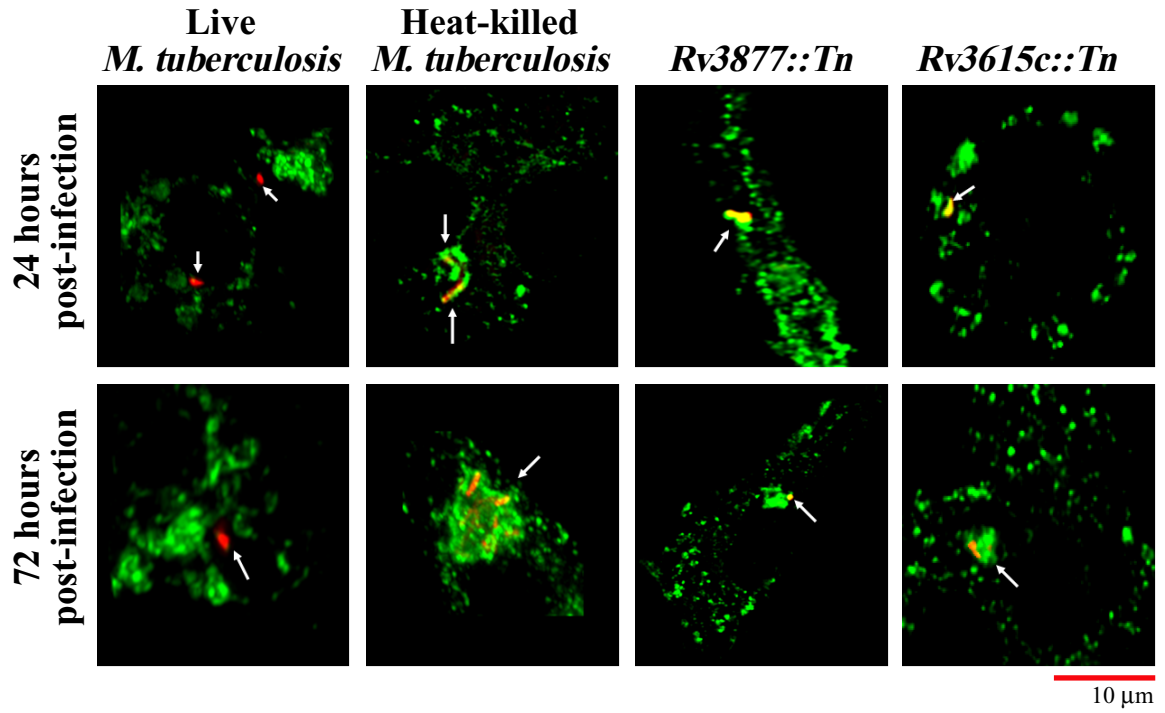
C   **Lamp-2 (green)**

Figure 3. *In vivo* growth defects of PMA mutant strains.

(A) Array filters were used to determine tag representation within pools of signature-tagged transposon mutants from culture (input) and infected mice (output). WT indicates representation of a strain in the pool of mutants that exhibited wildtype growth in mice at 3 weeks post-infection. **(B)** For each spot on the array filters, representation was determined by densitometry. For each mouse, the following equation was used to calculate a ratio of pixel intensities normalized to wildtype:

$(\text{mutant}^{\text{mouse}} / \text{wildtype}^{\text{mouse}}) / (\text{mutant}^{\text{input}} / \text{wildtype}^{\text{input}})$.
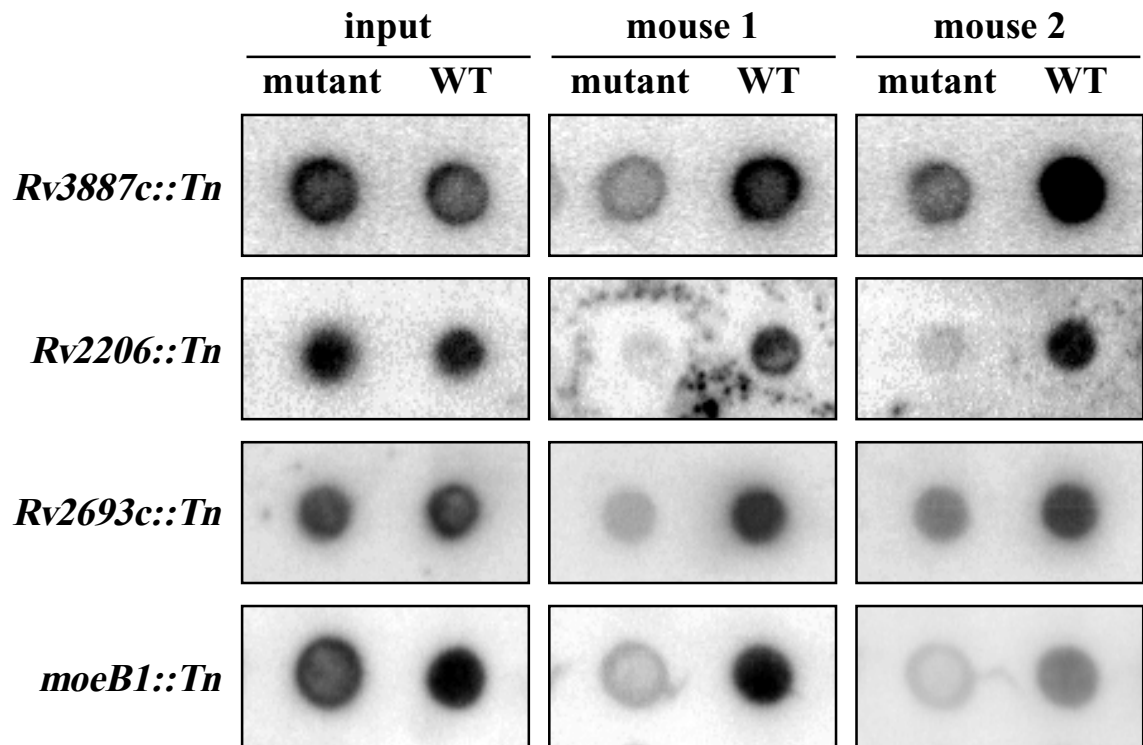
Fig. 3

A

Fig. 3

B
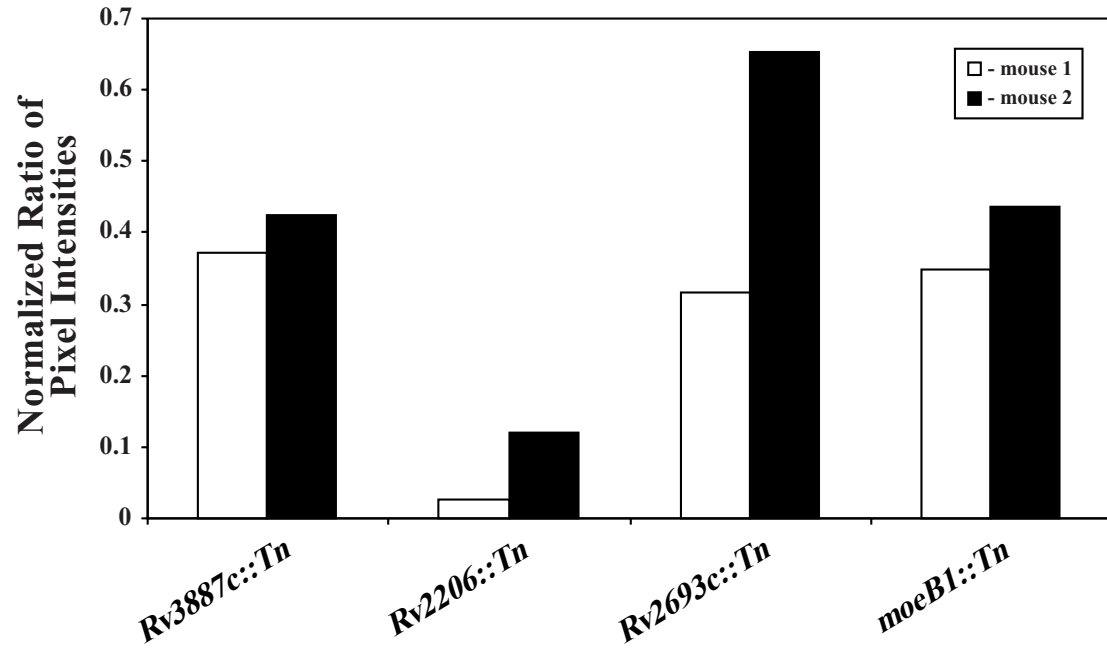
Figure 4. Analysis of intracellular survival of trafficking mutants.

Bone marrow-derived macrophage monolayers were infected with *M. tuberculosis* strains at an MOI of 1 for 2 hours and plated for CFU determination at 0, 24, 72, 120 and 168 hours post-infection. CFUs were determined for **(A)** *Rv2206::Tn*, **(B)** *Rv2693::Tn*, **(C)** *ΔmmpL9*, **(D)** *pcaA::Tn*, and **(E)** *moeB1::Tn*. Black bars indicate CFUs at 24 hours post-infection while gray bars represent CFUs at 72 hours post-infection. Values shown on the y-axis are from a dilution of the monolayer lysate and represent 1/400th of the actual number of CFUs in the monolayer. Growth curves shown are representative growth curves from at least two similar experiments. * indicates p value < 0.05. ** indicates p value < 0.01.

Fig. 4

A

wildtype vs. *Rv2206::Tn*

B

wildtype vs. *Rv2693c::Tn*

C

wildtype vs. Δ*mmpL9*

D

wildtype vs. *pcaA::Tn*

E

wildtype vs. *moeB1::Tn*
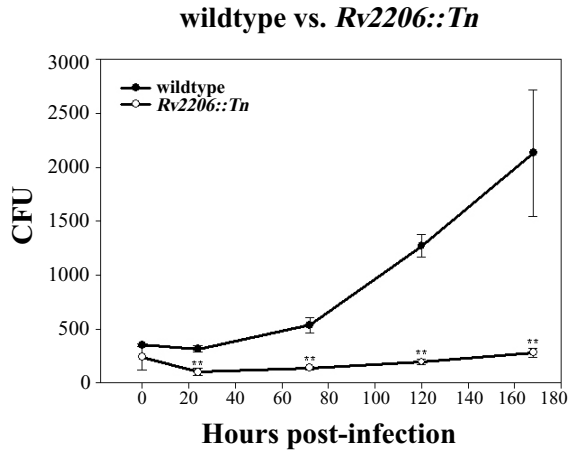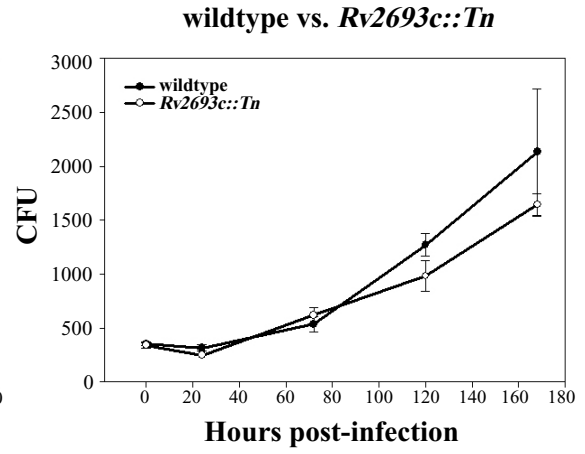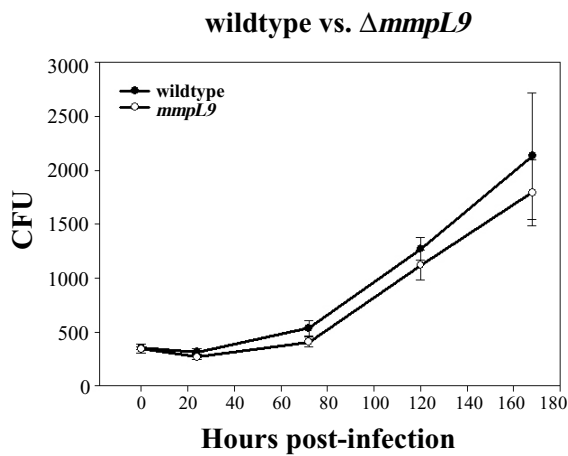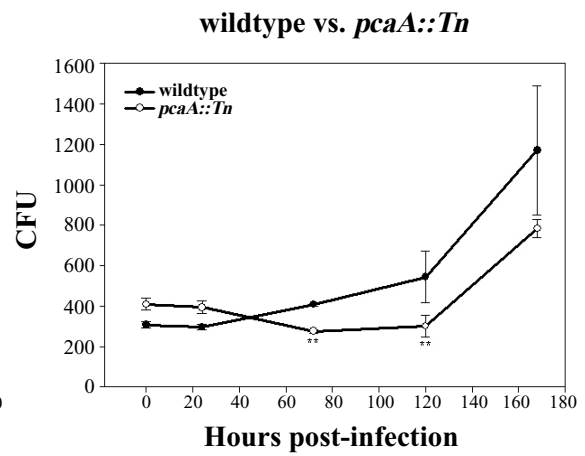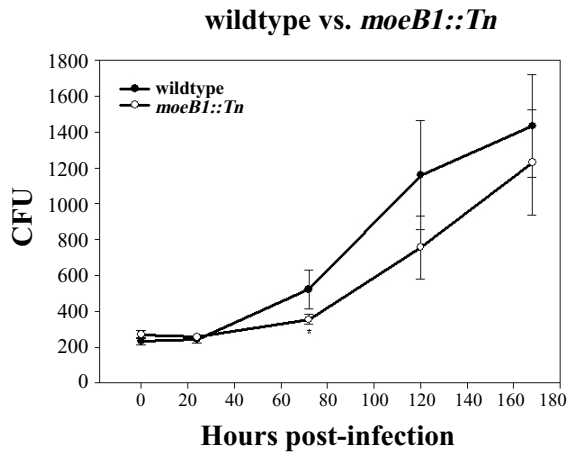
Figure 5. Quantification of trafficking defects of ESX-1 mutants.

Several mutants known to be defective for ESX-1 secretion (*Rv3877::Tn*, *Rv3870::Tn*, *Rv3871::Tn*, *ΔesxA, Rv3615c::Tn*) were scored for their ability to mediate PMA at 24 hours (black bars) and 72 hours (gray bars) post-infection. **(A)** A short dextran pulse and **(B)** transferrin were used as markers of early phagosomal compartments, while **(C)** LBPA and **(D)** Lamp-2 were used as markers of late phagosomal compartments. For each strain, fraction co-localization was averaged over at least three separate infections totaling > 200 phagosomes. ** indicates a significant difference (p value < 0.01) comared to both wildtype and *ΔesxA* strains.

Fig. 5

A

Dextran Pulse

B

Transferrin

Fig. 5 (cont.)

C

LBPA

D

Lamp-2
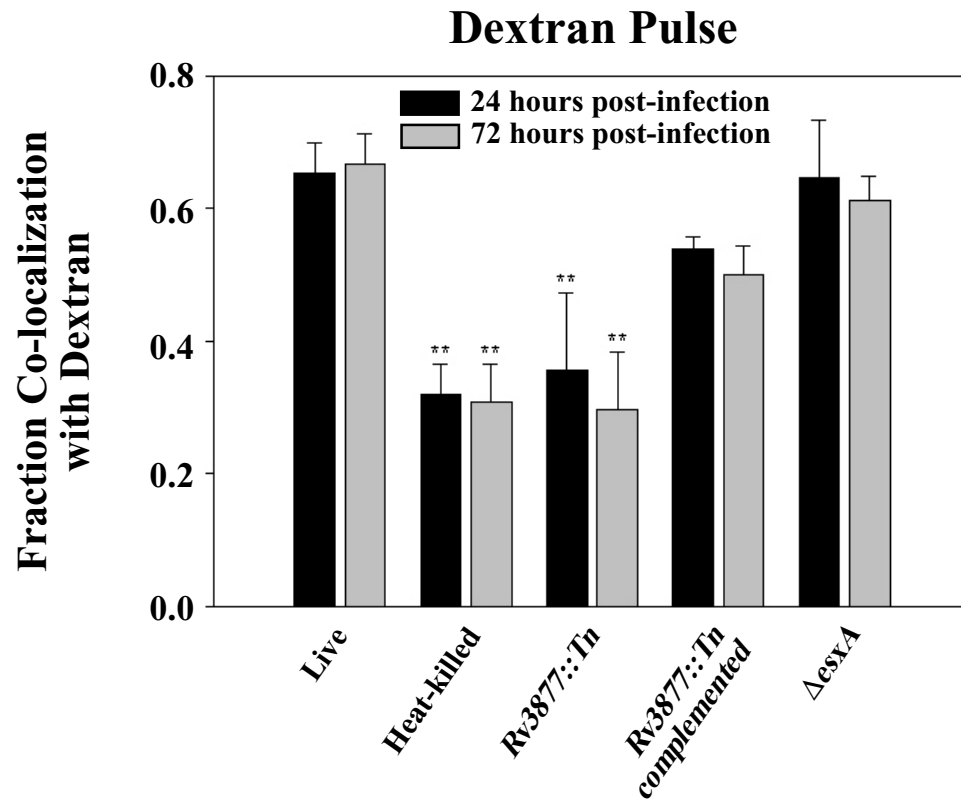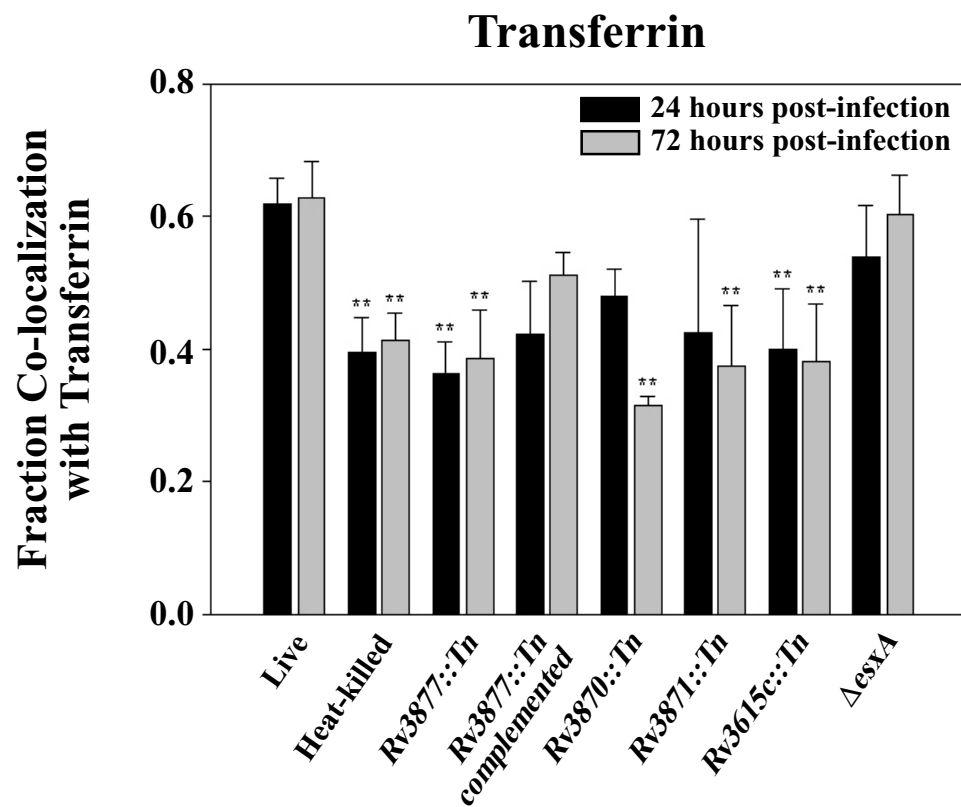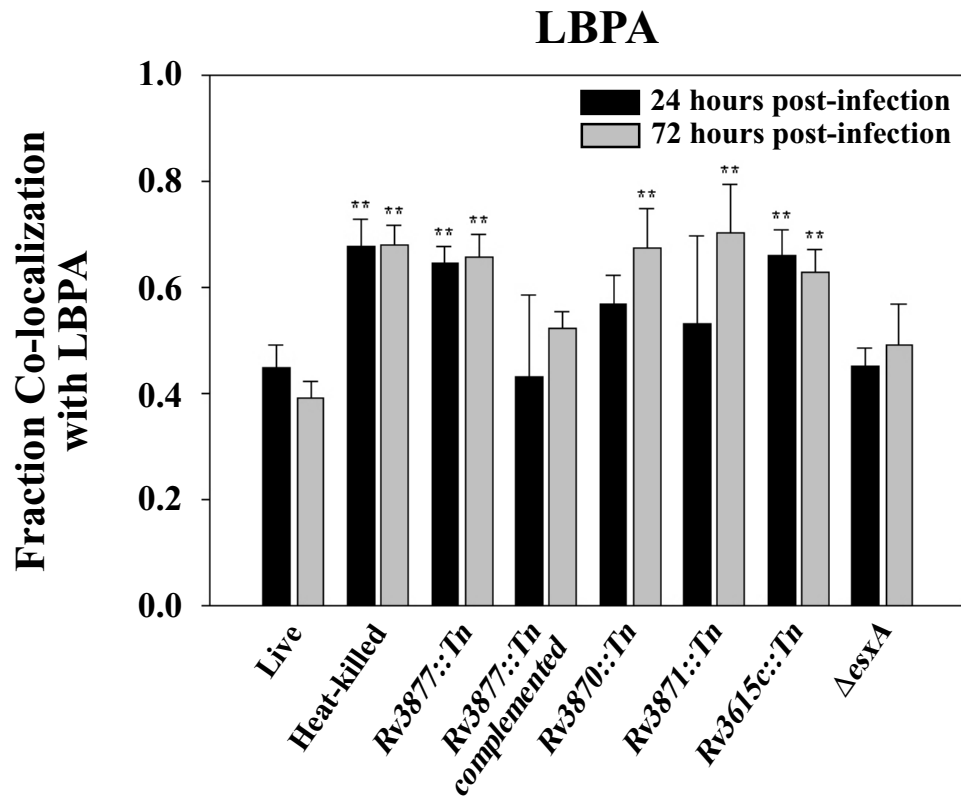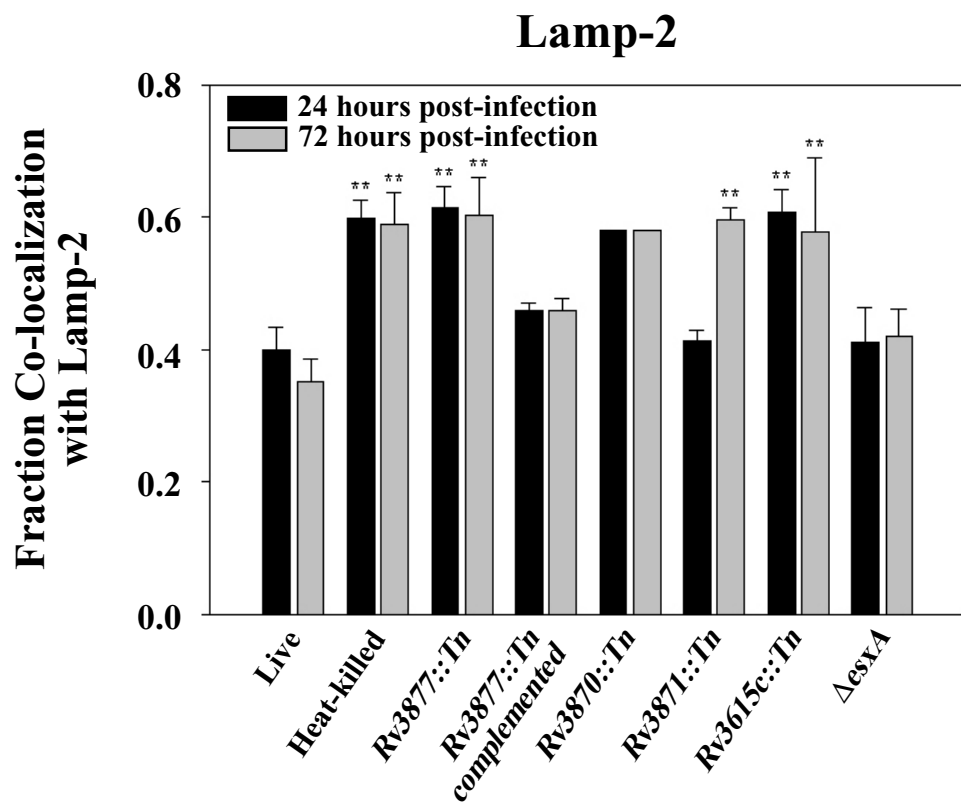
Figure 6. *ΔesxA* is not defective for PMA and does not traffic to a late phagosome.

(A) Macrophages were infected with *ΔesxA M. tuberculosis* and analyzed for co-localization with transferrin and LBPA using fluorescence deconvolution microscopy. Fluorescent markers are green while bacilli were stained red. White arrows point to individual bacilli. Scale bar = 10μm. **(B)** DIC (left), deconvolved fluorescent z slice (middle), and merged (right) images of individual macrophages infected with either *Rv3877::Tn* or *ΔesxA* were stained for the late marker LBPA by indirect immunofluorescence. Images are from 24 hours post-infection. Nuclei (blue) were stained with DAPI. **(C)** Z-stacks from macrophages infected with either *Rv3877::Tn* or *ΔesxA* mutants (stained red) were deconvolved and rendered to visualize and determine co-localization in three dimensions. LBPA stain is green. **(D)** *Rv3877::Tn* and *ΔesxA* mutants (green) expressing GFP were also used in some experiments as an alternative to post-fixation staining of bacteria. LBPA stain is red.

Fig. 6

A

Δ*esxA* (red)

	Transferrin (green)	**LBPA (green)**

10 µm

B

	DIC	Fluorescence	Merge
Rv3877::Tn			
ΔesxA			

43
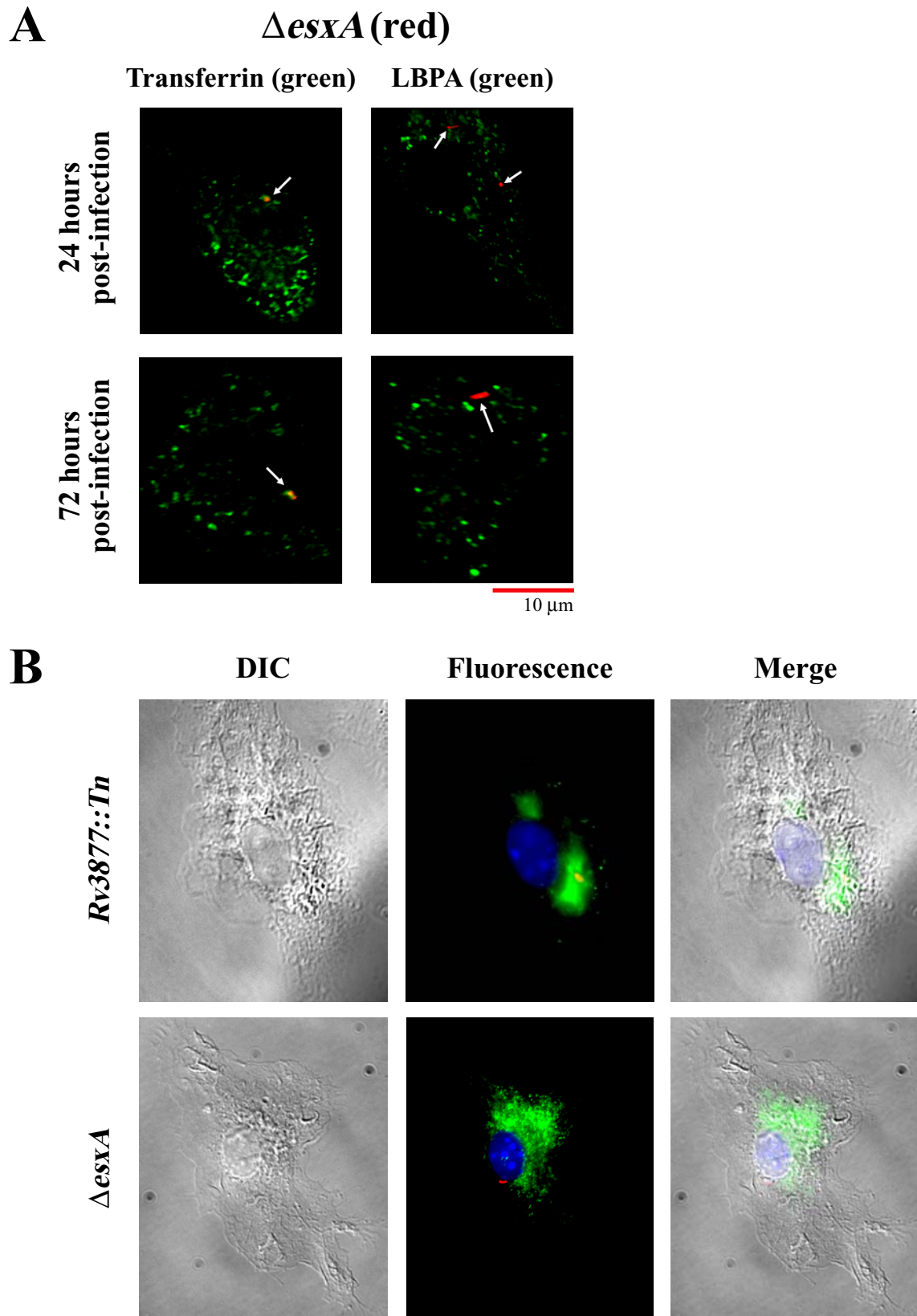
Fig. 6 (cont.)

C **LBPA Rendered**

Rv3877c::Tn   Δ*esxA*

24 hours post-infection
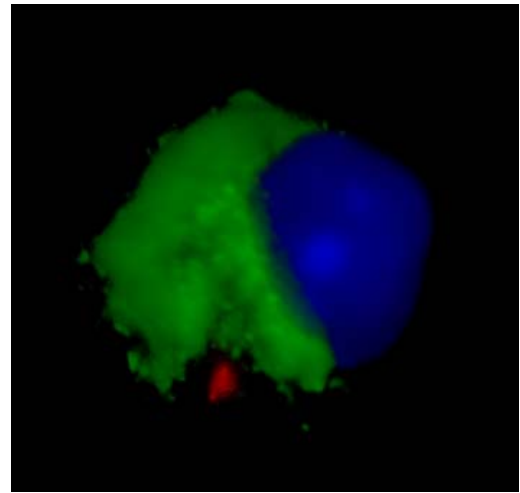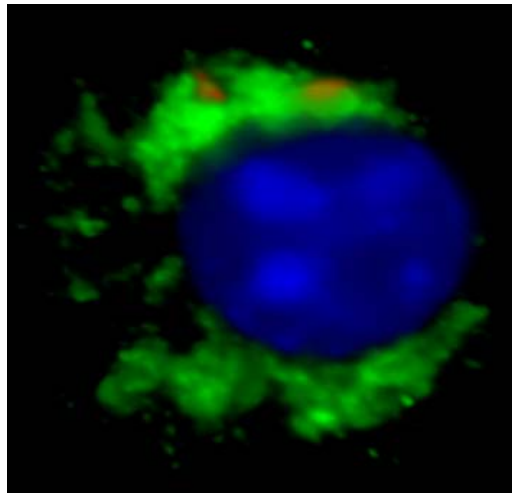
D **LBPA Rendered**

Rv3877c::Tn   Δ*esxA*

24 hours post-infection
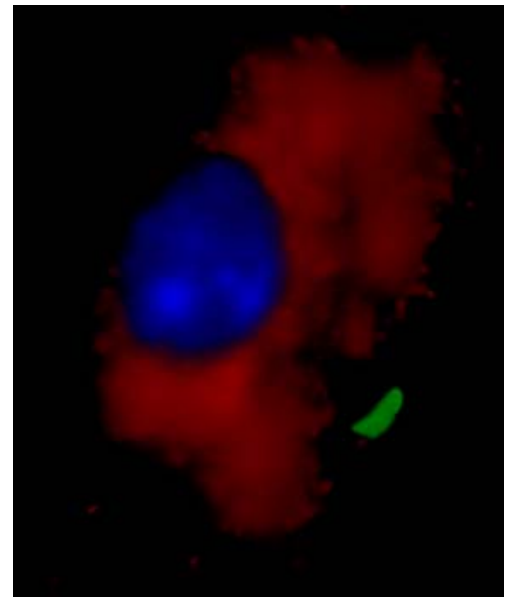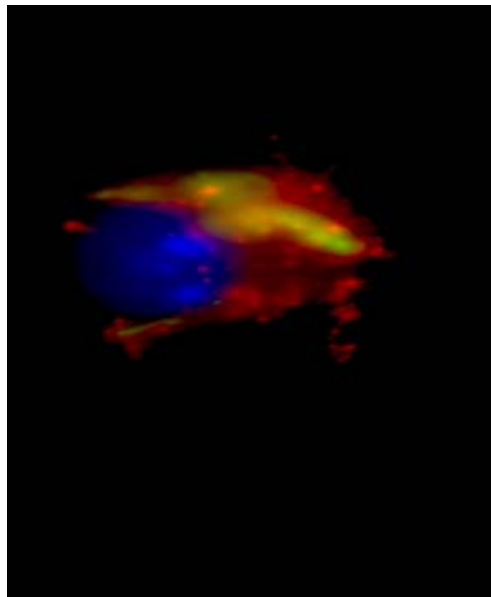
Table 1.   Plasmids and Strains used in this study

Strain/plasmid	Description/Genotype	Source
Plasmids		
pYUB921	**pGroEL, eGFP, oriE, oriM, KanR**	**W. R. Jacobs Jr.**
***M. tuberculosis* Strains**		
Erdman	Wildtype	W. R. Jacobs Jr.
Rv3870::Tn	HygR	Stanley *et al.* (2003)
Rv3871::Tn	HygR	Stanley *et al.* (2003)
Rv3877::Tn	HygR	Stanley *et al.* (2003)
ΔesxA	HygR	Stanley *et al.* (2003)
Rv3615c::Tn	HygR	MacGurn *et al.* (2005)
pcaA::Tn	HygR	This study
Rv3887c::Tn	HygR	This study
Rv2693c::Tn	HygR	This study
Rv2206::Tn	HygR	This study
moeB1::Tn	HygR	This study
ΔmmpL9	HygR	This study

Table 2.   Summary of fraction co-localization with markers used in this study

Strain	h.p.i.	Dextran		Transferrin		LBPA		LAMP-2	
		avg*	SD	avg	SD	avg	SD	avg	SD
Controls									
Erdman Live	24	0.654	0.045	0.619	0.039	0.447	0.044	0.399	0.033
	72	0.667	0.047	0.627	0.056	0.391	0.031	0.353	0.035
Erdman Heat-killed	24	0.320	0.045	0.395	0.053	0.678	0.051	0.598	0.027
	72	0.308	0.059	0.413	0.041	0.679	0.038	0.589	0.049
Class I mutants									
Rv3887::Tn	24	0.314	0.108	0.402	0.043	0.583	0.128	0.560	0.023
	72	0.356	0.050	0.381	0.015	0.687	0.007	0.559	0.070
Rv2206::Tn	24	0.390	0.056	0.372	0.024	0.688	0.069	0.617	0.001
	72	0.376	0.080	0.374	0.043	0.718	0.064	0.617	0.036
Rv2693c::Tn	24	0.440	0.109	0.401	0.002	0.664	0.060	0.605	0.032
	72	0.365	0.037	0.344	0.054	0.614	0.077	0.570	0.024
ΔmmpL9	24	0.464	0.074	0.330	0.042	0.638	0.086	0.519	0.087
	72	0.404	0.076	0.353	0.002	0.614	0.075	0.587	0.009
Class II Mutants									
pcaA::Tn	24	0.637	0.044	0.589	0.038	0.387	0.046	0.429	0.069
	72	0.338	0.037	0.442	0.060	0.580	0.010	0.571	0.014
moeB1::Tn	24	0.657	0.048	0.632	0.083	0.433	0.060	0.382	0.061
	72	0.319	0.074	0.393	0.027	0.622	0.042	0.589	0.062

*Average fraction co-localization with each marker was computed using >200 scored phagosomes from at least three experiments. h.p.i. indicates hours post infection. SD indicates standard deviation.

Chapter 3

A non-RD1 gene cluster is required for Snm secretion in *Mycobacterium tuberculosis*

Abstract

The Snm secretion system is a crucial virulence determinant of *Mycobacterium tuberculosis*. Genes encoding all known components of this alternative secretion pathway are clustered at the same genetic locus, known as RD1. Here, we show that a mutant *M. tuberculosis* strain containing a transposon insertion in the *Rv3615c* gene, which is situated outside of the RD1 locus, results in loss of Snm secretion. Complementation analysis revealed that both *Rv3615c* and the downstream gene *Rv3614c* are required for Snm secretion. Thus, we have renamed the two genes *snm9* and *snm10*, respectively. The *snm9::Tn* mutant phenocopies *bona fide snm* mutants, exhibiting attenuation in mice, macrophage growth defects and failure to suppress cytokine induction. Furthermore, yeast two-hybrid analysis revealed a physical interaction between Snm10 and Snm7 (Rv3882c), suggesting that Snm10 may function in complex with other Snm proteins during secretion. Thus, *snm9* and *snm10* are the first genes located outside the RD1 locus identified as critical components of Snm secretion. These data indicate that Snm secretion consists of an elaborate network of interactions that likely arose from multiple duplication events during the evolution of *M. tuberculosis*.

48

Introduction

A common theme in bacterial pathogenesis is the utilization of alternative secretion systems for delivery of virulence molecules to mediate interactions with the host. Although alternative secretion systems in Gram-negative bacteria have been described in mechanistic detail (Lee et al., 2001), little is known about alternative secretion pathways in gram-positive or acid-fast bacteria. Virulence of *Mycobacterium tuberculosis*, an acid-fast bacteria estimated to infect a third of the world's population (Dye *et al.*, 1999), requires secretion of ESAT-6 and CFP-10 (Wards et al., 2000; Hsu et al., 2003). These two small proteins, which are part of a large group of homologous proteins called the Esx family, lack traditional signal sequences and instead are secreted through an alternative secretion pathway called the Snm (secretion in mycobacteria) system (Stanley *et al.*, 2003) (Guinn *et al.*, 2004) (Hsu *et al.*, 2003). ESAT-6 and CFP-10 are encoded by genes at the RD1 (region of difference 1) locus, a part of the *M. tuberculosis* genome that has been deleted through repeated passaging of the *M. bovis* BCG vaccine strain (Behr *et al.*, 1999) (Mahairas *et al.*, 1996) (Cole *et al.*, 1998). Loss of RD1 is at least partially responsible for the attenuation of the BCG strain, as reintroduction restores some virulence (Pym *et al.*, 2002) (Majlessi *et al.*, 2005). Interestingly, many of the genes encoded at the RD1 locus are required for secretion of ESAT-6 and CFP-10, leading to the hypothesis that this region encodes for an alternative secretion complex essential for virulence.

Growing evidence suggests that the Snm secretion system is a critical virulence determinant in many acid-fast and Gram-positive bacteria. In *M. tuberculosis*, *snm* mutants are attenuated for virulence in mice, grow poorly in macrophages and fail to

49

suppress macrophage inflammatory responses such as the production of IL-12 and TNF-α (Stanley *et al.*, 2003) (Lewis *et al.*, 2003). *M. tuberculosis snm* secretion mutants also exhibit diminished cytolysis of pneumocytes (Hsu *et al.*, 2003). In *Mycobacterium marinum*, a relative of *M. tuberculosis* that causes disease in fish and amphibians, transposon insertions in various genes at the RD1 locus resulted in loss of ESAT-6/CFP-10 secretion as well as decreased haemolytic activity and cell-to-cell spreading (Gao *et al.*, 2004). Furthermore, *M. marinum* mutants missing the RD-1 region are defective for granuloma formation in the zebrafish embryo model of infection (Volkman *et al.*, 2004), suggesting a role for Snm secretion in determining host immune response. Despite its prominent role in the virulence of mycobacteria, the functional significance of Snm secretion has recently been extended to Gram-positive bacteria. In *Staphylococcus aureus*, *snm* homologues are required for secretion of ESAT-6-like proteins (Burts *et al.*, 2005). As with mycobacteria, loss of ESAT-6 secretion in *S. aureus* correlates with reduced virulence. It is noteworthy that several other Gram-positive pathogens, including *Bacillus anthracis, Corynebacterium diptheriae* and *Listeria monocytogenes* contain *snm* homologues (Pallen, 2002). While the role of these homologues in virulence is not yet determined, mounting evidence suggests that this alternative secretion system will be important for virulence in many acid-fast and Gram-positive pathogens.

Given its role in pathogenesis, it is curious that the Snm secretion system also functions in non-pathogenic mycobacteria. The fast-growing *Mycobacterium smegmatis* has a genetic locus homologous to RD1 and is able to secrete ESAT-6 and CFP-10 homologues (Gey Van Pittius et al., 2001; Converse et al., 2005). Interestingly, mutations in *M. smegmatis snm* homologues not only disrupt secretion of ESAT-6 and

CFP-10 (Converse et al., 2005), but also result in increased conjugal DNA transfer, a phenotype that is complemented by expression of *M. tuberculosis snm* genes (Flint *et al.*, 2004). In addition to *M. smegmatis*, many other non-pathogenic acid-fast and Gram-positive bacterial genomes encode *snm* homologues (Pallen, 2002), although their functions remain to be elucidated. While the Snm pathway may have different functions in various bacteria, similarity of *snm* genes suggests that the core mechanism of Snm secretion is conserved.

Several recent studies have begun to identify the individual proteins that form the Snm secretion complex. Physical interactions have been demonstrated between substrates ESAT-6 and CFP-10, between CFP-10 and Snm2, a pumping ATPase, and between Snm2 and Snm1, another pumping ATPase (Renshaw et al., 2002; Stanley et al., 2003; Iyer et al., 2004; Okkels et al., 2004). This suggests that a network of physical interactions that link substrates and Snm proteins may form the core machinery of this specialized secretion system. Other genes required for the secretion of ESAT-6 and CFP-10 in *M. tuberculosis* include *snm3* (*Rv3876*) (Guinn *et al.*, 2004) and *snm4* (*Rv3877*) (Stanley *et al.*, 2003). Additionally, a recent study in *M. smegmatis* disrupted several genes in the region homologous to *M. tuberculosis* RD1, demonstrating that in *M. smegmatis* Snm secretion requires *snm5* (*Rv3866*), *snm6* (*Rv3869*), *snm7* (*Rv3882c*), and *snm8* (*Rv3883c* or *MycP1*) (Converse et al., 2005). Furthermore, in *M. marinum*, transposon insertions in several other RD1 locus genes resulted in loss of Snm secretion (Gao *et al.*, 2004). So far, all the *snm* genes described are clustered at the RD1 locus.

Here we describe a second genetic locus in *M. tuberculosis*, outside the RD1 region, that is required for Snm secretion. Two genes at this locus, *Rv3615c* and

Rv3614c, are required for Snm secretion of ESAT-6 and CFP-10, prompting us to rename these genes *snm9* and *snm10*, respectively. The *snm9::Tn* mutant exhibits several pathogenesis defects associated with loss of Snm secretion in *M. tuberculosis*. Furthermore, we show that the Snm10 protein can physically interact with Snm7, which is encoded at the RD1 locus. Our data suggests that Snm secretion is a complex process that has evolved to require protein components encoded at multiple loci in the *M. tuberculosis* genome.

Results

The Rv3616c-Rv3614c gene cluster is conserved in pathogenic mycobacteria

In a genetic screen for *M. tuberculosis* mutants attenuated for growth in mice, we observed that a transposon insertion in *Rv3615c* resulted in loss of virulence (Figure 1). A recent study by Sassetti et al. also showed that transposon insertions in *Rv3616c*, *Rv3615c*, or *Rv3614c* resulted in attenuation of virulence in mice (Sassetti et al., 2003). The *Rv3616c-Rv3614c* gene cluster is highly conserved in *M. bovis* and in *M. leprae* (Figure 2A), but is absent from *M. avium paratuberculosis* and *M. smegmatis* genomes. This exclusive conservation among pathogenic mycobacteria may be indicative of a role for the gene cluster in virulence.

Within the *M. tuberculosis* genome, *Rv3616c*, *Rv3615c*, and *Rv3614c* are homologous to *Rv3864*, *Rv3865*, and *Rv3867* respectively (Sassetti et al., 2003) (Figure 2B). Interestingly, this homologous gene cluster is directly upstream of the RD1 locus and is interrupted by *Rv3866*, a gene that is required for Snm secretion in *M. smegmatis* (Converse et al., 2005). Motif analysis revealed conservation of the N-terminal 20 amino

acids in both Rv3615c and Rv3865, as well as several ESAT-6 family members (Figure

2C). Alignment of the N-terminal peptide sequence of Rv3615c and EsxW (Figure 2D)

reveals that 50% of the amino acids are highly similar. The conservation of this N-

terminal motif may indicate that *Rv3615c* and *Rv3865* are distantly related to the ESAT-6

family of proteins. Given the homology of the *Rv3616c-Rv3614c* gene cluster with genes

at the RD1 locus, we decided to test if this gene cluster functions in Snm secretion.

Secretion of ESAT-6 and CFP-10 is blocked in the *Rv3615c::Tn* mutant

To assess protein secretion in the *Rv3615c::Tn* mutant, we compared short-term

culture filtrate (STCF) from wildtype *M. tuberculosis* (Erdman) and the mutant cultures

using 2D gel electrophoresis. Several low molecular mass spots present in wildtype

STCF but missing from mutant STCF were identified using MALDI-TOF mass

spectrometry of trypsin-digested samples. Interestingly, all missing spots correspond to

different forms of either ESAT-6 or CFP-10 (Figure 3). Of the spots identified as ESAT-

6 (spot 1 and spot 2, Figure 3) one appeared to be acetylated between amino acids 2-33,

which is consistent with published results (Okkels *et al.*, 2004). Despite the observed

differences in isoelectric point for the different forms of CFP-10 (Figure 3, spots 3-6), the

m/z spectra of these spots did not reveal any differences to account for spot shifts. It is

likely that the different forms of CFP-10 result from post-translational modifications on

peptide fragments that are not efficiently ionized under the conditions of these

experiments. To determine if the secretion profile of *Rv3615c::Tn* mutants differs from

that of *snm4::Tn,* we compared STCF from each strain by 2D electrophoresis. Notably,

2D spot profiles of the two mutants were identical (data not shown), indicating that these mutants exhibit the same secretion defect.

Western blot analysis confirmed that both ESAT-6 and CFP-10 were abundant in STCF from wildtype cultures (Figure 4, lane 2) but missing in STCF from the *Rv3615c::Tn* mutant (Figure 4, lane 6). The secretion defect does not stem from a failure to express ESAT-6 or CFP-10, as both bands appear in cellular fractions of the mutant (Figure 4, lane 5). As with the 2D gel analysis, the *Rv3615c::Tn* mutant secretion defect was identical to the secretion defect of the *snm4::Tn* mutant (Figure 4, lanes 3 and 4). Thus, the *Rv3616c-Rv3614c* gene cluster represents the first locus outside of the extended RD1 region required for Snm secretion.

To confirm that the Snm secretion defect is due to the transposon insertion in the *Rv3616c-Rv3614c* gene cluster, we performed western-blot analysis on cellular and STCF fractions from strains with complementation constructs integrated in single copy. Introduction of the entire *Rv3616c-Rv3614c* gene cluster was sufficient to fully complement the secretion defect (Figure 4, lane 10), confirming that the transposon insertion at this locus is responsible for the secretion phenotype. Because it is likely that a transposon insertion in *Rv3615c* would affect expression of the downstream *Rv3614c*, abrogation of either gene could be responsible for loss of Snm secretion in the *Rv3615c::Tn* mutant.   To account for any polar effects, we attempted to complement the secretion defect with several constructs introducing different combinations of genes within the cluster (Figure 4, lanes 7-22). While reintroduction of the entire *Rv3616c-Rv3614c* gene cluster is sufficient for full complementation of the secretion defect, removal of *Rv3614c* from this construct fails to restore Snm secretion (Figure 4, lane 18)

despite wildtype levels of *Rv3615c* mRNA (Figure 5, C and D). Thus, the transposon

insertion in *Rv3615c* likely has a polar effect on the downstream gene *Rv3614c*, which is

required for Snm secretion. Transcriptional profiling by microarray revealed that

Rv3614c, like *Rv3615c*, is transcriptionally attenuated in the *snm9::Tn* mutant (Figure 5,

A and B), confirming the polar affect of the transposon insertion. *Rv3615c* is also

required for Snm secretion, as in-frame deletion of *Rv3615c* (Figure 4, lanes 16 and 20)

failed to complement the secretion defect despite wildtype levels of *Rv3614c* mRNA

(Figure 5, C and D).

While complementation with *Rv3615c-Rv3614c* restored some secretion of

ESAT-6 and CFP-10 (Figure 4, lane 22), this represents only partial complementation of

the secretion defect. Transcriptional analysis of this complementation strain revealed

mRNA levels of *Rv3615c* and *Rv3614c* that were lower than wildtype (Figure 5, C and

D), which could explain the partial complementation. Thus, we favor the hypothesis that

partial complementation resulted from aberrant transcription or mRNA stability of

Rv3615c or *Rv3614c* in the absence of a cis-copy of *Rv3616c*. While our

complementation analysis neither suggests nor excludes a potential role for *Rv3616c* in

Snm secretion, the complementation results demonstrate that both *Rv3615c* and *Rv3614c*

are required for Snm secretion. Here, we name these genes *snm9* and *snm10*,

respectively.

snm9* mutants have pathogenesis phenotypes similar to *snm4

Although the *snm9::Tn* mutant exhibited a secretion defect identical to other *snm*

mutants, it was still possible that the *snm9::Tn* mutant would exhibit pathogenesis

phenotypes different from other *snm* mutants, especially given the fact that *snm9* and *snm10* are encoded outside the RD1 locus. To assess growth in macrophages, we infected bone marrow-derived macrophages (BMDM) with wildtype (Erdman), *snm4::Tn, snm9::Tn,* and *snm9::Tn*-complemented strains and plated for CFU determination. While wildtype *M. tuberculosis* was able to grow in BMDM, the *snm9::Tn* mutant, like the *snm4::Tn* mutant, failed to grow over the course of a five day infection (Figure 6).

Given the inability of *snm* mutants to suppress proinflammatory responses of macrophages (Stanley *et al.*, 2003), we assessed IL-12 secretion, TNFα secretion, and nitric oxide production by macrophages after infection with an *snm9::Tn* mutant. Compared to wildtype *M. tuberculosis* (Erdman), the *snm9::Tn* mutant elicited high levels of IL-12 and TNFα secretion from macrophages (Figure 7A and B), indicating that these mutants are defective for suppressing the proinflammatory response. Additionally, macrophages infected with the *snm9::Tn* mutant strain produced higher levels of nitric oxide (Figure 7C), indicating that the macrophages are more responsive to mutant infection. The increased production of IL-12, TNFα , and nitric oxide during macrophage infection is also observed from infections with *snm4::Tn* mutant *M. tuberculosis* (Figure 7). Thus, the *snm9::Tn* mutant strain exhibited cellular pathogenesis defects to those observed in other *snm* secretion mutants.

Snm10 interacts physically with an Snm protein encoded at RD1

We hypothesized that Snm9 and Snm10 may physically interact with other Snm proteins as part of a larger Snm secretion complex. To test this hypothesis, we performed

a directed two-hybrid analysis in yeast to probe for physical interactions between Rv3616c, Snm9, Snm10, and other Snm proteins. Interestingly, Snm10 was found to interact with Snm7 (*Rv3882c*) (Figure 8, A and B). While it remains unclear if this physical interaction is required for Snm secretion, we hypothesize that these two Snm proteins may be structural or regulatory components of a larger Snm secretion complex that includes Snm1, Snm2, and Snm4. While no interactions were detected for the Rv3616c protein, 2-hybrid analysis revealed that Rv3615c interacts with itself (Figure 8, A and C), suggesting an ability to form multimers.

Discussion

We have shown that the *Rv3616c-Rv3614c* gene cluster encodes two genes required for Snm secretion in *M. tuberculosis*. These genes, which we have renamed *snm9* and *snm10*, are the first *snm* genes located outside the RD1 locus. The observation that both *snm9* and *snm10* have paralogues at the RD1 locus is not unique, as many RD1 locus genes have paralogues clustered throughout the *M. tuberculosis* genome. Indeed, genes encoding ESAT-6 and CFP-10, known as *esxA* and *esxB* respectively, are part of a homologous group known as the Esx family. There are 23 Esx family members encoded in the *M. tuberculosis* genome (H37Rv), 22 of which occur in tandem pairs, including *esxAB*. Of the 11 operons encoding Esx family pairs, five loci (including RD1) also contain paralogues of *snm* genes. This abundance of highly conserved gene clusters within the *M. tuberculosis* genome has been interpreted to represent extensive duplication of an ancestral locus during evolution. These observations, coupled with the evidence that *snm* genes at RD1 encode an alternative secretion pathway, have lead to the

hypothesis that each cluster of *snm* paralogues might constitute a discreet secretion pathway that is specific for the corresponding Esx family pair. Because *snm9* and *snm10* are located only 5 kilobases downstream of an Esx family pair, *esxV* and *esxW*, we believe that *snm9* and *snm10* may have originated from a duplication event of the ancestral locus, followed by a series of deletion and rearrangement events. Interestingly, although EsxW is encoded near *snm9* and *snm10*, the protein is secreted at wildtype levels in the *snm9::Tn* mutant (Figure 3). Thus, our evidence suggests that despite duplication of an ancestral RD1 locus several times during *M. tuberculosis* evolution, these homologous loci may not represent discrete, independent secretion pathways. Instead, we believe that some gene clusters with paralogues at RD1 may have retained their function in the secretion pathway encoded by the RD1 locus. This suggests that other non-RD1 genes in *M. tuberculosis* may be required for Snm secretion.

The *snm9::Tn* mutant exhibits pathogenesis defects observed in other *snm* mutants, including reduced virulence in mice, attenuated growth in macrophages, and an inability to suppress immuno-stimulatory cytokines such as IL-12. We hypothesize that Snm9 and Snm10 are integral components of the Snm secretion pathway which functions early during infection to combat the host response. Interestingly, transcriptional response studies have shown that *snm9* and *snm10* are coordinately upregulated in low iron (Rodriguez *et al.*, 2002) and low pH (Fisher *et al.*, 2002), conditions which may simulate the environment of a macrophage phagosome. The same data shows no significant changes in transcription of RD1 locus genes in response to these conditions. It is tempting to speculate that *M. tuberculosis* may respond to host infection by upregulating transcription of *snm9* and *snm10*, which in turn would activate Snm secretion.

Upregulation of the Snm pathway during infection might result in increased secretion of ESAT-6/CFP-10, or increased secretion of other, as yet undescribed, Snm substrates. Determination of Snm substrates secreted into host cells and how this process is regulated during infection will be fundamental to our understanding of *M. tuberculosis* pathogenesis.

Despite the requirement of *snm9* for Snm secretion, we were unable to detect interactions between Snm9 and other known Snm proteins in a yeast two-hybrid system. Thus, it is unclear if Snm9 functions in complex with other Snm proteins to mediate secretion. Interestingly, Snm9 contains an N-terminal motif that is conserved in several Esx family members, suggesting that Snm9 and its paralogue (*Rv3865*) may be distant relatives of the Esx family of proteins. Additionally, Snm9 is a small protein of 103 amino acids, similar to the small size of most Esx family proteins. Given these interesting similarities, we hypothesize that in addition to its requirement for Snm secretion, Snm9 might also be a substrate of the pathway. While we did not observe Snm9 among secreted proteins (Figure 8), we cannot rule out that Snm9 may be secreted at undetectable levels or under conditions not tested by our experiments. The generation of antibodies to Snm9 will greatly aid the determination of subcellular localization of this protein.

The physical interaction between Snm10 and Snm7 provides a direct link between an Snm protein encoded at the *Rv3616c-Rv3614c* gene cluster and another Snm protein encoded at the RD1 locus. As Snm7 is predicted to be a membrane protein with its large soluble domain located in the periplasm, it is likely that Snm10 and Snm7 proteins may be acting in complex as a periplasmic component of the Snm system. For both Snm10

and Snm7, determination of subcellular localization will be critical to understanding their role in Snm secretion. In addition to the Snm7-Snm10 interaction described here, an interaction between Snm1 and Snm2 has also been described (Stanley *et al.*, 2003). The identification of physical interactions between components suggests that Snm secretion requires one or more large protein complexes that function either as the core machinery or regulatory components of Snm secretion. Ultimately, deciphering the mechanism of Snm secretion will require identification of all required genes and an understanding of how they interact in the cell.

Materials and Methods

Strains and Plasmids. All strains and plasmids used in this study are listed in Table 1. *M. tuberculosis* (Erdman) cultures were grown as previously described (Cox *et al.*, 1999). Yeast media was purchased from Qbiogene (Carlsbad, CA).

Homology and Motif Analysis. Sequence data was retrieved from TIGR, and homologous loci were identified through BLAST searches. Motif analysis was performed using MEME/MAST (http://meme.sdsc.edu/meme/website/intro.html). Motifs were identified by training MEME on Rv3615c and Rv3865 peptide sequences. MAST analysis then identified other *M. tuberculosis* genes with matching motifs.

2D gels and Mass Spectrometry. Short-term culture filtrate (STCF) and cellular protein fractions were prepared as previously described (Stanley *et al.*, 2003). Briefly, *M. tuberculosis* (Erdman) strains were grown in Sauton's medium and culture supernatant

60

collected by filtration. Concentrated STCF was quantified using MicroBCA (Pierce) and processed using a 2D ReadyPrep Kit (BioRad) and resuspended in 8M Urea, 2% CHAPS, .2% ampholytes. 75µg of protein was hydrated onto 3.9-5.1 IPG strips (BioRad) overnight and then focused for 25,000 Vhrs. Strips were then embedded into 4-15% gradient SDS-PAGE gels to resolve the second dimension. Gels were stained using Coomassie Brilliant Blue.

For mass spectrometry, spots were excised, destained in 200mM ammonium bicarbonate with 40% acetonitrile, and subject to overnight digestion with trypsin (Sigma). The digest was concentrated on reversed-phase ZipTips (Millipore) and crystallized in CHCA matrix. MALDI-TOF was performed on a VoyagerPro workstation. Spot m/z profiles were analyzed by ProFound (http://prowl.rockefeller.edu/profound_bin/WebProFound.exe) to identify spots.

Complementation Strains and Western Blot. pMV306.Kan, which undergoes site-specific recombination at the mycobacterial *attB* locus, was used as the backbone for all complementation constructs. JMM1, JMM3, JMM4 were constructed by subcloning the *Rv3616c-Rv3614c* gene cluster, including the native promoter, from cosmid 2C11. The rest of the complementation strains were made by generating two primary amplicons with overlapping ends by PCR, then fusing these two primary amplicons into a third fusion amplicon by PCR (Tables 1, 2, and 3). Briefly, the following amplicons were cloned into pMV306.Kan to yield complementation strains: amplicon 2 (JMM43), amplicon 7 (JMM44), amplicon 8 (JMM45), amplicon 9 (JMM46), amplicon 10 (JMM47). These fusion amplicons were designed to maintain native intergenic sequences and preserve

start codon orientation. All complementation strains were sequenced and transformed into the *snm9::Tn* mutant background. Site-specific integration of the complementation constructs was confirmed by diagnostic PCR using the primers oAL44 and oAL46 (Table 2).

For complementation experiments, 2μg of STCF or cellular lysate protein fractions were loaded onto a 4-15% gradient SDS-PAGE gel. Proteins were transferred to nitrocellulose, which was blocked and blotted as previously described (Stanley *et al.*, 2003).

Macrophage Infection and ELISAs. All macrophages used in these experiments were derived from bone marrow cells of C57B6 mice that were differentiated for 6 days in L-cell supernatants. All infections were done using resting macrophages. *M. tuberculosis* (Erdman) strains were grown at 37ºC in 7H9 + Middlebrook oleic acid-albumin-dextrose-catalase (OADC) enrichment medium to an OD_{600} of 0.7 and innocula were prepared by washing and resuspending bacteria in PBS. Infections were performed at an MOI (multiplicity of infection) of 1 for colony forming unit (CFU) experiments and at MOI=10 for analysis of the macrophage proinflammatory response. For CFU analysis, inoculation was performed for 2 hours and monolayers were lysed and plated at 0, 24, 72, 120, and 168 hours post-infection. Normalization was achieved by dividing the CFUs of each time point by the post-innoculation CFU count. For IL-12, TNFα, and nitric oxide quantitation, macrophage monolayers were innoculated for four hours, followed by washing. Macrophage supernatants were collected and filtered at 24 hours post-infection. For IL-12 quantitation, P40 levels were determined by ELISA kit (BD Biosciences, Palo

Alto, CA). TNFα quantitation was performed using the mouse TNFα ELISA kit (BD Biosciences, Palo Alto, CA). Levels of nitric oxide in collected supernatants were quantified using the Griess reaction (Waters *et al.*, 2004).

Yeast Two-Hybrid Analysis. Directed two-hybrid fusion constructs were made by PCR amplification of target genes and cloning of the amplicon into bait (pEG202) or prey (pjsc401) constructs (Stanley *et al.*, 2003). All fusion constructs were made as full-length fusions, except membrane proteins, for which fusion constructs were made for each soluble domain (> 100 amino acids). Prey constructs were transformed into W303a and selected on CSM-Trp, while bait constructs were transformed into the EGY48 strain containing the LacZ reporter plasmid pSH18-34 and selected on CSM-His-Ura. Yeast transformants were confirmed by diagnostic PCR. Bait and prey yeast strains were mated, and diploids were selected on CSM-Ura-His-Trp. Equivalent amounts of diploid cells were then plated onto CSM-Ura-His-Trp plates containing galactose and XGal (5-bromo-4-chloro-3-indolyl-b-D-galactoside).

Quantitative beta-galactosidase assays were performed as previously described (Guarente et al., 1981). Briefly, diploid strains were cultured to mid-log phase in induction media, lysing yeast cells in SDS/chloroform, and adding o-nitrophenyl-beta-D-galactopyranoside (ONPG, 2mg/mL) to lysates. Reactions were quenched by addition of sodium carbonate, and OD420 was read. Arbitrary units of beta-galactosidase activity were calculated as: activity $= (1000 \text{ x } OD_{420}) / (\text{reaction time x vol. cells x } OD_{600})$.

63

Figure 1. An *Rv3615c* mutant was identified by signature-tagged mutagenesis.

Signature-tagged mutagenesis, mutant isolation, tag amplification, and insertion

determination were performed exactly as described (Cox *et al.*, 1999) **(A)** Singature

DNA tags from mutant mycobacteria harvested from innoculum pools or the lungs of two

mice (3 weeks post-infection) were amplified, radiolabelled, and hybridized to array

filters. The blots demonstrate that the DNA tag of the *Rv3615c::Tn* strain is

underrepresented in infected mice, compared to a control strain which was not

underrepresented in mice. **(B)** To quantify tag representation, pixel intensities of each

spot on each array were measured using ImageJ software (http://rsbweb.nih.gov/ij/). To

normalize tag representation for each array, the ratio of the pixel intensity of each spot to

the sum of all spot pixel intensities on the array was determined. Then, this ratio was

normalized to the innoculum pool to quantify tag representation in the mice compared to

tag representation in the innoculum. The degree of attenuation of the *Rv3615c::Tn*

mutant reported here is similar to that observed by Sassetti et al. for a different *Rv3615c*
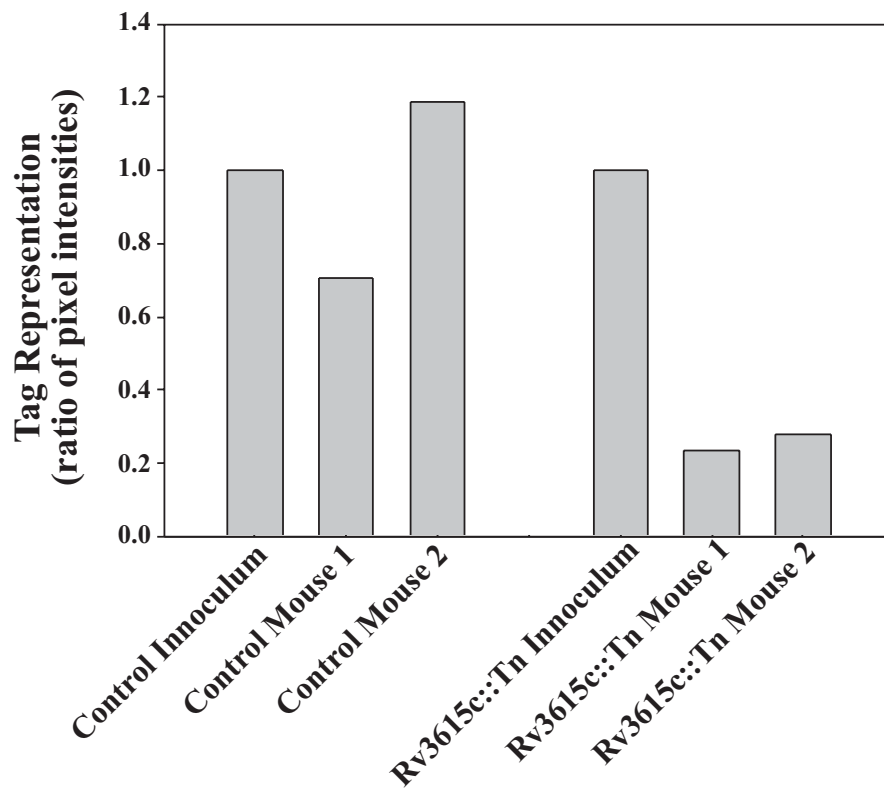
mutant (Sassetti et al., 2003).

Fig. 1

A
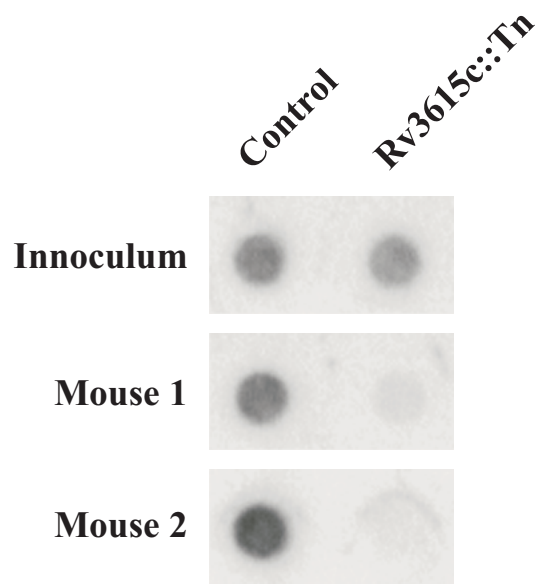
B

Figure 2. Sequence analysis of *the Rv3616c-Rv3614c* gene cluster reveals homology to genes at the RD1 locus.

(A) The *Rv3616c-Rv3614c* gene cluster conserved in *M. bovis* and *M. leprae*. Percentages indicate percent identity of amino acid sequence. **(B)** *Rv3616c*, *Rv3615c* and *Rv3614c* have paralogs within the *M. tuberculosis* genome just upstream of the RD1 locus. Percentages indicate percent identity of amino acid sequence. **(C)** MAST/MEME analysis revealed an N-terminal motif of 20 amino acids which is conserved in several ESAT-6 family members. E-values indicate the expected number of sequences in a random database of the same size matching the motif as well as the sequence. Motif identities are as follows:
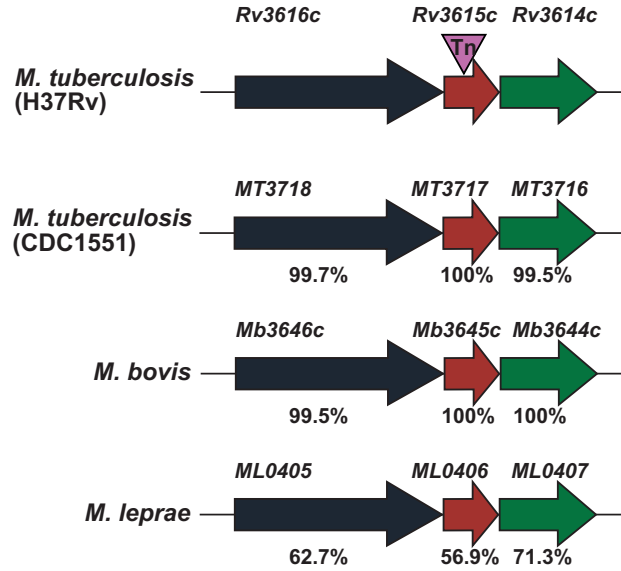
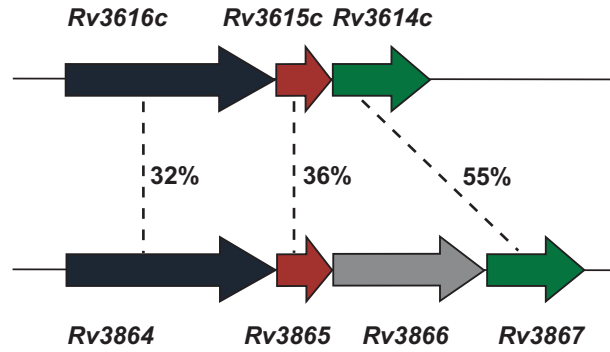Motif #1: "MTERLMVDPHRLKVLAGHH" Motif #2: "THGPYCSKFNDTLNEY" Motif #3: "DEAWRK" Motif #4: "ISEAGW" Motif #5: "IHNMLD" Motif #6: "NNYEQKEQ" Motif #7: "IDKIF" **(D)** Sequence alignment of Rv3615c with esxW reveals 50% of the amino acids in this motif are identical (boxed, dark shade) or strongly similar (boxed, light shade).
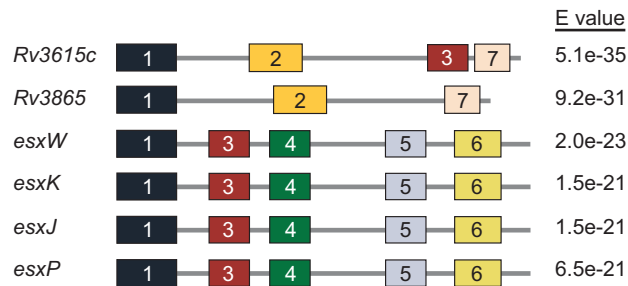
Fig. 2
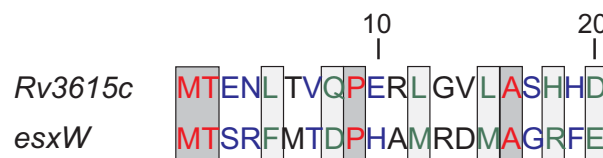
A

B

C

D

Figure 3. The _Rv3615c::Tn_ mutant fails to secrete ESAT-6 and CFP-10.

Short-term culture filtrate (STCF) was collected from wildtype (Erdman) and mutant

cultures and 75ug or protein was analyzed by two-dimensional electrophoresis. For the

first dimension, protein samples were hydrated onto 3.9-5.1 IPG strips and focused. For

the second dimension, strips were run on SDS-PAGE gels. Proteins were stained with

Coomassie Brilliant Blue. Spots were excised and identified by MALDI-TOF mass

spectrometry analysis. Although spots co-migrated with spots 1, 3, 4 and 6, no ESAT-6

or CFP-10 protein was detected in any of the co-migrating spots. MT2420 is a member

of the Esx family of proteins that has been deleted from _M. tuberculosis_ H37Rv genome,

but is present in CDC1551 and Erdman genomes.

Fig. 3

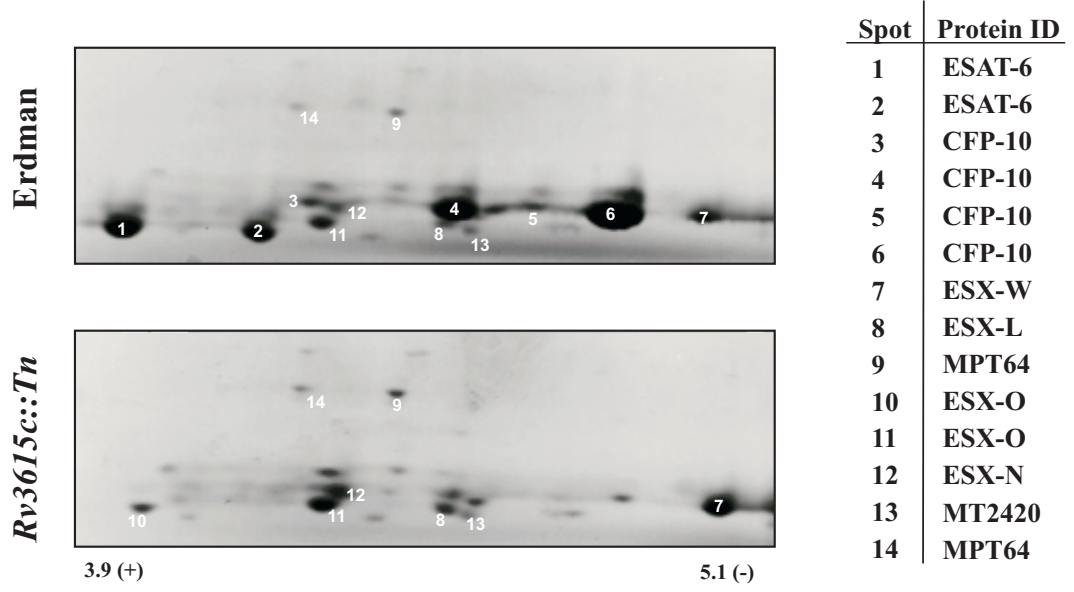| Spot	Protein ID
1	ESAT-6
2	ESAT-6
3	CFP-10
4	CFP-10
5	CFP-10
6	CFP-10
7	ESX-W
8	ESX-L
9	MPT64
10	ESX-O
11	ESX-O
12	ESX-N
13	MT2420
14	MPT64

3.9 (+)　　　　　　　　　　5.1 (-)

Figure 4. Both *Rv3615c* and *Rv3614c* are required for Snm secretion.

The complementation constructs diagrammed were inserted into a *Rv3615c::Tn*

background in single copy by site-specific integration at the *attB*. ESAT-6, CFP-10, and

GroEL (GroEL2) western blots were performed on STCF (S) and cellular (P) fractions

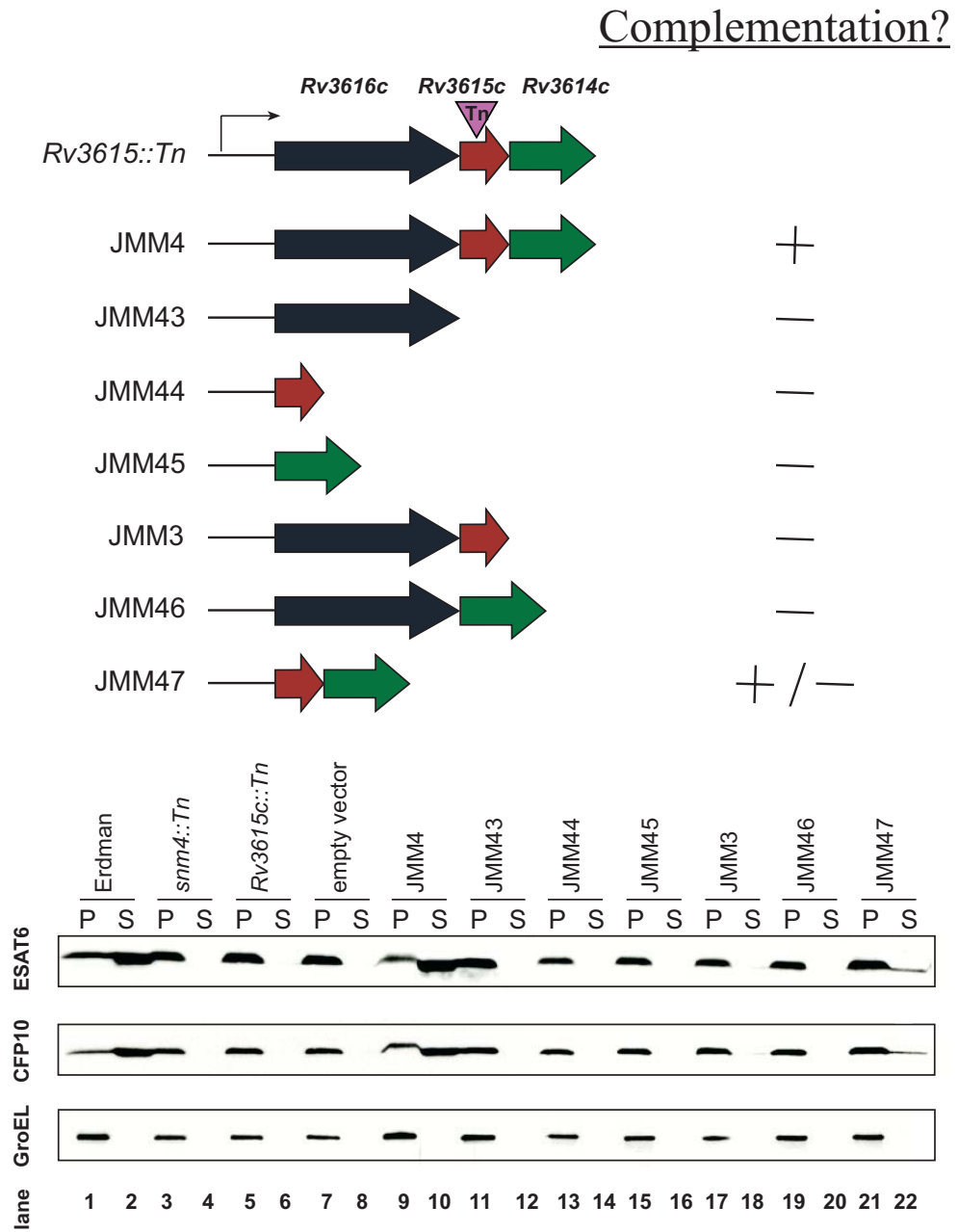collected from each strain.

Fig. 4

Figure 5. Transcription of *Rv3616c* is not affected in the *snm9::Tn* mutant strain.

DNA microarray analysis was used to comprehensively measure relative levels of mRNA

transcripts during growth of *snm9::Tn* mutant and complemented *M. tuberculosis* strains.

RNA from cultures grown in Sauton's medium was collected as previously described

(Rodriguez *et al.*, 2002). Briefly, pellets were bead-beat in TRIzol reagent (Invitrogen),

chloroform extracted, and aqueous fractions precipitated overnight in isopropanol. RNA

samples were then resuspended in water, DNAse treated, purified by Qiagen RNeasy kit

(Qiagen), and quantified by OD260. Integrity of RNA was assessed by agarose gel

electrophoresis. 5μg of RNA from each sample was random-primed with nonamers and

reverse transcribed in the presence of amino-allyl dUTP using StrataScript reverse

transcriptase (Stratagene). Residual RNA was then hydrolyzed by addition of 0.2N

NaOH / 0.1M EDTA and incubation at 65º for 15 minutes, followed by addition of 0.2N

HCl to neutralize. cDNA samples were then purified by Zymo binding columns (Zymo).

Erdman cDNA samples were then conjugated to Cy3, while cDNA samples from

snm9::Tn or complemented (JMM4) strains were conjugated to Cy5. Dye-conjugated

cDNA samples were mixed and hybridized on microarray slides containing

oligonucleotide spots representing every gene in *M. tuberculosis* (Qiagen). After 3 days

of hybridization at 65º Celsius, arrays were washed and scanned using a GenePix 3000B

scanner (Axon Instruments). Data analysis was performed in GenePix Pro 4.1 and

Cluster 3.0. RNA samples were generated and analyzed from triplicate experiments. **(A)**

Ratios (Cy5 / Cy3) of median pixel intensity are shown for selected genes. **(B)** These

ratios were then converted to color based on a continuous linear scale. Green spots

represent decreased mRNA levels relative to wildtype (Erdman), while red spots

represent increased mRNA levels. *Rv3613c* and *Rv3612c* transcription is attenuated in the mutant, indicating the polar affect of the transposon insertion extends beyond *Rv3614c*. Complementation analysis indicates that these genes are not required for Snm secretion. From three independent experiments, no other genes exhibited significant transcriptional differences compared to wildtype levels. **(C and D)** Similar microarray analysis was performed to profile transcription in complementation backgrounds, demonstrating that wildtype transcription of either *Rv3615c* (JMM3) or *Rv3614c* (JMM46) is not sufficient to complement the Snm secretion defect. The partial complementation observed in JMM47 is likely due to low levels of *Rv3615c* and *Rv3614c* transcripts.

Fig. 5

A

Erdman vs. *snm9::Tn*			Erdman vs. *snm9::Tn* comp.			
#1	#2	#3	#1	#2	#3	
1.062	1.336	0.758	2.44	3.261	2.191	*Rv3616c*
0.055	0.036	0.058	1.377	1.847	1.321	*Rv3615c*
0.035	0.046	0.074	1.394	1.627	1.283	*Rv3614c*
0.135	0.151	0.338	0.148	0.179	0.469	*Rv3613c*
0.314	0.294	0.623	0.405	0.327	0.718	*Rv3612c*

Experiment: is noted before the #1 #2 #3 columns.

B
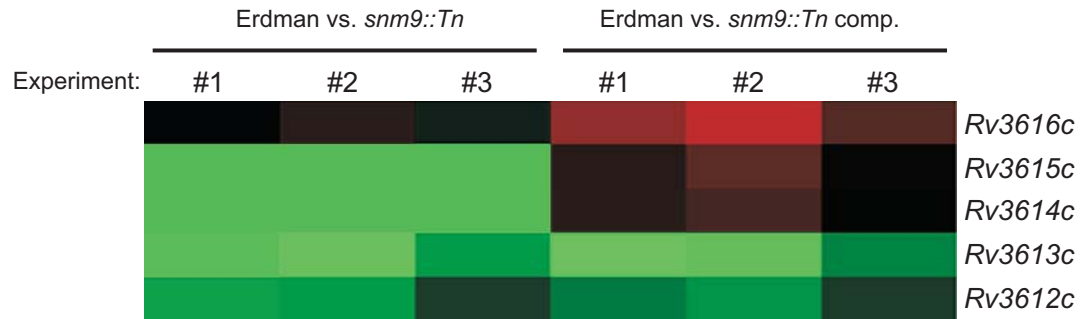
C

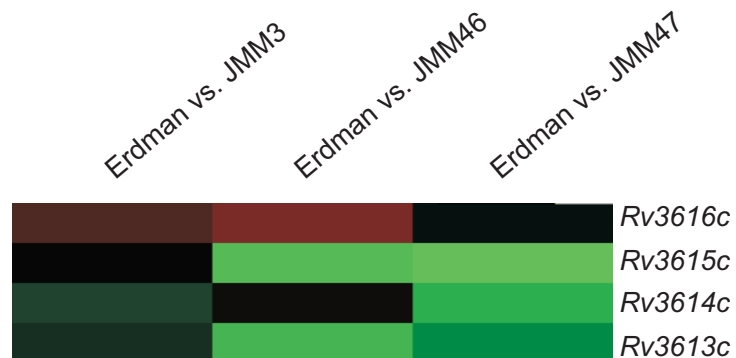| Erdman vs. JMM3	Erdman vs. JMM46	Erdman vs. JMM47	
1.711	2.340	.769	*Rv3616c*
1.056	.080	.173	*Rv3615c*
.530	1.288	.244	*Rv3614c*
.614	.246	.349	*Rv3613c*

D

Figure 6. The *snm9::Tn* mutant strain fails to grow in bone marrow-derived macrophages.

(A) Macrophages were infected at a mulitiplicity of infection of 1. CFUs determined by lysing infected monolayers and plating lysates at indicated time points. **(B)** Data was normalized for three experiments. *snm9::Tn* complementation strain is JMM4.

Fig. 6
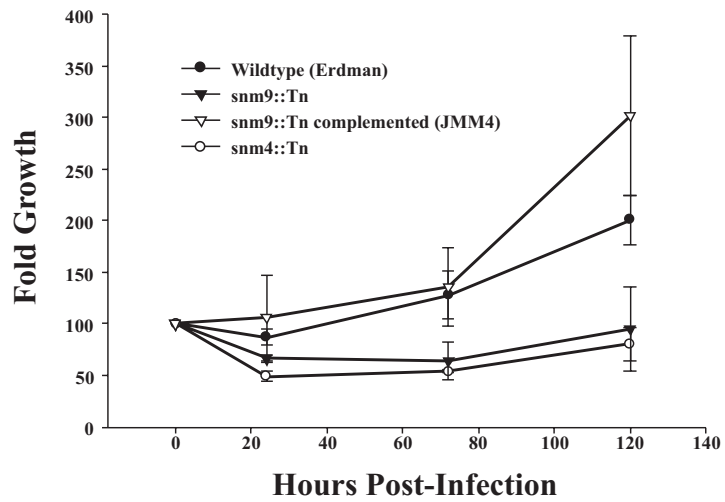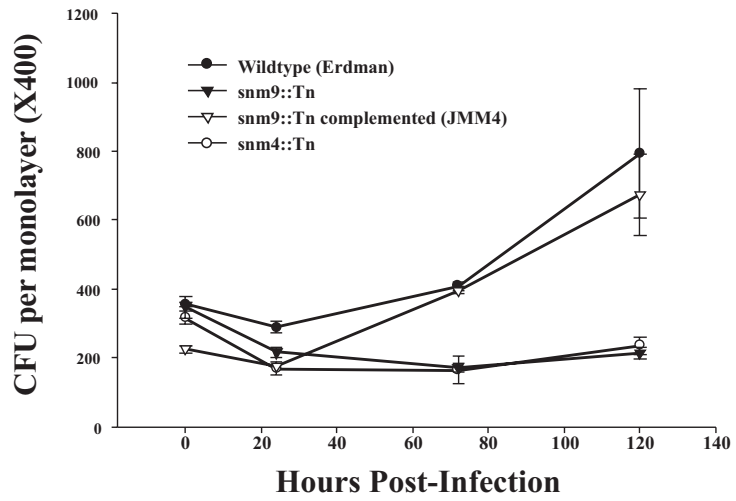
Figure 7. The *snm9::Tn* mutant is defective for suppressing the macrophage proinflammatory response.

Bone marrow-derived macrophages were infected and culture supernatants collected at 24 hours post-infection. **(A)** Concentration of IL-12 (p40 subunit) was determined by ELISA. The graph shown is a representative example of five experiments. **(B)** Concentration of TNFα was determined by ELISA. The graph shown is an average of two independent experiments. **(C)** Concentration of nitric oxide was determined by the Griese reaction. The graph shown is an average of two independent experiments. *snm9::Tn* complementation strain is JMM4.

Fig. 7

A
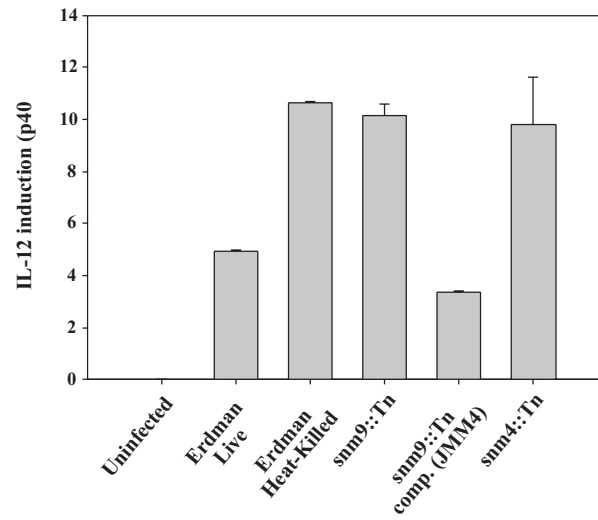
B
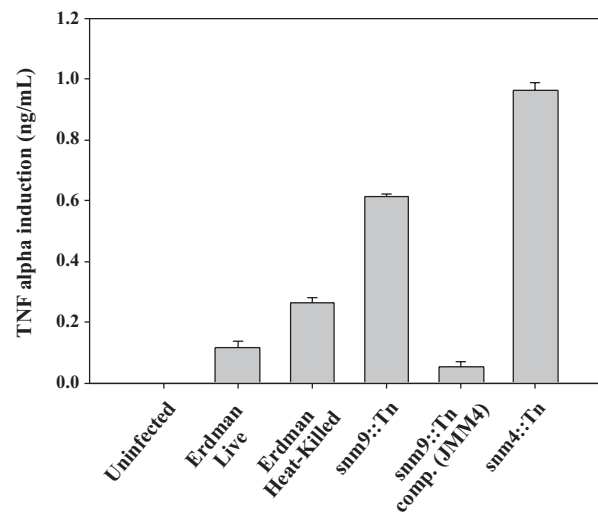
C
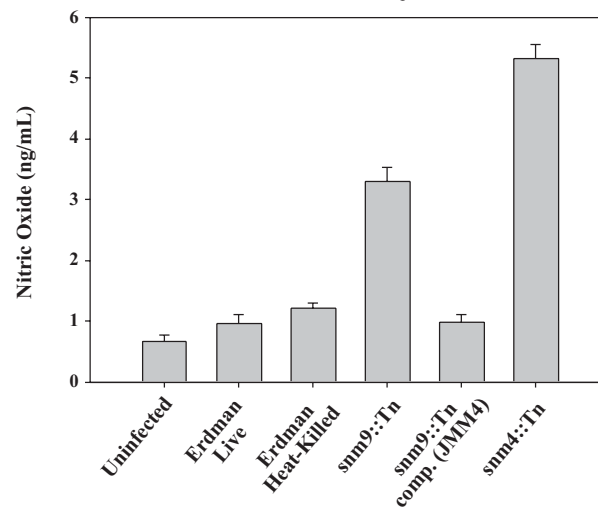
Figure 8.   Snm10 protein interacts with Snm7.

(A) Diploid yeast strains pairing prey fusion constructs (empty vector, Rv3616c, Snm9 (Rv3615c), Snm10 (Rv3614c)) with bait fusion constructs (vector, Rv3616c, Snm9 (Rv3615c), Rv3864 (soluble domain 1 (SD1) and 2 (SD2)), Rv3865, Snm5 (Rv3866), ESAT6, CFP10, Snm2 (Rv3871), Snm1 (Rv3870, soluble domain 1 (SD1) and 2 (SD2)), Snm6 (Rv3869), Snm7 (Rv3882c), MycP1 (Rv3883c)) were grown on diploid-selective media and replica plated to Xgal indicator plates. Snm10 (Rv3614c) and Rv3867 bait fusion constructs were ommited from this analysis due to strong autoactivation. Quantitative beta-galactosidase assays were performed on observed interactions of Rv3614c with Rv3882c **(B)** and Rv3615 with itself **(C)**.

Fig. 8

A
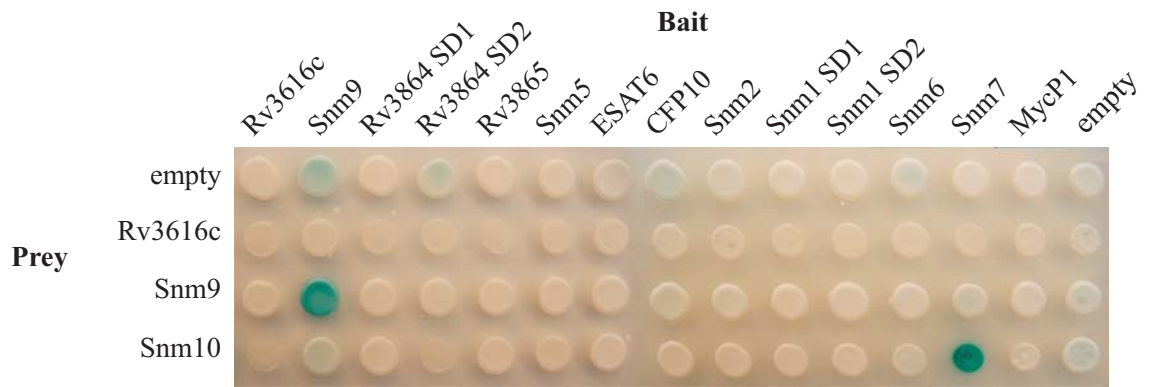
B
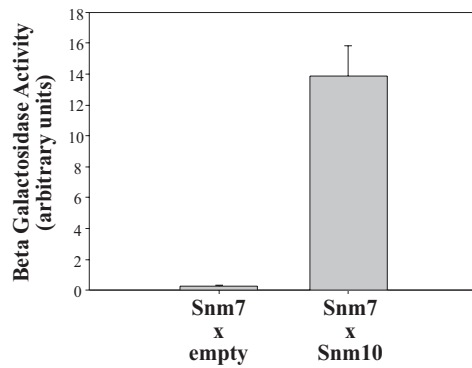
C

TABLE 1. Strains and plasmids used in this study

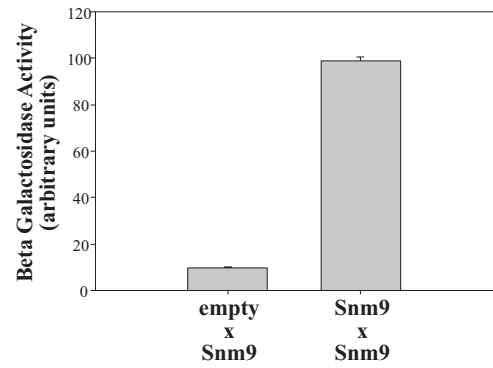| Strain/plasmid	Gentoype/description	Source
	M. tuberculosis	
Erdman	Wild-type	W. R. Jacobs Jr.
snm9::Tn (*Rv3615c::Tn*)	Erdman *snm9::Tn5370*, HygR	This study
snm4::Tn	Erdman *snm4::Tn5370*, HygR	Stanley et. al
JMM1	*snm9::Tn* + empty vector, HygR, KanR	This study
JMM4	*snm9::Tn* + *Rv3616c-Rv3614c*, HygR, KanR	This study
JMM43	*snm9::Tn* + *Rv3616c*, HygR, KanR	This study
JMM44	*snm9::Tn* + *Rv3615c*, HygR, KanR	This study
JMM45	*snm9::Tn* + *Rv3614c*, HygR, KanR	This study
JMM3	*snm9::Tn* + *Rv3616c-Rv3615c*, HygR, KanR	This study
JMM46	*snm9::Tn* + *Rv3616c+Rv3614c*, HygR, KanR	This study
JMM47	*snm9::Tn* + *Rv3615c-Rv3614c*, HygR, KanR	This study
	S. cerevisiae	
W303-1a	MATa; ura3-1; leu2-3, -112; his3-11, -15; trp1-1; ade2-1; can1-100	P. Walter (UCSF)
EGY48	MATα; trp1, his3, ura3, lexAop-LEU2	R. Brent
	Plasmids	
pEG202	LexA bait plasmid, HIS3, 2μm	Stanley et. al
pJSC401	pJG4-5 + ClaI linker in MCS	Stanley et. al
pMV306.Kan	*int*, *oriE*, KanR,	W. R. Jacobs Jr.
pJAM35	pJSC401 + *Rv3616c*	This study
pJSC557	pJSC401 + *Rv3615c*	This study
pJAM37	pJSC401 + *Rv3614c*	This study
pJAM36	pEG202 + *Rv3616c*	This study
pJAM556	pEG202 + *Rv3615c*	This study
pJAM38	pEG202 + *Rv3614c*	This study
pJAM40	pEG202 + *Rv3864* SD1	This study
pJAM48	pEG202 + *Rv3864* SD2	This study
pJSC559	pEG202 + *Rv3865*	This study
pJAM42	pEG202 + *Rv3866*	This study
pJAM44	pEG202 + *Rv3867*	This study
pWH1	pEG202 + *esxA (esat6)*	Stanley et. al
pWH3	pEG202 + *esxB (cfp10)*	Stanley et. al
pJSC540	pEG202 + *snm2*	Stanley et. al
pJAM46	pEG202 + *snm1* SD1	This study
pJSC538	pEG202 + *snm1* SD2	Stanley et. al
pJAM52	pEG202 + *Rv3869*	This study
pJAM54	pEG202 + *Rv3882c*	This study
pJAM56	pEG202 + *Rv3883c (mycP1)*	This study

TABLE 2. Oligonucleotides

Oligonucleotide	Sequence
oJAM5	CTTCGCCGATCTTGCC
oJAM6	GCCTGCCGCCTATCTCAAC
oJAM7	TGATCGTGTCCCTTCCGTTTA
oJAM8	CCGTTGAGATAGGCGGCAGGCATGACGGAAAACTTGACC
oJAM9	CGTCCCTTCGGAATTCAT
oJAM10	CCGTTGAGATAGGCGGCAGGCGTGGACTTGCCCGGAAAT
oJAM11	TAAACGGAAGGGACACGATCAGTGGACTTGCCCGGAAAT
oJAM12	TTCCACCCGTGCTCTATTAATG
oAL44	GTCGCACAAGAGTTGCAGAC
oAL46	GTACAGTCGCGCTCGACTAA

TABLE 3. Primary Amplicons

Amplicon	Primers	Spanning sequence	Fusion overhang to:
1	ojam5, ojam6	Native promoter	None
2	ojam5, ojam7	Native promoter thru *Rv3616c*	None
3	ojam8, ojam9	*Rv3615c*	ojam6
4	ojam8, ojam12	*Rv3615c + Rv3614c*	ojam6
5	ojam10, ojam12	*Rv3614c*	ojam6
6	ojam11, ojam12	*Rv3614c*	ojam7

TABLE 4. Fusion Amplicons

Amplicon	Template Mix	Primers
7	Amplicon 1 + 3	ojam5, ojam9
8	Amplicon 1 + 5	ojam5, ojam12
9	Amplicon 2 + 6	ojam5, ojam12
10	Amplicon 1 + 4	ojam5, ojam12

Chapter 4

An Esx-1 effector protein of *Mycobacterium tuberculosis* forms a high molecular weight complex with a sphingomyelinase activity

Abstract

Many pathogenic bacteria use specialized secretion systems to deliver virulence factors into the host where they interact with target molecules and affect the host response. *Mycobacterium tuberculosis*, for instance, requires a specialized secretion system known as the Esx-1 pathway for full virulence, but very little is known about the substrates of this pathway and their potential for interactions with the host. Here, we describe a novel substrate of the Esx-1 secretion pathway which we call Esx-1 substrate protein C, or EspC. Although the protein itself is only ~10 kDa, secreted EspC was sized between ~130-270 kDa using gel filtration chromatography. While some of this is the result of homomultimerization, we provide evidence that at least some of this higher order complex is the result of interactions between different protein species. Immunoprecipitation of secreted EspC revealed multiple copurifying species including substrates of SecYEG, TAT, and Esx secretion pathways. Bioinformatic analysis of one copurifying species, Rv0888, suggested that the protein may be a neutral sphingomyelinase. We show that a sphingomyelinase activity copurifies with EspC and that this activity is independent of any phospholipase activity. We hypothesize that once secreted, EspC interacts with substrates of multiple secretion systems, including SecYEG, TAT, and multiple Esx pathways, to form a large complex that is important for targeting a sphingomyelinase activity to host membranes. Such a sphingomyelinase activity secreted and targeted in the host could have multiple implications for interfering with the host response.

84

<u>Introduction</u>

   Bacterial pathogens often use specialized secretion systems to deliver important virulence factors into host cells (Lee et al., 2001). Many such virulence factors have been shown to interfere with various host functions, including G protein signaling (Alto et al., 2006), MAP kinase signaling (Arbibe et al., 2007; Kramer et al., 2007; Li et al., 2007), and membrane trafficking (Nagai et al., 2002; Shohdy et al., 2005). While mechanisms of specialized secretion and virulence functions of effector proteins are well described for Gram negative pathogens, relatively little is known about specialized secretion in acid-fast and Gram positive pathogens. *Mycobacterium tuberculosis*, the acid-fast bacillus responsible for the disease tuberculosis, is known to utilize at least four secretion systems: the SecYEG pathway, the twin arginine translocation (TAT) pathway, the SecA2 pathway, and the Esx pathway. The SecYEG and TAT pathways are both essential for *in vitro* growth (Sassetti et al., 2003; Saint-Joanis et al., 2006) and thought to secrete largely housekeeping proteins, although substrates of both pathways have been implicated in pathogenesis (Berthet et al., 1998; Saint-Joanis et al., 2006). The SecA2 and Esx secretion pathways are both non-essential for growth *in vitro* but required for full virulence in mice (Braunstein et al., 2003; Hsu et al., 2003; Stanley et al., 2003; Guinn et al., 2004). We are interested in the Esx secretion pathway because it is a crucial virulence determinant in *M. tuberculosis* yet it is conserved in many acid-fast and Gram positive pathogens (Gey Van Pittius et al., 2001; Burts et al., 2005; Desvaux et al., 2005).

   In *M. tuberculosis*, the two most abundantly secreted proteins in culture are ESAT-6 and CFP-10, two small proteins that lack SecYEG signal sequences and interact to form a dimer (Renshaw et al., 2002; Lightbody et al., 2004; Renshaw et al., 2005).

ESAT-6 and CFP-10, encoded by *esxA* and *esxB* genes, respectively, are part of a large family of 23 (strain H37Rv) or 25 (strain CDC1551) genes, known as the Esx family (Pallen, 2002). These Esx family members are small proteins (~100 amino acids), typically encoded in pairs, many of which are known to be secreted despite lacking SecYEG signal sequences. In the case of ESAT-6 and CFP-10, secretion is dependent on several genes encoded at the same genetic locus (*Rv3870, Rv3871, Rv3876, Rv3877*) (Hsu et al., 2003; Stanley et al., 2003; Guinn et al., 2004), called the Esx-1 locus (Fig. 1A). In the case of 6 other Esx family operons, the surrounding genes are conserved, encoding proteins similar to those observed at the Esx-1 locus (Gey Van Pittius et al., 2001). Thus, there are 7 conserved Esx loci. While only Esx-1 and Esx-5 (Abdallah et al., 2006) have been shown to encode specialized secretion systems, it is tempting to speculate that each locus could encode related yet distinct secretion pathways.

Several recent studies focusing on Esx-1 secretion have begun to elucidate potential roles during host infection. Mutants defective for Esx-1 secretion exhibit a range of diverse phenotypes, including defects in immune modulation, *in vivo* growth, phagosome trafficking, and growth in macrophages (Stanley et al., 2003; Guinn et al., 2004; Hsu et al., 2003; Tan et al., 2006). Despite the plethora of virulence phenotypes exhibited in Esx-1 mutants, a direct role for ESAT-6 / CFP-10 dimers in the molecular pathogenesis of mycobacteria has not been demonstrated. Furthermore, two additional proteins, EspA (Rv3616c) and PE35, were recently shown to be secreted in an Esx-1 dependent manner, and secretion of EspA was mutually dependent upon secretion of ESAT-6 / CFP-10 dimers (Fortune et al., 2005). Thus, the pleiotropy of Esx-1 mutants

coupled with the mutually-dependent secretion of known effectors has made it difficult to attribute specific pathogenic functions to individual effectors of the pathway.

Previously, we showed that *Rv3615c* is required for Esx-1 secretion (MacGurn et al., 2005) (Figure 1A). Here, we report that *Rv3615c* encodes a protein secreted in an Esx-1 dependent manner, and we rename the protein <u>E</u>sx-1 <u>s</u>ubstrate <u>p</u>rotein <u>C</u>, or EspC. We observed that secreted EspC exists in a high molecular weight complex and copurifies with various Esx family proteins as well as proteins secreted by the SecYEG and TAT pathways. One protein that copurified with EspC, Rv0888, was predicted to be a secreted neutral sphingomyelinase. We showed that a sphingomyelinase activity specifically copurifies with EspC, and that a mutant attenuated for *Rv0888* transcription exhibits decreased sphingomyelinase activity. We hypothesize that a large complex of secreted proteins including EspC, EspA, and multiple Esx proteins may be involved in targeting a bacterial sphingomyelinase activity in the host. This activity could modify the host response to infection, and we consider the possible signaling pathways that such a bacterial sphingomyelinase might affect.

Results

EspC is secreted in an ESX-1-dependent manner

Previous motif analysis of the Rv3615c amino acid sequence revealed similarity to several Esx family proteins which are known to be secreted (MacGurn et al., 2005). We therefore hypothesized that Rv3615c itself might be secreted, despite the lack of a traditional signal sequence for secretion. To localize the protein, we used an antibody generated against Rv3615c to probe cell lysates and short-term culture filtrates (STCFs).

Rv3615c was detected by immunoblot of *M. tuberculosis* cell lysates but only when blotted against very large amounts (~100 μg) of protein (Fig. 1B). In contrast, the antibody detected a size-appropriate (~10 kDa) band as well as higher molecular weight (MW) species (~15-20 kDa) in modest amounts of STCF (~15 μg). All of the bands detected by immunoblot were absent in the *Rv3615c::Tn* mutant cell fractions and restored by addition of a wildtype copy of *Rv3615c* (Fig. 1B). To confirm that all of the species detected by the antibody correspond to Rv3615c, we complemented the *Rv3615c::Tn* mutant with an N terminal 3X FLAG-tagged version of the protein. Blotting with antibodies to FLAG revealed that the FLAG-tagged Rv3615c was secreted at approximately wildtype levels and exhibited the same banding pattern as untagged Rv3615c (Fig. 1C).

The presence of higher-than-expected MW species of Rv3615c in *M. tuberculosis* STCF suggested some sort of post-translational modification associated with secretion, but tandem mass spectrometry analysis of the protein identified only a few modified peptides (Table 2) and could not explain the observed heterogeneity. We hypothesized that Rv3615c could be subject to complex glycosylation. To test this, we subjected STCFs to a chemical deglycosylation procedure and found that this treatment resulted in loss of the high MW species (Fig. 1D). In an attempt to conclusively demonstrate that the nature of the modification is glycosylation, we subjected Rv3615c to treatment with a panel of enzymatic deglycosylases but were unable to identify any susceptibilities to common enzymes that hydrolyze N-linked or O-linked glycans (data not shown). Therefore, while we cannot definitively attribute the high MW species to covalent

addition of glycans, we conclude that Rv3615c undergoes significant post-translational modification in a manner that is associated with secretion.

Since it lacks a traditional signal sequence for SecYEG secretion, we hypothesized that Rv3615c could be a substrate for the Esx-1 secretion system. To test this hypothesis, we analyzed Rv3615c secretion in several Esx-1 secretion mutants. Although Rv3615c was detected in the cell lysates of every strain examined, we failed to detect secreted Rv3615c in any of the mutants known to be defective for Esx-1 secretion (Fig. 1E), indicating that Rv3615c is secreted in an Esx-1-dependent manner. To confirm this observation, we looked for Rv3615c secretion in *Mycobacterium bovis* BCG which lacks the ESX-1 locus but still encodes the *Rv3616c-Rv3614c* gene cluster. While Rv3615c was not detected in the cell lysate or STCF of wildtype BCG, ectopic expression of the ESX-1 locus restored secretion of Rv3615c in BCG (Fig. 1F). Thus, we conclude that Rv3615c is a substrate of the Esx-1 secretion pathway and we have renamed the protein Esx-1 secreted protein C, or EspC.

To visualize Rv3615c secretion, we performed immunofluorescence staining of FLAG-tagged Rv3615c in fixed *M. tuberculosis* under non-permeablizing conditions. Interestingly, Rv3615c does not seem to be expressed evenly across the population of cells, and instead seems to be highly expressed in some bacilli (Fig. 2A). Futhermore, immunoelectron microscopy analysis revealed that Rv3615c is not evenly distributed across the cell perimeter, and instead seems to exist in concentrated patches along an individual bacillus (Fig. 2B). These observations suggest that Rv3615c secretion is not uniform in a population of mycobacteria and that its secretion appears localized to specific foci at the cell perimeter.

Secreted EspC exists in a high molecular weight complex

Previously, we showed that EspC interacted with itself in a yeast two-hybrid system (MacGurn et al., 2005), suggesting the potential for multimerization. To determine if native EspC forms higher order structures, we performed size exclusion chromatography on whole STCF and analyzed which fractions contained EspC. Our sizing analysis of native STCF revealed that most total secreted protein (A_{280}) appeared between 4 and 40 kDa (Fig. 3A). ESAT-6 and CFP-10, the two most abundant proteins in the STCF, eluted from the column with apparent molecular weights at or below the predicted dimer size of ~20 kDa, while the SecYEG substrate Mpt32 appeared at a MW of ~45-50 kDa, consistent with the size of this protein on an SDS-PAGE immunoblot (Fig. 3A). In contrast, 3X FLAG-tagged EspC, which has a predicted MW of ~13 kDa, appeared mostly between 130 and 270 kDa (Fig. 3A). Thus, native EspC seems to exist in a higher order structure far larger than its predicted molecular weight.

Given its ability to interact with itself in a yeast 2-hybrid system, we hypothesized that this higher order structure might exist exclusively of EspC proteins. To test this, we compared the estimated size of native EspC to recombinant EspC using size exclusion chromatography. The majority of recombinant EspC appeared between 40-85 kDa, far smaller than the native EspC (Fig. 3B). Although recombinant EspC does not contain the post-translational modifications observed in the native, such slight increases in native MW are not enough to account for the observed difference on the sizing column. While this result suggests that EspC may form homomultimeric structures up to ~80-100 kDa,

we hypothesized that the higher observed MW of native EspC may be attributable to interactions with other proteins in the STCF.

Secreted EspC copurifies with proteins secreted by multiple pathways

To determine if native EspC interacts with other secreted proteins, we immunoprecipitated 3X FLAG-tagged EspC from STCF and analyzed the IP by SDS-PAGE followed by silver staining. This approach revealed several bands that copurified with EspC from STCF, none of which copurified in the absence of the 3X FLAG epitope (Fig. 4A). Mass spectrometry analysis of these copurifying species identified an assortment of known secreted proteins including Esx proteins and Esx-associated proteins as well as proteins with strong SecYEG and TAT signal sequences (Fig. 4B, Table 2). Similar mass spectrometry analysis of 3X FLAG-tagged Mpt32 or 3X FLAG-tagged Mpt64, two canonical SecYEG substrates whose secretion has been described (Andersen et al., 1991; Oettinger et al., 1994) (Laqueyrerie et al., 1995) (Dobos et al., 1995), did not reveal any copurifying species (data not shown). It is possible that the species we observed copurifying with EspC were the result of non-specific interactions or a general "stickiness" of the protein. However, it is noteworthy that the two most abundant proteins in *M. tuberculosis* STCF, ESAT-6 and CFP-10, did not copurify with EspC, suggesting that the copurifying species are not the result of non-specific interactions. Furthermore, when we performed mass spectrometry analysis on EspC immunopurified from high molecular weight gel filtration fractions, we observed many of the same copurifying species (Figure 4B), suggesting a very stable complex. Thus, our identification of multiple secreted proteins that copurify specifically with EspC in the

STCF strongly suggests that this protein exists in a large complex resulting from EspC homomultimerization and interactions with several other secreted proteins.

Of the proteins that copurified with EspC, seven were Esx family members and one, EspA, is a known substrate of the Esx-1 secretion system that is encoded directly upstream of EspC. Of the three copurifying proteins that are part of the PE/PPE family of proteins, only one (PPE18) is encoded at an Esx locus. It is interesting that so many of the proteins that copurified with secreted EspC were Esx-related. However, while EspC is Esx-1 dependent, many of the Esx family proteins that copurified with EspC are secreted independently of Esx-1 (MacGurn et al., 2005). Furthermore, 4 of the copurifying species are predicted to have signal sequences for either the SecYEG or TAT secretion pathways (Fig. 4B, Table 2). Thus, our results suggest that substrates of multiple pathways including Esx, SecYEG, and TAT secretion systems may form interactions once they are secreted by their respective pathways.

We were intrigued by the possibility that substrates of distinct export pathways might cooperate following secretion. While none of the SecYEG or TAT substrates that copurified with EspC have any defined functions, analysis of primary sequence and secondary structure predictions led to putative functions for Rv2525c, which is related to a family of transglycosidase enzymes, and Rv0888, which is part of a diverse family of Mg^{2+}-dependent phosphodiesterases (Table 2) (Dlakic, 2000).

The EspC complex exhibits sphingomyelinase activity

We decided to focus on the copurifying protein Rv0888. Bioinformatic analysis of the primary structure of Rv0888 revealed a striking similarity to DNase I, but we were

unable to detect any DNase activity copurifying with EspC (data not shown). However, when we analyzed the predicted secondary structure of Rv0888, we found that the Rv0888 protein is most closely related to a *Listeria ivanovii* secreted neutral sphingomyelinase (nSMase), a Mg^{2+}-dependent phosphodiesterase that hydroylzes sphingomyelin. Sequence alignment with secreted nSMases of other Gram positive pathogens revealed that Rv0888 contains important conserved amino acids crucial for Mg^{2+} coordination, substrate recognition, and catalysis (Fig. 5A). Interestingly, phylogenetic analysis demonstrated that Rv0888 from *M. tuberculosis* is actually more closely related to human and yeast nSMases than many secreted nSMases from other Gram positive pathogens (Fig. 5B). Furthermore, comparison of a predicted structure for Rv0888 and the crystal structure of the secreted nSMase of *L. ivanovii* revealed striking structural similarities (Fig. 5C), suggesting that Rv0888 might be acting as a neutral sphingomyelinase.

We next examined whether the purified EspC complex exhibited SMase activity using a fluorometric assay for sphingomyelin hydrolysis. Wildtype STCF contained sphingomyelinase activity, but the specific activity of purified EspC was far greater than that of wildtype STCF (Fig. 5D). In contrast, neither purified Mpt32 nor Mpt64 exhibited any appreciable sphingomyelinase activity (Fig. 5D). This is consistent with our observation that Rv0888, a putative nSMase, copurifies specifically with EspC and is enriched in the purified EspC fraction.

Since the *M. tuberculosis* genome encodes four phospholipases that can hydrolyze either phosphatidylcholine or sphingomyelin (Johansen et al., 1996), it is possible that the observed sphingomyelinase activity is the result of one or more phospholipases in the

93

STCF. However, analysis using a fluorometric assay for phospholipase activity showed that neither wildtype STCF nor purified EspC exhibited any phospholipase activity (Fig. 5E). This demonstrates that the observed sphingomyelinase activity is the result of an nSMase and not due to the presence of a phospholipase. Furthermore, this result demonstrates that the sphingomyelinase that copurifies with EspC can discriminate between the two similar substrates sphingomyelin and phosphatidylcholine, an important consideration given that some bacterial nSMases can hydrolyze both sphingomyelin and phosphatidylcholine (Clarke et al., 2006).

Our data is consistent with the hypothesis that Rv0888, which copurifies with secreted EspC, is the nSMase responsible for the observed sphingomyelinase activity. However, in the absence of solid genetic data we cannot conclude that Rv0888 is required for the observed sphingomyelinase activity in the STCF. Although we do not currently have a mutant in Rv0888, we do have a strain, *Rv3849::Tn*, that harbors a mutation in a transcription factor and is attenuated for *Rv0888* transcription (Sridharan Raghavan, unpublished results). STCF collected from the *Rv3849::Tn* strain had significantly less sphingomyelinase activity than wildtype STCF, and this defect was rescued by complementation (Fig. 5F). Incidentally, the Rv3849::Tn mutant is also attenuated for transcription of the *EspA/EspC/Rv3614c* genetic locus (Fig. 1A), and thus the decrease in sphingomyelinase activity observed in the mutant STCF could be linked to a decreased capacity for Esx-1 secretion rather than a specific defect in *Rv0888* transcription. However, our analysis of STCF from other Esx-1 defective mutants demonstrates that the sphingomyelinase activity is not dependent on Esx-1 secretion (Fig. 5G), supporting our hypothesis that the activity can be attributed to the Rv0888 protein.

Esx and Sec Secretion Components Copurify with Cell-Associated EspC

Given our ability to identify proteins that copurified with secreted EspC in STCF, we decided to apply the same methodology to attempt to identify protein species that copurify with EspC in *M. tuberculosis* cell lysates. As with STCF, we observed multiple copurifying species that were not observed in immunoprecipitation of cell lysates lacking the 3X FLAG epitope (Fig. 6A). Copurifying species were identified by mass spectrometry (Fig. 6B). Although this method does not distinguish between cytosolic, cell membrane, periplasmic, or cell-wall localized EspC, it is noteworthy that the only protein that copurifies in both STCF and cell lysates is PPE18. This suggests that most of the species that copurify with EspC from STCF form interactions post-secretion. It is also noteworthy that several Esx locus proteins copurified with EspC, most notably proteins encoded at the *esxG/esxH* locus (Rv0281, Rv0282, Rv0284 and Rv0292). Proteins known to be required for Esx-1 secretion (Rv3870, Rv3871, Rv3877, Rv3616c, Rv3614c) were not seen to copurify with EspC from cell lysates. Finally, it is interesting that EspC copurified with secA2, a protein translocase that is involved in specialized secretion of some proteins (Kurtz et al., 2006) but has not been implicated in Esx secretion.

Discussion

In this study, we demonstrate that EspC (Rv3615c) is secreted in an Esx-1 dependent manner. Compared to ESAT-6 and CFP-10, which are the two most abundantly secreted proteins in *M. tuberculosis*, EspC is expressed and secreted in very

low abundance. Indeed, EspC has not previously been observed in *M. tuberculosis* STCF. It is not altogether surprising that EspC is secreted, since we showed previously that it contains an amino acid motif conserved in several Esx family members. Furthermore, EspC is encoded directly downstream of EspA, another Esx-1 pathway substrate. Combined with our previous results that *espC* is required for Esx-1 secretion, we conclude that secretion of EspC, like secretion of EspA, is mutually dependent upon secretion of ESAT-6/CFP-10 dimers. This codependent secretion appears to be a recurring theme of Esx-1 secretion, and although this is not unprecedented (Pettersson et al., 1999), the biological significance remains unclear.

Although this codependent secretion appears to be a shared characteristic of all known Esx-1 substrates, several features of secreted EspC make it unique. Unlike ESAT-6, CFP-10, or EspA, EspC appears to undergo significant post-translational modifications. The observed modifications, which decrease the mobility on SDS-PAGE by ~4-8 kDa, appeared heterogenous and resulted in a fuzzy smear by Western blot. While our mass spectrometry analysis identified a few peptides that were modified, including potential lysine lipidation with 4-hydroxynonenal, these modifications were not sufficient to explain the drastic and heterogenous modifications observed by SDS-PAGE. We hypothesized that the observed modifications may due to glycosylation of EspC. Although our mass spectrometry analysis did not identify hexose modification of any observed peptides, and no sensitivities were observed to enzymatic deglycosylases, we cannot rule out modification by more complex glycans. Importantly, a chemical deglycosylation reaction resulted in loss of the observed modification, suggesting either glycosylation or some other acid-sensitive modification. Very little is known about

protein glycosylation in *M. tuberculosis*, and only two proteins, Mpt32 (Dobos et al., 1995) (Dobos et al., 1996) and the 19-kilodalton lipoprotein (Herrmann et al., 1996), have characterized glycan modifications, both O-linked mannose residues. Interestingly, Mpt32 mannosylation was shown to be dependent on secretion through the SecYEG pathway (VanderVen et al., 2005), similar to our observation that EspC modification requires Esx-1 secretion. It is tempting to speculate that EspC undergoes post-translational modification, perhaps glycosylation, following secretion via the Esx-1 pathway. Clearly, further analysis will be required to better characterize the post-translational modifications observed for EspC.

Unlike secreted ESAT-6 or CFP-10, which were not observed to exist in forms larger than dimers, secreted EspC existed at molecular weight (~130-270 kDa) much higher than its monomer size (~13 kDa for the 3X FLAG-tagged variant). Only in the case of Esx family member dimerization (Lightbody et al., 2004) and PE/PPE family member dimerization (Strong et al., 2006) have higher order structures of secreted proteins been described in *M. tuberculosis*. Recombinant EspC ran at a molecular weight (~58-85 kDa) significantly higher than predicted monomers, suggesting that the protein has the potential interact with itself in homomultimers. This is consistent with our previous observation that EspC can interact with itself in a yeast 2-hybrid system (MacGurn et al., 2005). Further experimentation will be required to determine exact stoichiometry and symmetry of recombinant EspC homomultimers.

Since we were able to tag the N terminus of the EspC protein without affecting its secretion profile, we were able to purify native EspC from *M. tuberculosis* STCF. Consistent with the high observed molecular weight, we found that native EspC

copurified with several other secreted proteins, including many Esx family members, one protein encoded at an Esx locus (PPE61), and one known Esx-1 substrate, EspA. All of the copurifying species identified in this study were specific to the presence of EspC and were not observed to copurify with control proteins, Mpt32 or Mpt64. Furthermore, EspC did not copurify with any of the most abundant proteins in *M. tuberculosis* STCF, such as ESAT-6, CFP-10, EsxW or Mpt64. Importantly, PPE18, EspA, and several Esx family members also copurified with EspC in the sizing fractions, suggesting that these proteins form a stable core complex that accounts for the high molecular weight observed with gel filtration chromatography. Although not all of the species that copurified with EspC from STCF were observed to copurify with sized EspC, we believe these may represent transient or low affinity interactions with a stable core complex.

In addition to identifying many copurifying species that are implicated in Esx secretion, we also identified two copurifying species with SecYEG signal sequences and two with TAT signal sequences. Overall, our observation that EspC copurifies with substrates of Esx, TAT, and SecYEG secretion pathways suggests that multiple proteins secreted by different systems can form interactions post-secretion. This adds a layer of complexity to our understanding of *M. tuberculosis* secretion, and the cooperation between different secretion systems could represent a general strategy for robust bacterial manipulation of the host cell.

One of the SecYEG substrate proteins observed to copurify with EspC was Rv0888, a protein similar to the family of neutral sphingomyelinase (nSMase) proteins. Many Gram positive pathogens have been shown to encode secreted nSMases which are important for full virulence (Clarke et al., 2006). Importantly, we showed that a SMase

activity copurifies with EspC, and that this activity is specific to sphingomyelin. Additionally, a mutant known to be attenuated for Rv0888 transcription was abrogated for the sphingomyelinase acivity, implicating this gene as a putative SMase. Although the SMase activity was Esx-1 independent, we hypothesize that interaction of secreted Rv0888 with the EspC complex might be important for targeting the nSMase activity to the lumenal leaflet of the host phagosomal membrane, where hydrolysis of sphingomyelin can occur.

A secreted sphingomyelinase activity has important implications for *M. tuberculosis* cellular pathogenesis. Ceramide generated by nSMase activity is an important signal for apoptosis (Chatterjee, 1999), and *M. tuberculosis* is known to induce some level of apoptosis during macrophage infection (O'Sullivan M et al., 2007). It will be interesting to see if *Rv0888* mutants of *M. tuberculosis* are defective in inducing apoptosis of host cells. There is also evidence that nSMase generation of ceramide can interfere with signaling through toll-like receptors by disrupting lipid rafts on host membranes, thus altering the host innate immune response (Walton et al., 2006). Ceramide has also been shown to inhibit phagocytosis by the scavenger receptor (Luan et al., 2006), which could affect host phagocytosis and mechanism of reinfection. Given that ceramide production and sphingolipid homeostasis can affect multiple signaling pathways and host processes, it is tempting to speculate that a secreted bacterial sphingomyelinase activity could play an important role in *M. tuberculosis* cellular pathogenesis. Future experiments will be aimed at demonstrating whether Rv0888 is directly involved in generating cermaide in the host and modulating the host response to infection.

Materials and Methods

Bacterial Strains, Culture Conditions and STCF Collection. Strains of

Mycobacterium tuberculosis (Erdman) used in this study are listed in Table 1. All strains

were grown as previously described (Cox et al., 1999). Briefly, cultures for macrophage

infection were grown to mid-logarithmic phase in 7H9 media supplemented with 10%

Middlebrook OADC (BD Biosciences), 0.5% glycerol and 0.05% Tween 80. Cultures

were grown for collection of short term culture filtrate (STCF) as previously described

(Stanley et al., 2003). Briefly, *M. tuberculosis* cultures were grown in Sauton's medium

and culture supernatant was collected by filtration. STCFs were concentrated using

Amicon Ultra-15 Centrifugal Filter Units (5000 MWCO, Millipore).

Antibodies, Reagents, and Chemical Deglycosylation. Polyclonal mouse antibodies

generated against EspC (Rv3615c) were obtained from the Center for Innovation in

Medicine Antibody Core at University of Texas, Southwestern. Mouse monoclonal

antibodies targeting KatG and Mpt32 were obtained from Colorado State University

under the TB Vaccine Testing and Research Materials Contract. Antibodies against

ESAT-6 (mouse monoclonal) and CFP-10 (rabbit polyclonal) were kind gifts of P.

Andersen (Statens Serum Institut, Copenhagen, Denmark). Anti-FLAG M2 antibody

(mouse monoclonal) and EZView Anti-FLAG M2 Affinity Gel were purchased from

Sigma. Alexa488-conjugated anti-mouse secondary antibodies and TALON Dynabeads

were purchased from Invitrogen.

Western blots were performed as previously described. Antibodies were diluted diluted in blocking solution accordingly: Rv3615c/EspC (1:100), KatG (1:20), Mpt32 (1:20), ESAT-6 (1:5000), CFP-10 (1:5000), anti-FLAG M2 (1:5000), Alexa488-conjugated anti-mouse (1:200).

Chemical deglycosylation reaction was performed using a GlycoFree Chemical Deglycosylation Kit (Prozyme) according to manufacturer's instructions.

Immunofluorescence and Immunoelectron Microscopy. For immunfluorescence and immunoEM visualization of FLAG-tagged EspC, cultures were grown under the same conditions used for STCF collection. Bacteria were fixed in PBS containing 4% paraforlmaldehyde.

For immunofluorescence, bacteria were incubated on polylysine-treated glass coverslips prior to fixation. Coverslips were washed, blocked in PBS containing 0.1% BSA and 0.05% Saponin, and subsequently stained with anti-FLAG M2 and Alexa488 anti-mouse antibodies.

For immunoelectron microscopy, bacteria samples were washed to remove fix and samples were processed and imaged as previously described (McCaffery et al., 1995). Briefly, fished and washed samples were cryoprotected with 20% poly(vinyl pyrrolidone) (#M-6385, Sigma) in 2M sucrose overnight and frozen in liquid nitrogen. Frozen thin section were cut with Leica Ultracut UCT with EMFCS attachment (Leica Microsystems Inc.,IL.). Sections were treated with 0.2% glycine, blocked with 2% each fish gelatin, BSA in PBS, pH 7.4. incubated with the anti-FLAG M2 antibody for 3 hours at 1:50 or no dilution, and incubated with goat anti-mouse conjugated with 10 nm gold

(Ted Pella Inc, Ca.) at 1:50 dilution for 60 minutes. The sections were then stained with Oxalate uranyl acetate and embedded in 1.5% methyl cellulose (Sigma, Mo.),0.3% aqueous uranyl acetate (Ted Pella Inc., Ca.). The sections were examined in Philips Tecnai 10 electron Microscope.

Gel Filtration and Sizing Analysis. Prior to size separation by gel filtration, samples were dialyzed into TBS and centrifuged at 50,000g to clarify the sample. For sizing of *M. tuberculosis* STCF, 3mg of total protein was run over a Superose 6 gel filtration column using a TBS buffer system. The column exhibited a void volume of 7.5 mLs and was calibrated using the following standards: thyroglobulin (670 kDa), ferritin (440 kDa), catalase (232 kDa), γ-globulin (158 kDa), ovalbumin (44 kDa), myoglobin (17 kDa), vitamin B12 (1.35 kDa).

Following size separation, collected fractions were analyzed by SDS-PAGE followed by immunoblot to determine which fractions contained a given protein species. For quantitation, samples were loaded onto slot blots and antibody detection was quantified by densitometry using ImageJ software (NIH). OD280 was used to measure the total protein contained in each fraction.

Protein Purification. Prior to immunoprecipitation, STCFs were dialyzed against TBS. 3X FLAG-tagged proteins were immunoprecipitated using Anti-FLAG M2 EZView affinity gel (Sigma) according to manufacturer's protocol. All elutions from M2 beads were done using excess 3X FLAG peptide. For proteins tagged with a 3X-FLAG and a 6X His, tandem purification was achieved by binding of the sample to TALON

Dynabeads and washing according to manufacturer's protocol. If elution was required, sample was eluted from TALON Dynabeads by addition of 150mM imidazole.

Mass Spectrometry Analysis. For mass spectrometry analysis, samples were prepared either by on-bead digestion or in-gel digestion. For on-bead digestion, samples bound to TALON Dynabeads (Invitrogen) were digested in 50mM ammonium bicarbonate buffer containing 20ng/μL trypsin (Roche) for 2 hours at 37ºC, followed by magnetic separation of the digested peptides from the beads.

For in-gel digestion, samples were processed by SDS-PAGE and stained with colloidal coomassie (GelCode Blue, Pierce). The entire gel lane was cut into thin horizontal slices, and each excised slice was finely diced and destained in freshly made 50mM ammonium bicarbonate buffer in 50% methanol. After destaining, each piece was dehydrated by shaking in acetonitrile followed by a vacuum dry step. Dried gel samples were rehydrated with 50mM ammonium bicarbonate buffer containing 20ng/μL trypsin (Roche). Gel samples were allowed to rehydrate on ice for 30 minutes followed by incubation at 37º for 4 hours. The digestion was stopped by addition of a solution of 7% formic acid / 0.1% TFA in water. Peptides were extracted from the gel by shaking the sample for 12 hours at 4º in the presence of of 2μL of Porous 50 C18 beads to the sample. Following the extraction, the mixture containing the C18 beads was transferred to a gel loading pipet tip plugged with a C8 membrane, which was then centrifuged to create a C18 column at the end of the tip. The beads were then washed with 0.1% TFA and eluted using 60% acetonitrile.

For MALDI-MS and MALDI-MS/MS, samples were eluted directly onto target, followed by the addition of matrix (α–cyano-4-hydroxycinnamic acid). Each sample was analyzed first by MALDI-MS using a prOTOF 2000 MALDI-OTOF Mass Spectrometer (Perkin Elmer SCIEX). The MS spectra were analyzed and peaks were selected using MoverZ software. The selected peaks were then subject to MALDI-MS/MS analysis using a Finnigan vMALDI LTQ Mass Spectrometer (ThermoElectron Corporation).

For analysis by LC-MS/MS, peptide samples were dried under vacuum to eliminate organic solvent and formic acid was added to the sample to a final solution of 0.1%. Samples were then run on a QTRAP LC/MS/MS Mass Spectrometer (Applied Biosystems MSD SCIEX). Mass spectra were analyzed using Analyst 1.4.1 software.

The ions identified by mass spectrometry were used to identify parent proteins from *M. tuberculosis* using Mascot Search Engine (Matrix Science). Significance levels of protein identification were based on a Mowse scoring algorithm(Pappin et al., 1993).

Bioinformatic Analysis and Structural Prediction. Sequences of known bacterial sphingomyelinases were aligned using ClustalX and phylogenetic relationships were determined using the MAFFT Phylogeny Server. Secondary structural predictions were done using Phyre, the successor to 3D-PSSM(Kelley et al., 2000). 3-dimensional structure was predicted using the ESyPred3D algorithm(Lambert et al., 2002).

Sphingomyelinase and Phospholipase Assays. Sphingomyelinase and phospholipase fluorometric assays were performed using Amplex Red kits according to manufacturer protocol (Invitrogen). Data was collected on a SpectraMax microplate fluorometer

(Molecular Devices) and analyzed using Microsoft Excel. For determination of specific

activity, the Vmax (RFU $\bullet$ min^{-1}) was divided by the total protein added to the reaction,

as determined by Micro BCA Protein Assay (Pierce).

Figure 1. EspC is secreted in an Esx1-dependent manner.

(A) Two genetic loci of *M. tuberculosis* known to encode genes required for Esx-1 secretion are the ESX-1 locus and the *Rv3616c-Rv3614c* gene cluster. Genes labeled in blue have been shown to be required for Esx-1 secretion, while genes colored in red are known substrates of the pathway. Interestingly, all described substrates of the Esx-1 system seem to be secreted in a mutually-dependent manner. **(B)** Rv3615c is a secreted protein. Using antibodies that recognize Rv3615c, we probed for the presence of the protein in cell pellets (P) and STCFs (S) from wildtype (Erdman), mutant (*Rv3615c::Tn*), and complementation strains. Samples were blotted with αKatG antibodies as a control for cell lysis. **(C)** An N terminal 3X FLAG tagged version of Rv3615c complements secretion in the *Rv3615c::Tn* mutant and runs at the expected molecular weight on an SDS-PAGE gel. Immunoblotting with αFLAG antibodies reveals the same pattern of detection as the αRv3615c antibody. **(D)** The smear detected by the αRv3615c antibody that runs slightly higher than the expected size of the protein (~10 kDa) is sensitive to a chemical deglycosylation reaction. Antibodies recognizing the 45-kDa glycoprotein (Apa) from *M. tuberculosis* were also sensitive to the reaction and underwent expected size shifts. **(E)** Genetic analysis of Rv3615c secretion. αRv3615c antibodies were used to probe for the presence of the protein in cell pellets (P) and STCFs (S) of various strains harboring mutations at the Esx-1 genetic locus (upper) and two additional loci also required for Esx-1 secretion (below). Importantly, all strains known to be defective for Esx-1 secretion were also defective for secretion of Rv3615c. As such, we henceforth refer to Rv3615c as <u>E</u>sx-1 <u>s</u>ecreted <u>p</u>rotein <u>C</u>, or EspC. **(F)** Western blot analysis of cell pellets (P) and STCFs (S) from *M. bovis BCG* and a variant of BCG with an episomal

copy of the Esx-1 locus from *M. tuberculosis* (Erdman) reveals that EspC secretion

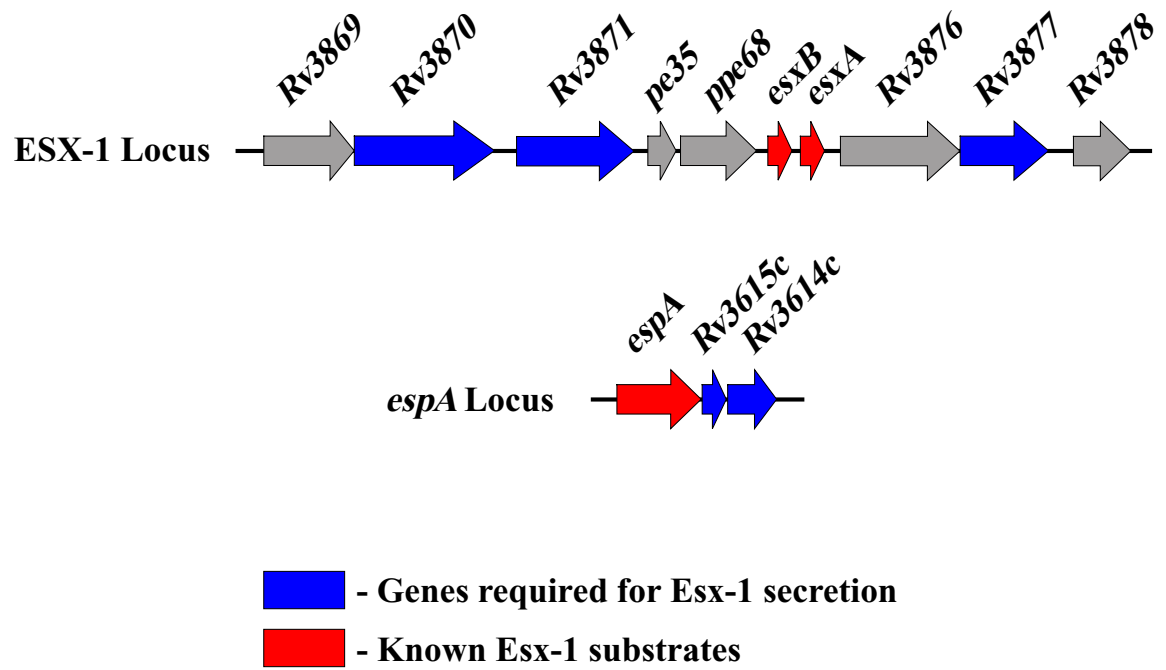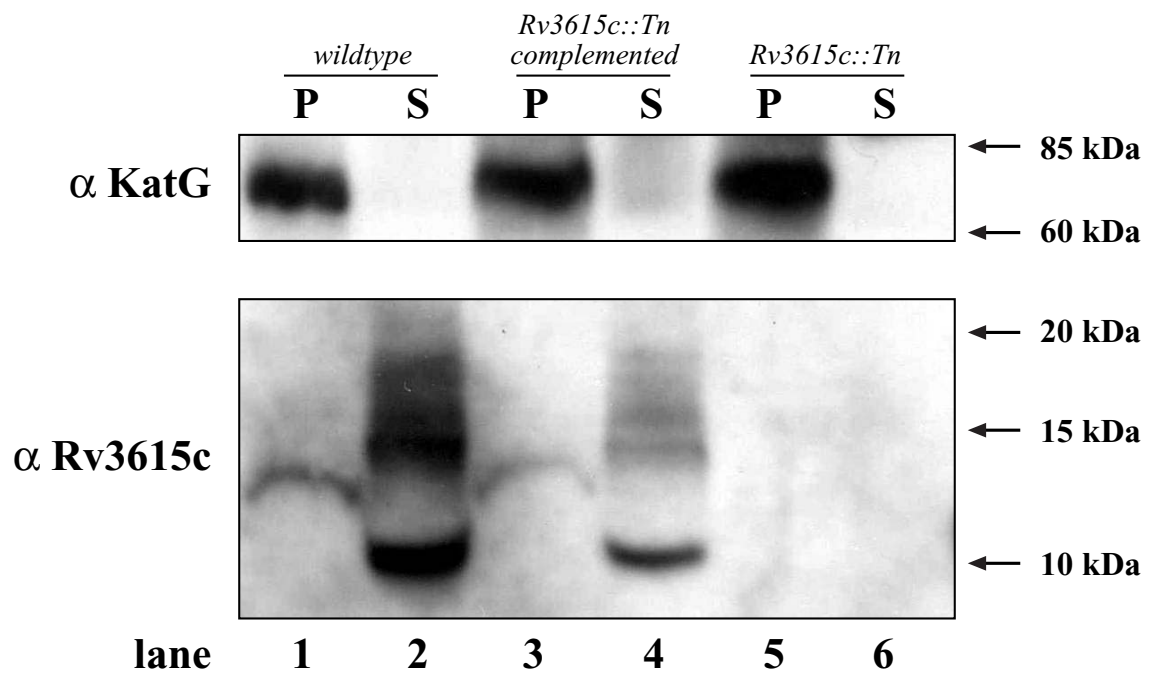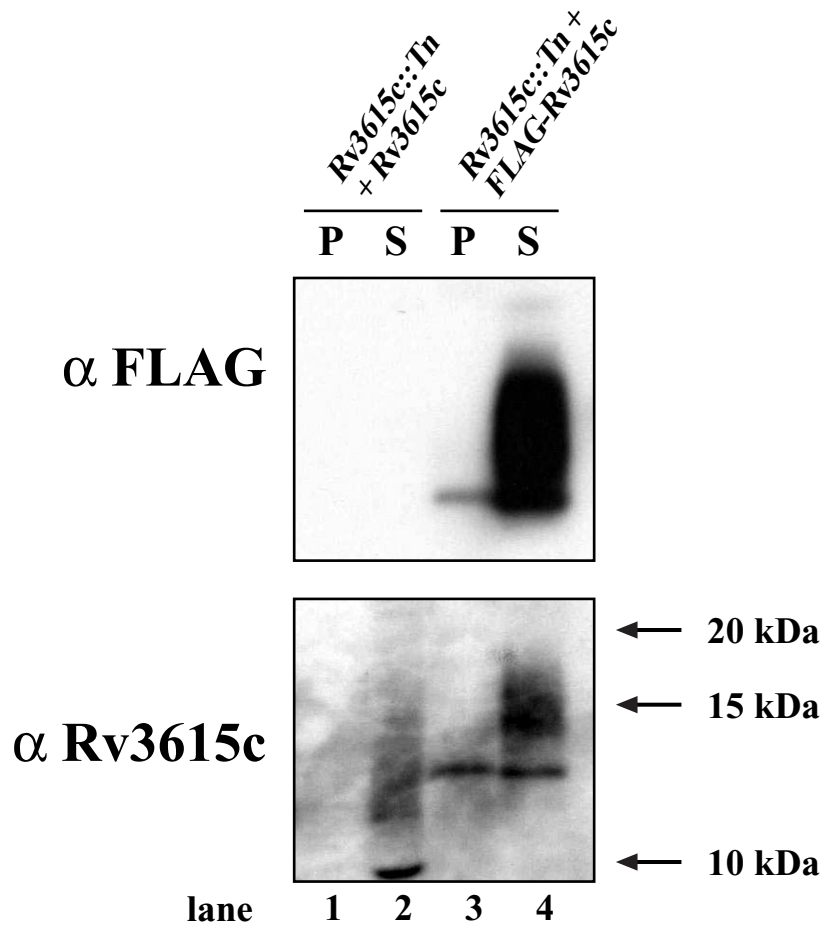requires expression of the Esx-1 secretion system.

Fig. 1

A

ESX-1 Locus

Rv3869 *Rv3870* *Rv3871* *pe35* *ppe68* *esxB* *esxA* *Rv3876* *Rv3877* *Rv3878*

espA Locus

espA *Rv3615c* *Rv3614c*

■ - Genes required for Esx-1 secretion
■ - Known Esx-1 substrates

Fig. 1

B

Fig. 1

C

Fig. 1

D

α Mpt32

α Rv3615c

Untreated   Mock   Chemical Deglycosylation

← 48.8 kDa
← 37.1 kDa
← 20 kDa
← 15 kDa
← 10 kDa

lane   1   2   3
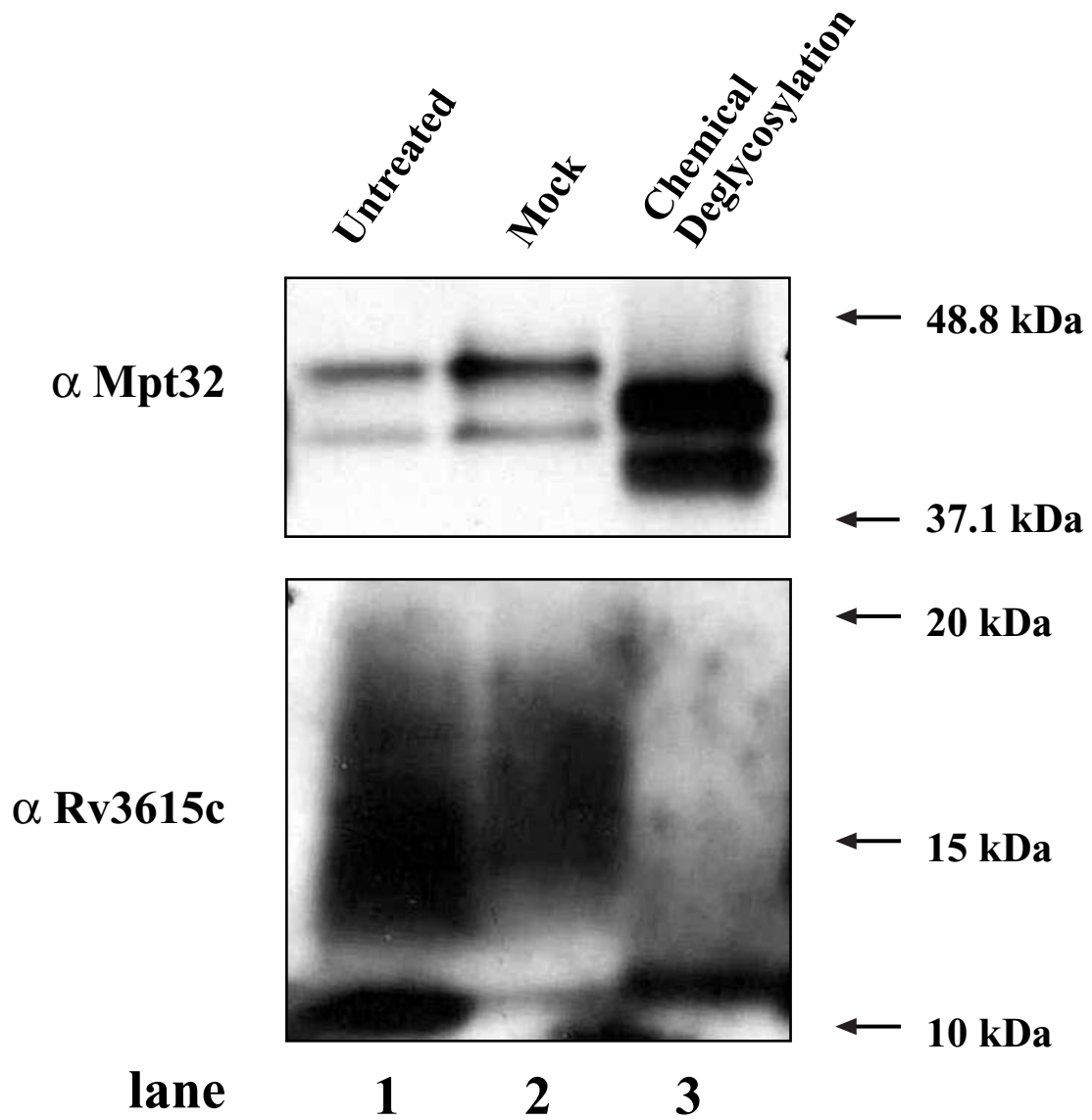
Fig. 1

E
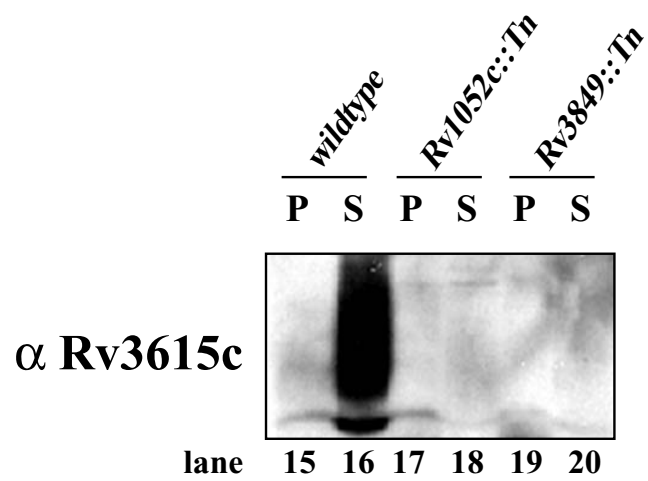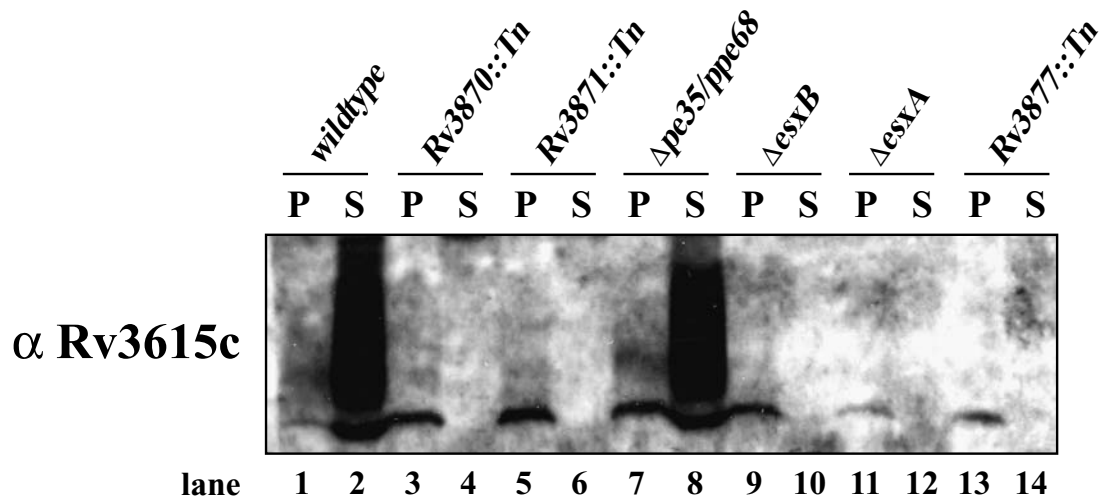
Fig. 1

F
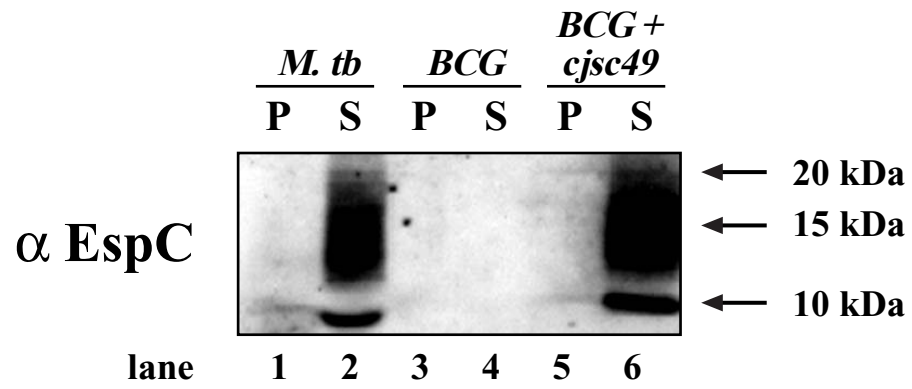
Figure 2. Immunodetection of EspC from *M. tuberculosis*.

(A) Surface staining of *M. tuberculosis* expressing 3X FLAG-tagged EspC was performed by fixing bacteria on glass coverslips and visualizing the FLAG epitope by indirect immunofluorescence. Green indicates fluorescent staining of FLAG epitope.

(B) Electron micrographs with immunogold labeling of the FLAG epitope in *M. tuberculosis* expressing the 3X FLAG-tagged EspC reveals a localization pattern similar to that observed with immunofluorescence microscopy. Arrows indicate immunogold staining of the FLAG epitope.
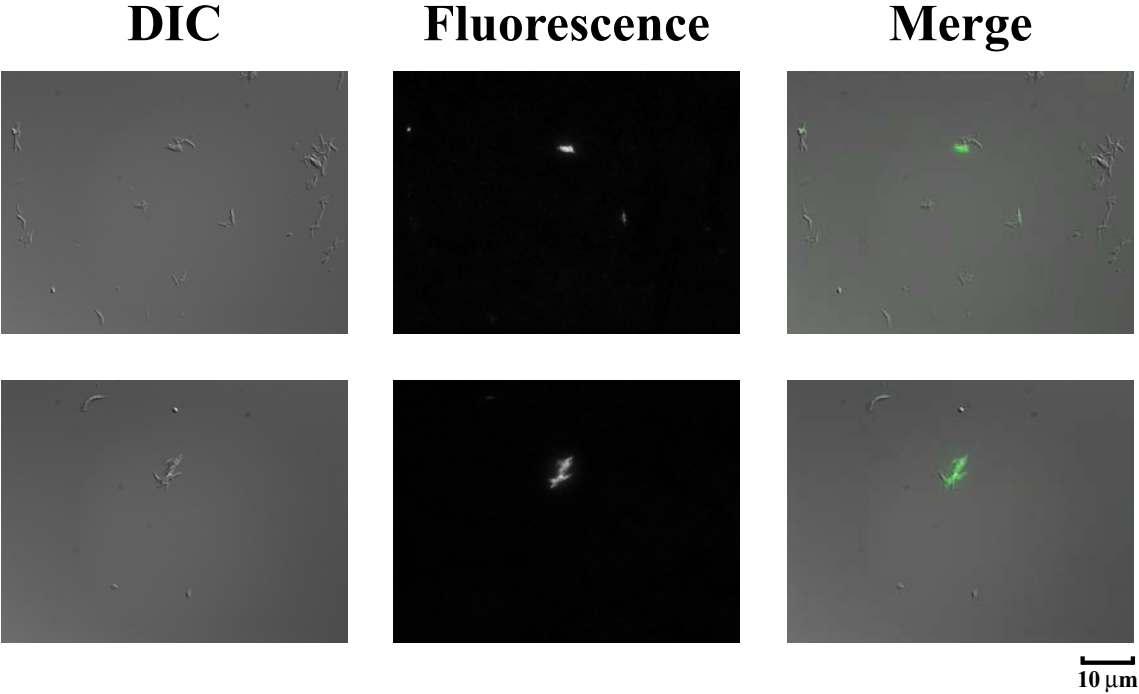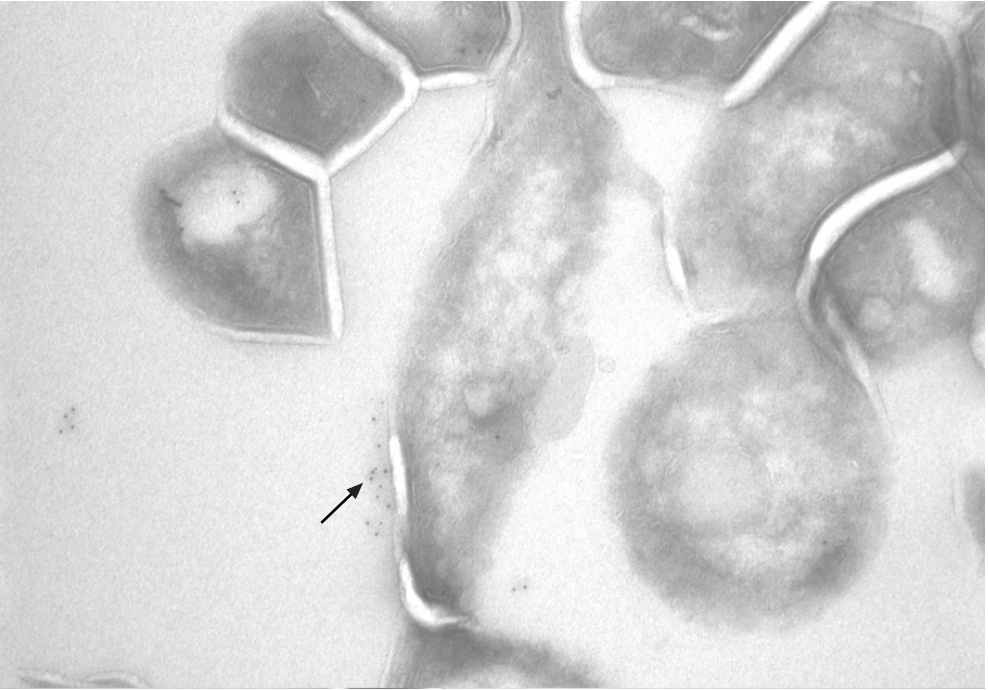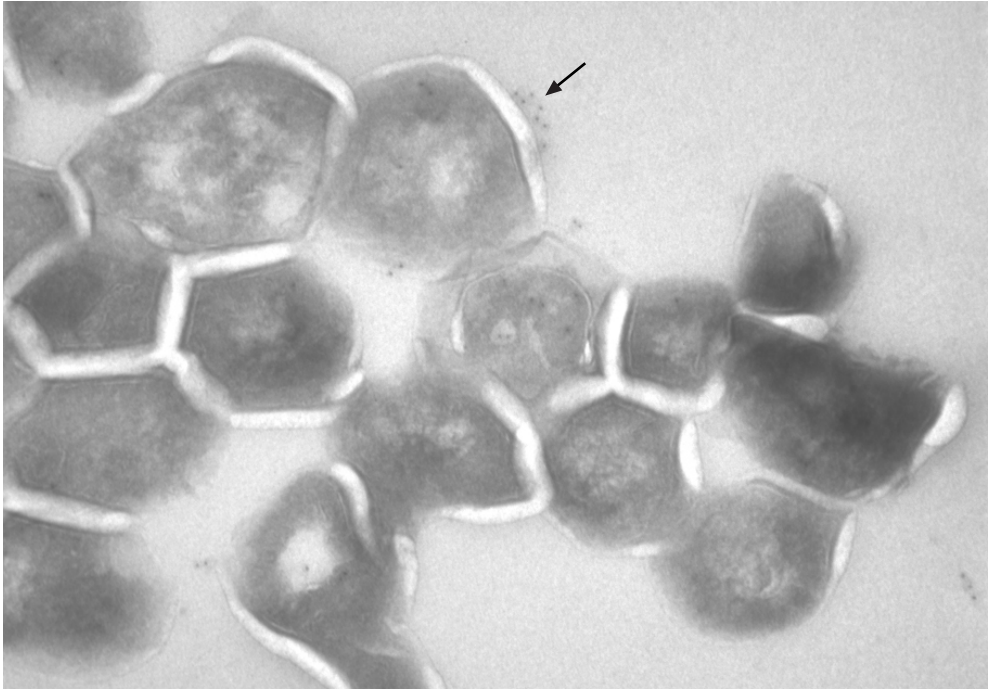
Fig. 2

A

DIC	Fluorescence	Merge

10 μm

Fig. 2

B

0.5 μm

Figure 3. EspC from *M. tuberculosis* STCF exists in a higher order complex.

(A) STCF from *M. tuberculosis* expressing 3X FLAG-tagged EspC was run over a gel

filtration column and individual fractions were analyzed by slot-blotting with quantitation

by densitometry (top) or SDS-PAGE followed by Western blot (bottom) using αFLAG,

αCFP-10, αESAT-6, or αMpt32 (45-kDa glycoprotein) antibodies. Fraction indicates

the fraction number from the start of the run collection, while molecular weight (MW)

represents the estimated weight in kDa expected for each fraction based on calibration of

the column with known standards. Arrows (top) indicate where known standards appear

during the fractionation. OD_{280} was used as an estimate of total protein represented in

each fraction. **(B)** Sizing analysis of native 3X FLAG-tagged EspC from STCF

compared to recombinant 3X FLAG-tagged EspC expressed and purified from *E. coli*.

Recombinant 3X FLAG-tagged EspC (~13kDa) appears larger than expected but is

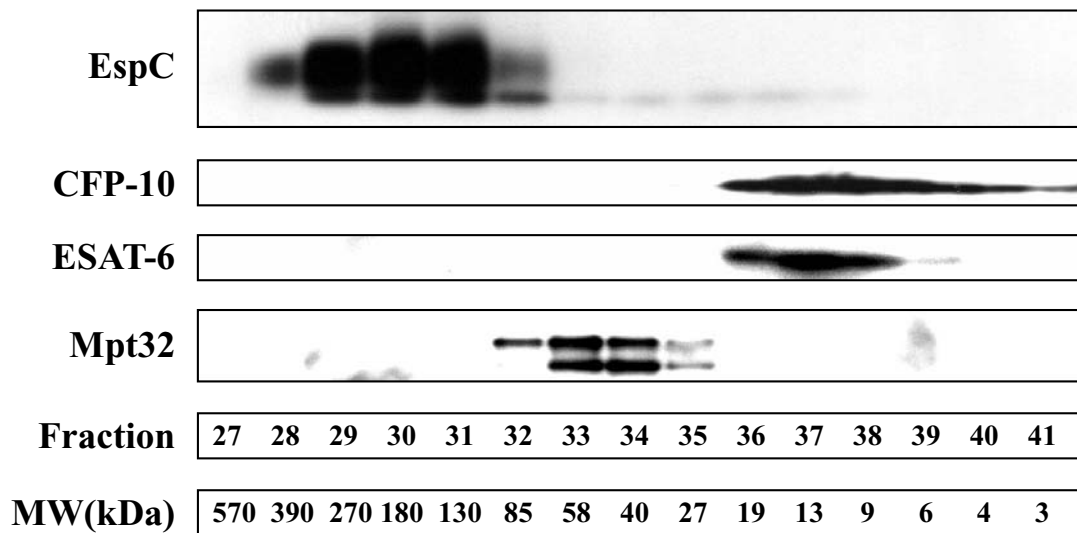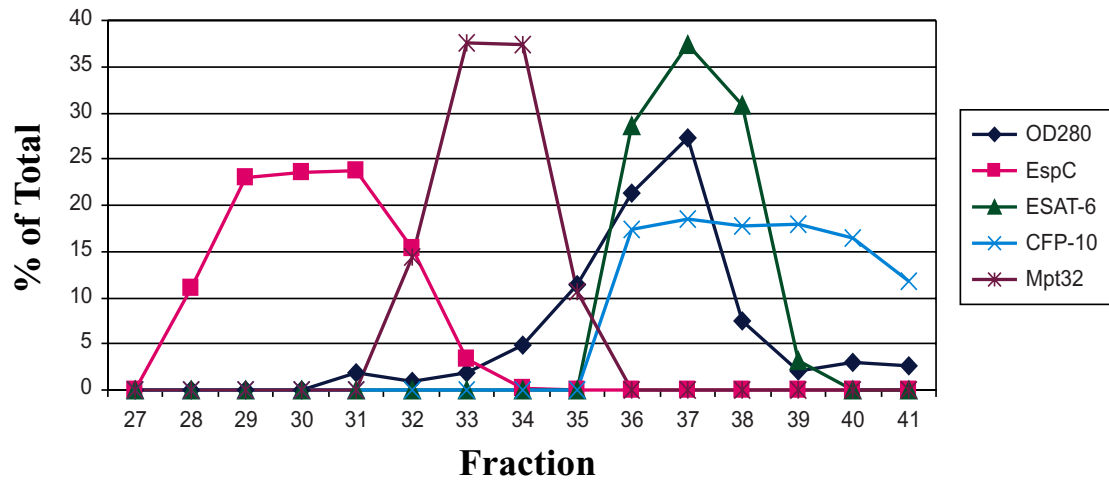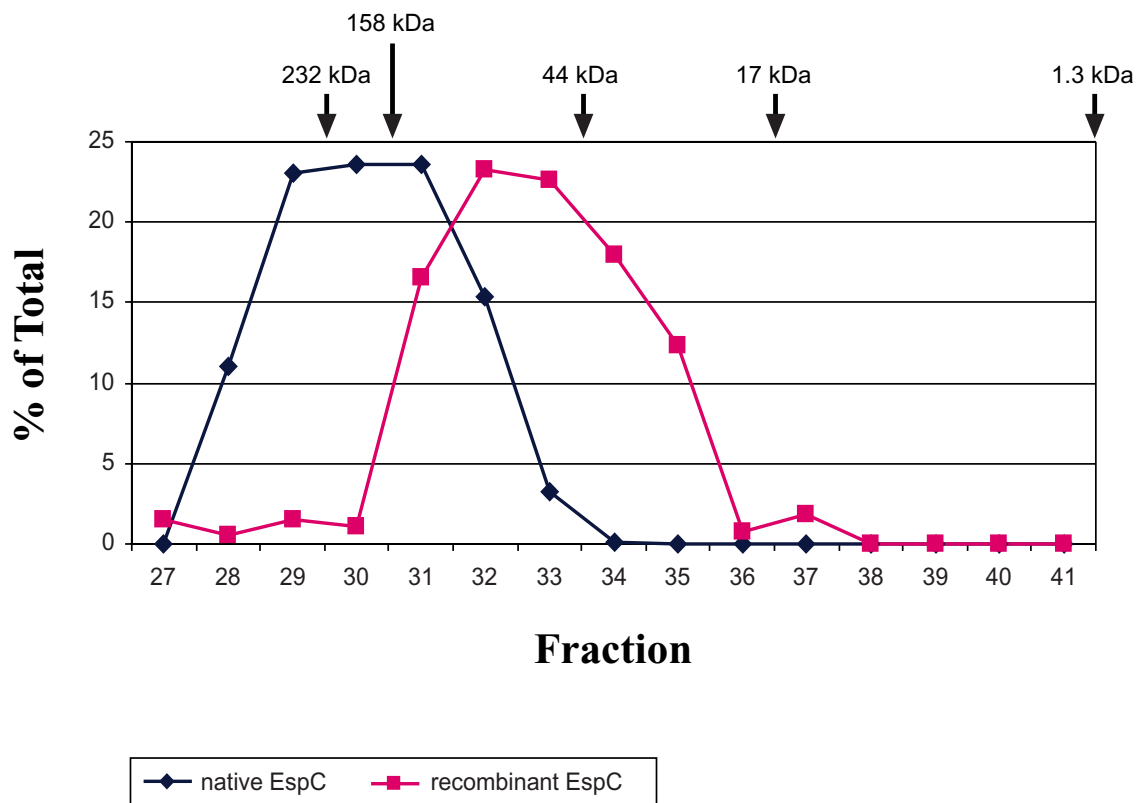considerably smaller than native EspC.

Fig. 3

A

Fig. 3

B

Figure 4. Several secreted proteins copurify with EspC from *M. tuberculosis* STCF.

(A) 3X FLAG-tagged EspC was immunopurified from *M. tuberculosis* STCF, run on SDS-PAGE and silver-stained (lane 1). As a control, the same protocol was performed on wildtype *M. tuberculosis* STCF lacking the 3X FLAG epitope (untagged control, lane 2). **(B)** Mass spectrometry peptide fingerprinting was used to identify species that specifically copurified with secreted EspC. All copurifying species listed were identified with 100% certainty. Most gel slices analyzed contained at least two copurifying species, making it impossible to identify specific bands on the gel. * indicates a protein that also copurified with EspC following gel filtration fractionation.
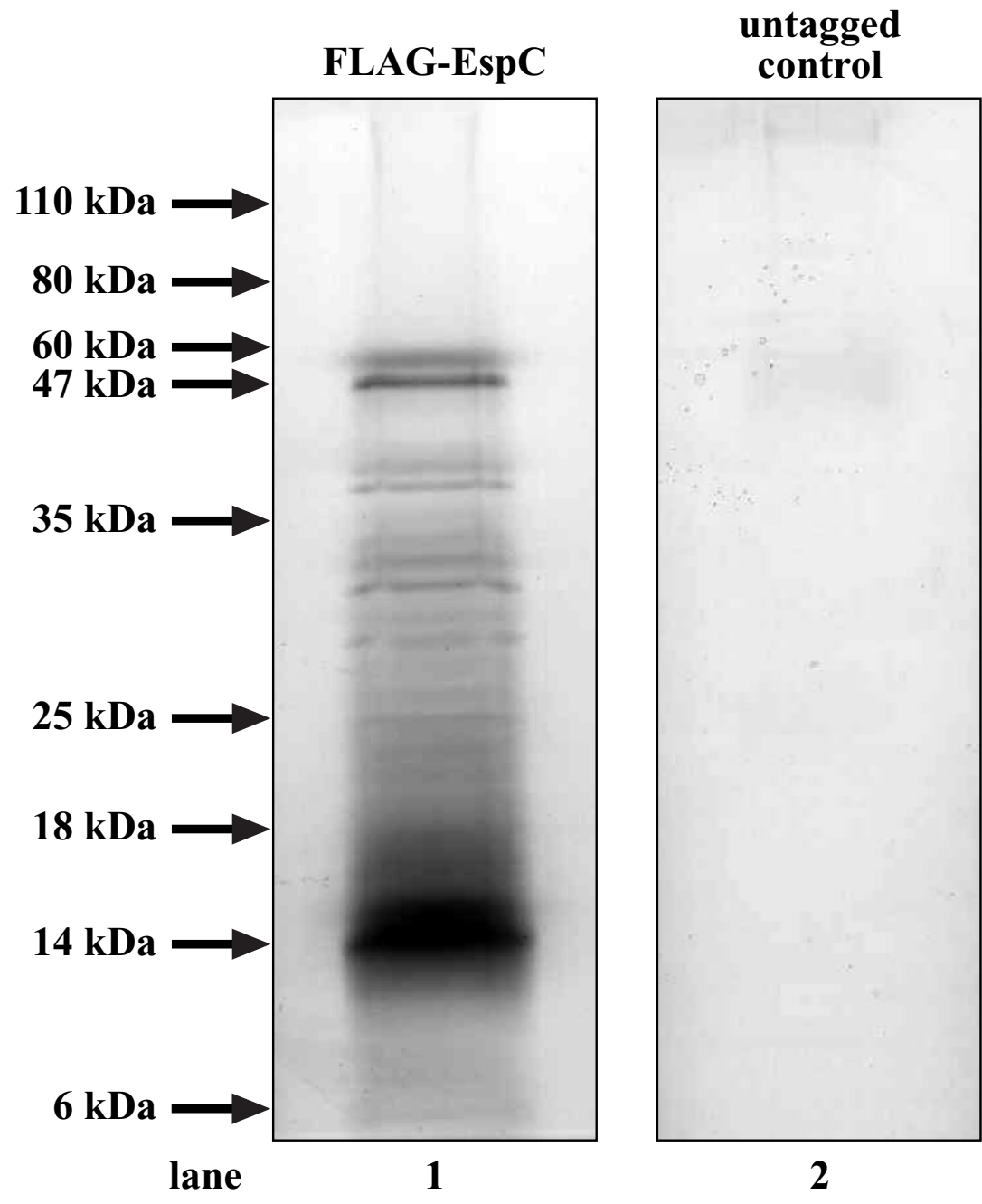
Fig. 4

A

FLAG-EspC   **untagged control**

110 kDa ➡

80 kDa ➡

60 kDa ➡
47 kDa ➡

35 kDa ➡

25 kDa ➡

18 kDa ➡

14 kDa ➡

6 kDa ➡

lane   **1**   **2**

Figure 4

B

Protein	MW by PAGE
Esx Family Proteins	
EsxL*	6-25 kDa
EsxG	6-14 kDa
EsxK*	6-25 kDa
EsxN	6-25 kDa
EsxM*	6-18 kDa
EsxO*	6-25 kDa
MT2420	6-14 kDa
MT2421	6-14 kDa
Esx-1 Substrates	
EspA*	35-47 kDa
PE/PPE Family Proteins	
PPE18*	35-47 kDa
PE31	6-14 kDa
PPE60	35-47 kDa
Putative Secreted Proteins	
Rv0888	47-60 kDa
Rv2525c	18-25 kDa
Rv3491	14-18 kDa
Rv1754c	47-60 kDa

Figure 5. Immunopurified EspC contains a sphingomyelinase activity.

(A) Sequence alignment of *M. tuberculosis* protein Rv0888 with known neutral

sphingomyelinase proteins from human (neutral sphingomyelinase 2 and 3),

Saccharomyces cerevisiae, Streptomyces coelicolor, and *Listeria ivanovii.* The line

beneath the alignment indicates degree of similarity across the alignment. • Indicates a

conserved residue, while ∗ indicates a highly conserved residue. Red triangles indicate a

conserved residue involved in catalysis. Red circles indicate conserved residues involved

in Mg^{2+} coordination. Red squares indicate residues that surround the catalytic pocket

and are thought to be involved in substrate recognition. **(B)** Phylogenetic tree

constructed from neutral sphingomyelinase sequences encoded in various bacteria and

eukaryotes. **(C)** Crystal structure of neutral sphingomyelinase from *L. ivanovii*

compared to the predicted structure of Rv0888 from *M. tuberculosis*. Colors indicate

secondary structure patterns. **(D)** A fluorometric assay was used to detect

sphingomyelinase activity from *M. tuberculosis* STCF or immunopurified EspC, Mpt64

and Mpt32. Specific activity (RFU • min^{-1} • μg^{-1}) was calculated by dividing the Vmax

(RFU • min^{-1}) by the total protein added (μg) to the reaction. **(E)** A similar fluorometric

assay was performed using the same samples to detect phospholipase activity.

Phospholipase (PLC) from *Bacillus cereus* was used as a positive control. Neither *M.*

tuberculosis STCF nor purified EspC exhibited any phospholipase acitivty. **(F)** STCF

from a mutant strain (*Rv3849::Tn*) known to be attenuated for Rv0888 expression

exhibits less sphingomyelinase activity than STCF from wildtype or complemented *M.*

tuberculosis. **(G)** Sphingomyelinase activity was determined for STCF collected from

Esx-1 secretion mutants. Loss of Esx-1 secretion does not affect sphingomyelinase

activity in the STCF.

Fig. 5

A

Fig. 5

B

Fig. 5

C

L. ivanovii **sphingomyelinase**	*M. tuberculosis* **Rv0888**
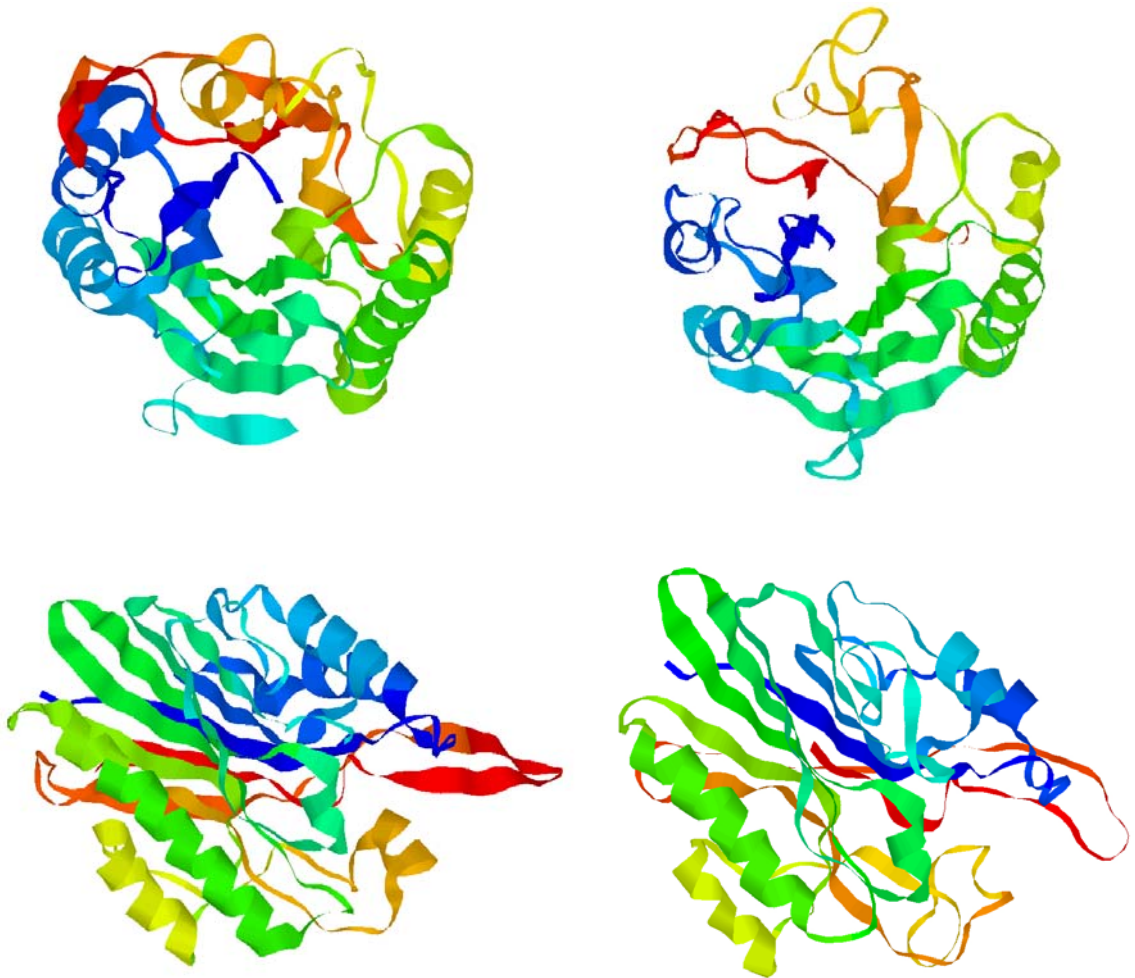
Fig. 5

D
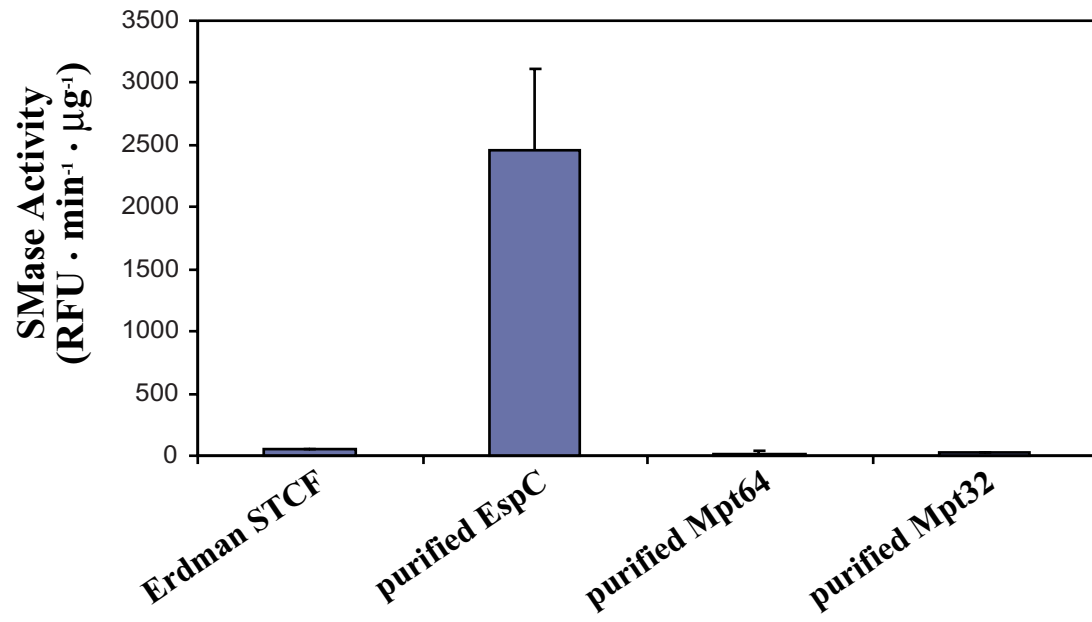
Fig. 5

E
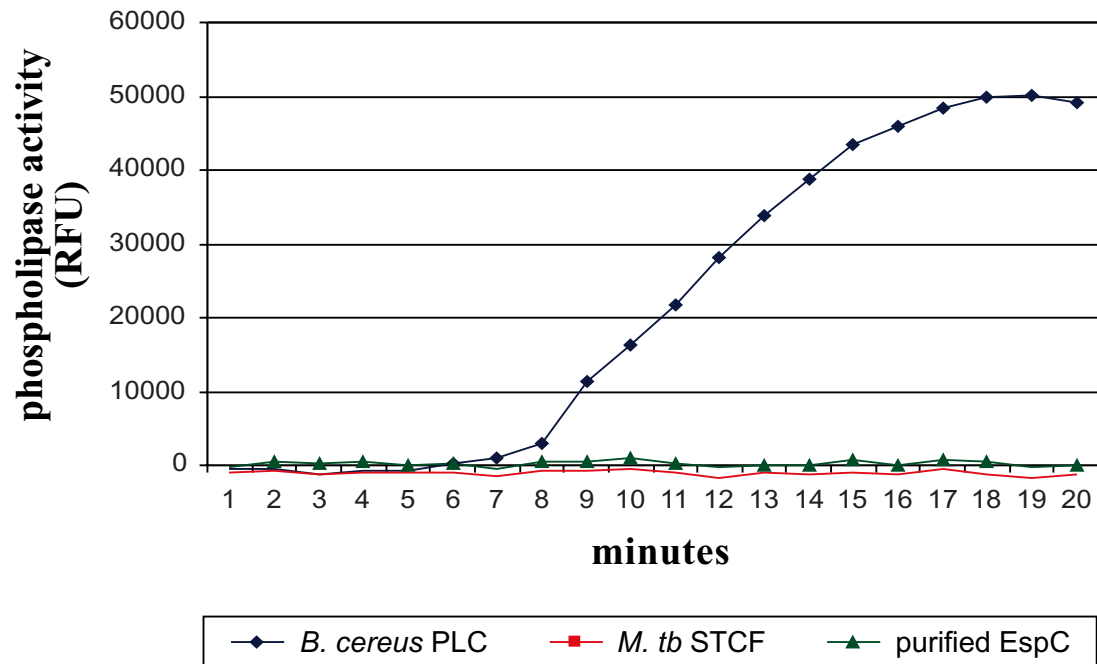
Fig. 5

F
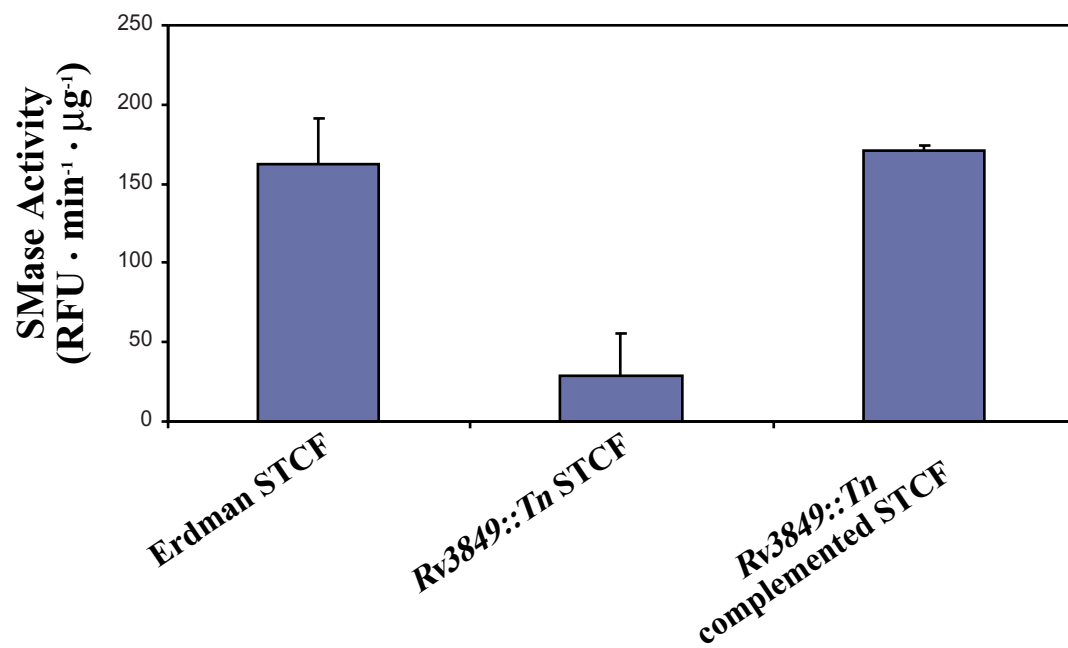
Fig. 5

G
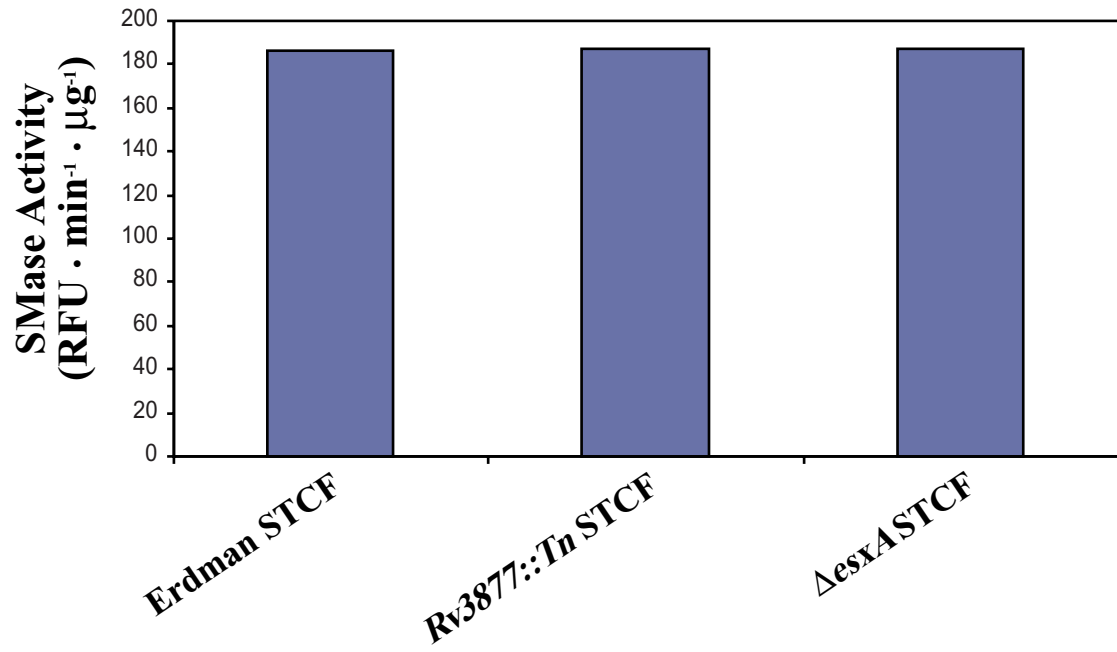
Figure 6. Proteins copurify with EspC from _M. tuberculosis_ cell lysates.

(A) 3X FLAG-tagged EspC was immunopurified from _M. tuberculosis_ whole cell lysates, run on SDS-PAGE and silver-stained (lane 1). As a control, the same protocol was performed on wildtype _M. tuberculosis_ whole cell lysates lacking the 3X FLAG epitope (untagged control, lane 2). **(B)** Mass spectrometry peptide fingerprinting was used to identify species that specifically copurified with cell-associated EspC. All copurifying species listed were identified with 100% certainty. Species that copurified non-specifically were identified in both tagged and untagged samples and are not represented in the table.

Fig. 6
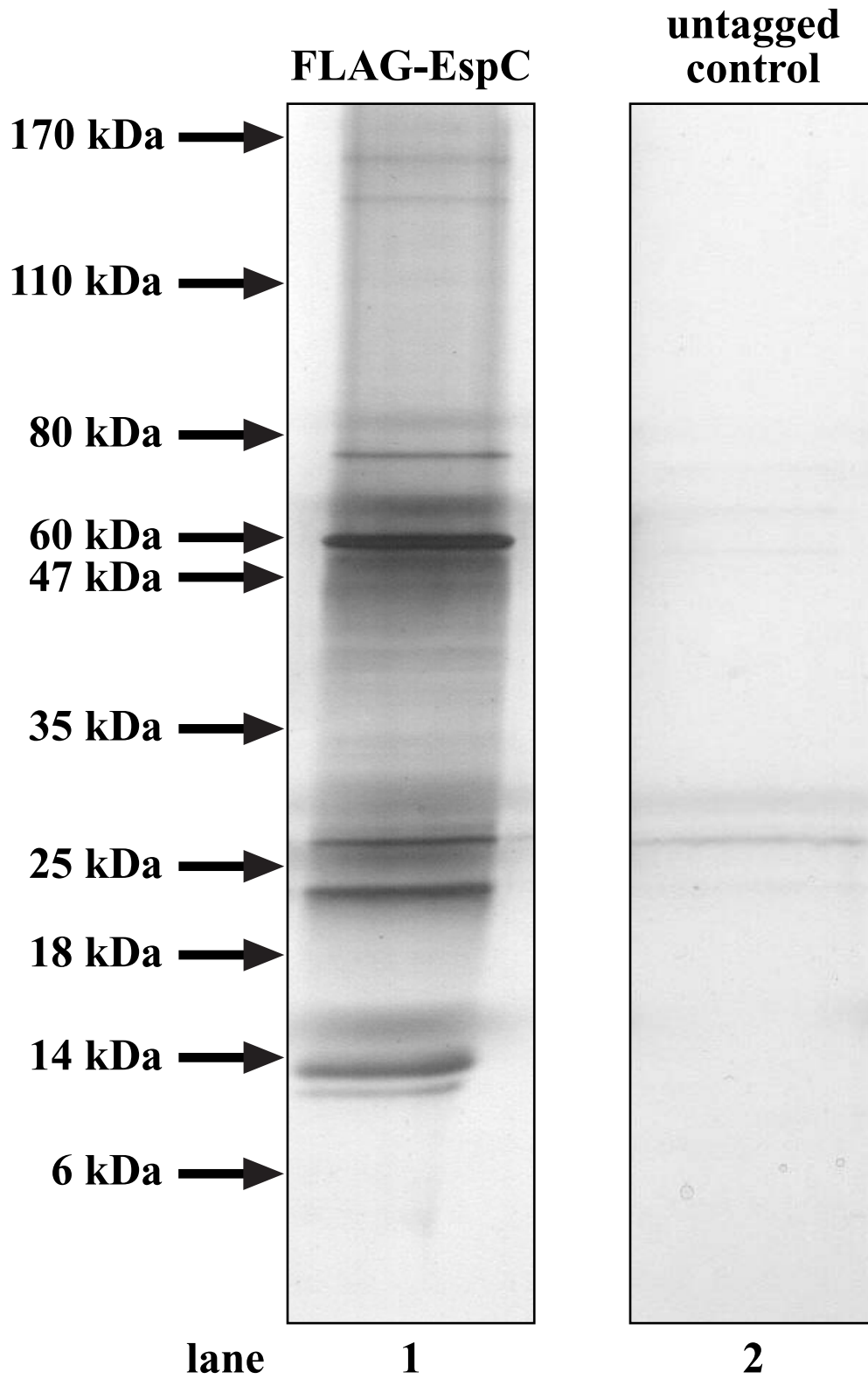
Fig. 6

B

Protein	MW by PAGE	Putative function
Esx Locus Proteins		
Rv0281	25-35 kDa	SAM-dependent methyltransferase domain, sig. sequence
Rv0282	60-80 kDa	CHP with ATP/GTP binding domain, Rv3868 homolog
Rv0284	110-170 kDa	Putative ATPase, Rv3870 homolog
Rv0292	25-35 kDa	Conserved transmembrane protein
PPE18	35-47 kDa	PE/PPE family protein
Known Secretory Proteins		
secA2	80-110 kDa	Involved in protein secretion
Other Proteins with Known Functions		
Rv0251c	14-18 kDa	Transcriptional regulatory protein
Rv0818	25-35 kDa	Transcriptional regulatory protein
Rv1543	25-35 kDa	Fatty-acyl CoA reductase
Rv1872c	35-47 kDa	Lactate dehydrogenase
Rv3296	14-18 kDa	Helicase
Rv3648c	6-14 kDa	Probable cold shock protein
Rv3801c	60-80 kDa	Fatty-acid CoA synthetase
Proteins with Unknown Functions		
Rv3528c	18-25 kDa	CHP
Rv2005c	25-35 kDa	CHP
Rv2159c	25-35 kDa	Possible ATP-binding protein
Rv2161c	25-35 kDa	Contains TIM beta/alpha-barrel domain
Rv2204c	14-18 kDa	Contains putative HesB-like domain
Rv2676c	18-25 kDa	Ferredoxin-like domain
Rv0831c	25-35 kDa	CHP, similar to Rv0347
Rv0347	25-35 kDa	CHP, similar to Rv0831c

Table 1. Strains and plasmids used in this study

Strain/plasmid	Gentoype/description	Source
M. tuberculosis		
Erdman	Wild-type	W. R. Jacobs Jr.
espC::Tn (Rv3615c::Tn)	Erdman *espC::Tn5370*, HygR	MacGurn et. al
JMM4	*espC::Tn* + pJAM3, HygR, KanR	MacGurn et. al
Rv3870::Tn	Erdman *Rv3870::Tn5370*, HygR	Stanley et. al
Rv3871::Tn	Erdman *Rv3871::Tn5370*, HygR	Stanley et. al
Δpe35/ppe68	Erdman *Δpe35/ppe68*, HygR	Stanley et. al
ΔesxB	Erdman *ΔesxB*, HygR	Stanley et. al
ΔesxA	Erdman *ΔesxA*, HygR	Stanley et. al
Rv3877::Tn	Erdman *Rv3877::Tn5370*, HygR	Stanley et. al
Rv1052c::Tn	Erdman *Rv1052c::Tn5370*, HygR	Raghavan et. al
Rv3849::Tn	Erdman *Rv3849::Tn5370*, HygR	Raghavan et. al
BCG	*Mycobacterium bovis, variant BCG*, Pasteur strain	W. R. Jacobs Jr.
BCG + cjsc49	BCG with episomal cosmid containing Esx-1 locus from *M. tb*	Stanley et al.
JMM70	*espC::Tn* + pJAM69, HygR, KanR	This study
JMM122	*espC::Tn* + pJAM104, HygR, KanR	This study
JMM134	Erdman + pJAM106, KanR	This study
JMM135	Erdman + pJAM107, KanR	This study
Rv3849::Tn complemented	*Rv3849::Tn* + complementation plasmid	Raghavan et. al
Plasmids		
pMV306.Kan	Integrating plasmid containing *int*, *oriE*, KanR,	W. R. Jacobs Jr.
pJAM3	pMV306.Kan with Rv3616c-Rv3614c (native promoter)	MacGurn et. al
pJAM69	pJAM3 with N terminal 3X FLAG tag on *espC*	This study
pJAM104	pJAM3 with N terminal 3X FLAG/6X His on *espC*	This study
pJAM106	pJAM306 + C terminal 3X FLAG/6X His on *mpt32* (*espC* promoter)	This study
pJAM107	pJAM306 + C terminal 3X FLAG/6X His on *mpt64* (native promoter)	This study

Table 2. Mass Spectrometry Analysis of EspC and Potential Modifications

Peptide mass	Parent Peptide	Parent Mass	Δ Mass	E-value*	Site	Potential Modification**
1777.96	IAAKIYSEADEAWR	1621.84	156.12	1.1E-7	K4	4-hydroxynonenal (post-translational)
3442.85	GVLASHHDNAAVDASSG VEAAAGLGESVAITHGPY	3386.83	57.02	7.1E-10	H6	Carbamidomethyl (chemical artifact)
3481.22	LGVLASHHDNAAVDASS GVEAAAGLGESVAITH	3125.03	356.19	3E-5	E27	unknown

* E-value is the is the number of matches with equal or better scores expected to occur by chance alone.
** Potential modifications were identified using the Unimod server (http://www.unimod.org).

Table 3. Bioinformatic Analysis of secreted proteins that copurify with EspC

Protein	Secretion Signal Sequence	Putative Function*
Rv0888	SecYEG signal sequence	Neutral sphingomyelinase; DNAse I
Rv2525c	TAT signal sequence	Putative transglycosidase
Rv1754c	TAT signal sequence	Unknown
Rv3491	SecYEG signal sequence	Unknown

* Putative function was determined using PSI-BLAST searches for comparing primary structures and the PHYRE server for comparing secondary protein structures.

Chapter 5

Conclusions and Perspectives

A consensus is emerging that multiple factors from *M. tuberculosis*, including secreted lipids and proteins, are important for mediating phagosome maturation arrest (PMA) during macrophage infection{Pethe, 2004 #61}{Mueller, 2006 #154}{Deretic, 2006 #31}. Concurrent with our genetic screen for mutants with phagosome trafficking defects in macrophage cells, two other groups published studies that identified mutants of mycobacteria with trafficking defects. Pethe et al. used magnetic isolation of lysosomal compartments to select for mutants of *M. tuberculosis* that preferentially trafficked to lysosomes at early time points post-infection {Pethe, 2004 #61}. Many of the mutants isolated in this study exhibit very severe growth defects in macrophages, making it difficult to determine if the trafficking defect or susceptibility to macrophage killing is the primary defect. Furthermore, some of the mutants isolated in this genetic selection, including a septation mutant, could have gross defects not related to pathogenesis. Another study by Stewart et al. identified mutants of *M. bovis BCG* that were enriched in acidified phagosomes during macrophage infection, but most of these mutations affected genes involved in bacterial cell metabolism{Stewart, 2005 #78}. Our strategy for identification of *M. tuberculosis* mutants with phagosome trafficking defects was limiting since we only screened a set of 67 mutants known to be attenuated for virulence in mice. Furthermore, while the other studies focused on isolation of trafficking defects very early post-infection, our study was biased to later time points post-infection. Thus, given the procedural differences between the three studies, it is not surprising that each identified a mutually exclusive set of mutants defective for PMA.

Given the inhospitable environment of the lysosome, it is widely accepted that PMA is a crucial determinant of *M. tuberculosis* survival inside the host macrophage. Interestingly, Pethe et al. and our study each identified mutants that trafficked to lysosomal compartments without consequence to intracellular survival. These results are important because they demonstrate that PMA is not strictly required for intracellular survival of *M. tuberculosis*. This goes against the prevailing opinion that PMA is important for survival in the macrophage. Instead, our results support the alternative hypothesis that PMA may benefit *M. tuberculosis* pathogenesis by sequestering the bacteria away from antigen presenting compartments, thereby altering the host immune response {Ramachandra, 2001 #65} {Singh, 2006 #76} {Flynn, 2003 #36}. Future experiments using this important class of mutants will determine if failure to mediate PMA affects antigen presentation and host immune response during infection.

Recently, the Esx-1 secretion system, a crucial virulence determinant of *M. tuberculosis* and other pathogenic mycobacteria, has become the subject of intense study. Although our knowledge of this specialized secretion system is growing, many questions surrounding the mechanism of Esx-1 secretion and the molecular interactions it facilitates with the host remain to be elucidated. Our identification of several trafficking mutants that were defective for Esx-1 secretion led us to study what role Esx-1 secretion plays in PMA. We hypothesized that Esat-6 and Cfp-10, two known substrates of the Esx-1 pathway, might be involved in mediating PMA. However, this hypothesis proved incorrect, since mutations in either *esxA* or *esxB* (which encode Esat-6 and Cfp-10, respectively) had no affect on phagosome trafficking in the host. We therefore hypothesized that novel Esx-1 substrates might play a role in mediating PMA during

macrophage infection (Figure 1). Identification of this mystery substrate will require systematic characterization of each Esx-1 effector as they are identified.

In the second part of this thesis, we determined that one of the uncharacterized PMA mutants harboring a mutation in a gene called *espC* (*Rv3615c*) was in fact an Esx-1 mutant. We show that, in addition to being required for Esx-1 secretion, the EspC protein is secreted in an Esx-1 dependent manner. Although it is tempting to speculate that EspC could be the Esx-1 effector responsible for mediating PMA during host infection, our data show that *esxA* and *esxB* knockout strains fail to secrete EspC despite exhibiting normal phagosome maturation arrest. Thus, EspC isn't likely to function in modulating phagosome trafficking during infection since its secretion is not a requirement for PMA (Figure 2). Although this co-dependent secretion is a curious feature of Esx-1 secretion that has been described for three other characterized effectors of the pathway (Esat-6, Cfp-10, and EspA {Stanley, 2003 #77} {Fortune, 2005 #2}), the mechanism remains unclear.

Having ruled out a role for EspC in PMA, we decided to employ biochemical methodologies to probe potential functions of this novel Esx-1 substrate. Initial characterization of secreted EspC led to the identification of significant post-secretion modifications. Some potential modifications were identified by mass spectrometry, but none of these could account for the drastic and heterogenous differences observed by SDS-PAGE and western blot. Although we provide some evidence that EspC may be subject to glycosylation, future experiments using rigorous mass spectrometry methods will need to demonstrate how and where the EspC protein is modified post-secretion.

Since Esat-6 and Cfp-10 interact to form a dimer, we wondered if EspC might interact with other secreted proteins in a similar manner. Using gel filtration chromatography followed by immunopurification and mass spectrometry, we discovered that secreted EspC associates in a high molecular weight complex that contains several Esx family members and another Esx-1 substrate, EspA. Although dimers between Esx family members and PE/PPE family members have been described, this is the first example of a large, secreted multi-protein complex in *M. tuberculosis*. Interestingly, all of the Esx family members associating in this complex are known to be secreted in an Esx-1 independent manner. Furthermore, the EspC complex also exhibited the ability to copurify with substrates of the SecYEG and TAT secretion pathways, but these may be the result of weaker or transient interactions. We propose that secreted EspC interacts in a complex of proteins that includes substrates of multiple secretion pathways (Figure 3). Future experiments using analytical ultracentrifugation and cryo-EM tomography should shed light on the stoichiometry and structure of this complex.

One of the Sec substrates that associates with the EspC complex is a protein called Rv0888. Our bioinformatics and structural investigation of this protein led us to hypothesize that it might function as a neutral sphingomyelinase (nSMase). Many Gram positive pathogens have been shown to encode secreted nSMases which are important for full virulence {Clarke, 2006 #10}. Consistent with the idea that Rv0888 is a nSMase, we showed that a SMase activity copurifies with EspC, and that this activity is specific to sphingomyelin. Additionally, a mutant known to be attenuated for Rv0888 transcription was abrogated for the sphingomyelinase acivity, implicating this gene as a putative SMase. Although the SMase activity was Esx-1 independent, we hypothesize that

interaction of secreted Rv0888 with the EspC complex might be important for targeting the nSMase activity to the lumenal leaflet of the host phagosomal membrane, where hydrolysis of sphingomyelin can occur (Figure 4).

A secreted sphingomyelinase activity has important implications for the host-pathogen interaction that occurs during *M. tuberculosis* infection. Ceramide, one of the products of sphingomyelin hydrolysis, is known to affect multiple signaling pathways in eukaryotic cells. Generally, ceramide is thought to dissolve lipid rafts and has been shown to antagonize raft-associated signaling, including signaling through toll-like receptors {Walton, 2006 #144}. Thus, it is feasible that the secreted sphingomyelinase activity observed in *M. tuberculosis* could dampen the host innate immune response. Additionally, ceramide has been shown to be an important signal that can lead to apoptosis {Chatterjee, 1999 #11}. Some apoptosis is known to occur during M. tuberculosis infection of macrophages {O'Sullivan M, 2007 #143} and it will be interesting to test if this requires *Rv0888*. Future experiments using a knockout of the Rv0888 mutant will be important for determining what role this sphingomyelinase plays in the host-pathogen interaction.

In addition to broadening our understanding Esx-1 secretion and identifying a potentially important host-pathogen interaction, these studies also have important implications for tuberculosis vaccine development. The current vaccine, an attenuated strain of *Mycobacterium bovis* called BCG, is effective during childhood but is not protective in adults {Skeiky, 2006 #160}. Although *M. bovis* is highly similar to *M. tuberculosis*, BCG is attenuated because it has undergone many genome deletions, including deletion of the locus that encodes Esx-1 {Mahairas, 1996 #54}. Since ESAT-6

and CFP-10 are neither synthesized nor secreted in BCG, one prominent strategy for improving TB vaccination is to supplement BCG with factors that stimulate an immune response to ESAT-6 and CFP-10 {Skeiky, 2006 #160}. We propose that engineering a vaccine to stimulate an immune response to EspC, which is encoded by BCG but not expressed or secreted, could further enhance protective efficacy. Ultimately, since BCG that expresses the Esx-1 secretion system is enhanced for virulence {Pym, 2002 #114} and thus not an ideal candidate for vaccination, development of an improved vaccine will likely necessitate the design of a BCG strain that secretes variants of Esx-1 effectors without enhancing virulence.

Figure 1. A model for Esx-1 involvement in PMA.

Our data indicate that Esx-1 secretion is required for PMA, but known substrates are dispensible. Novel Esx-1 effectors may be involved in mediating PMA. CM = bacterial cell membrane. PG = peptidoglycan. mAG = mycolyl-arabinogalactan.

Fig. 1
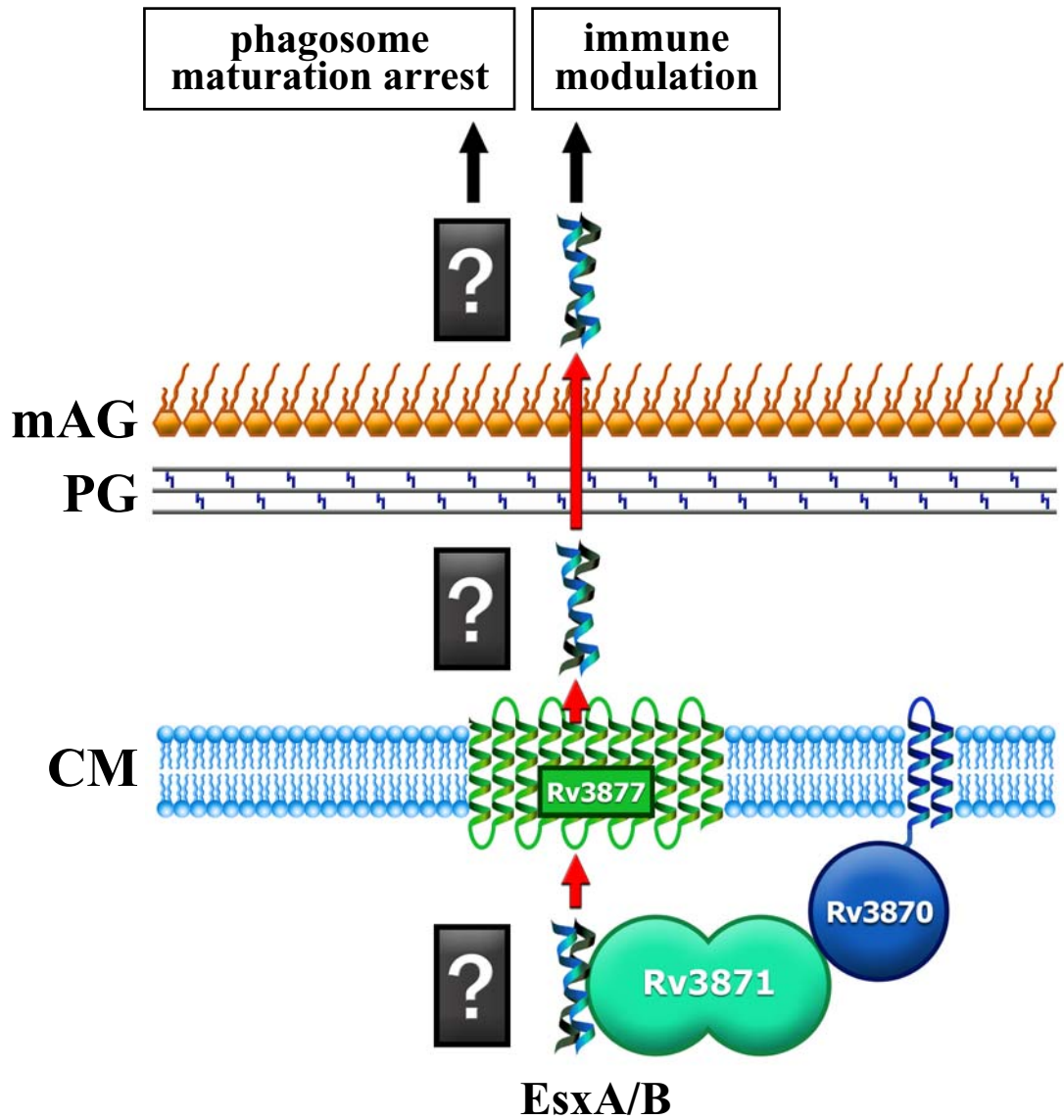
Figure 2. A model for EspC secretion.

We show that EspC is secreted in an Esx-1 dependent manner. CM = bacterial cell

membrane. PG = peptidoglycan. mAG = mycolyl-arabinogalactan.

Fig. 2
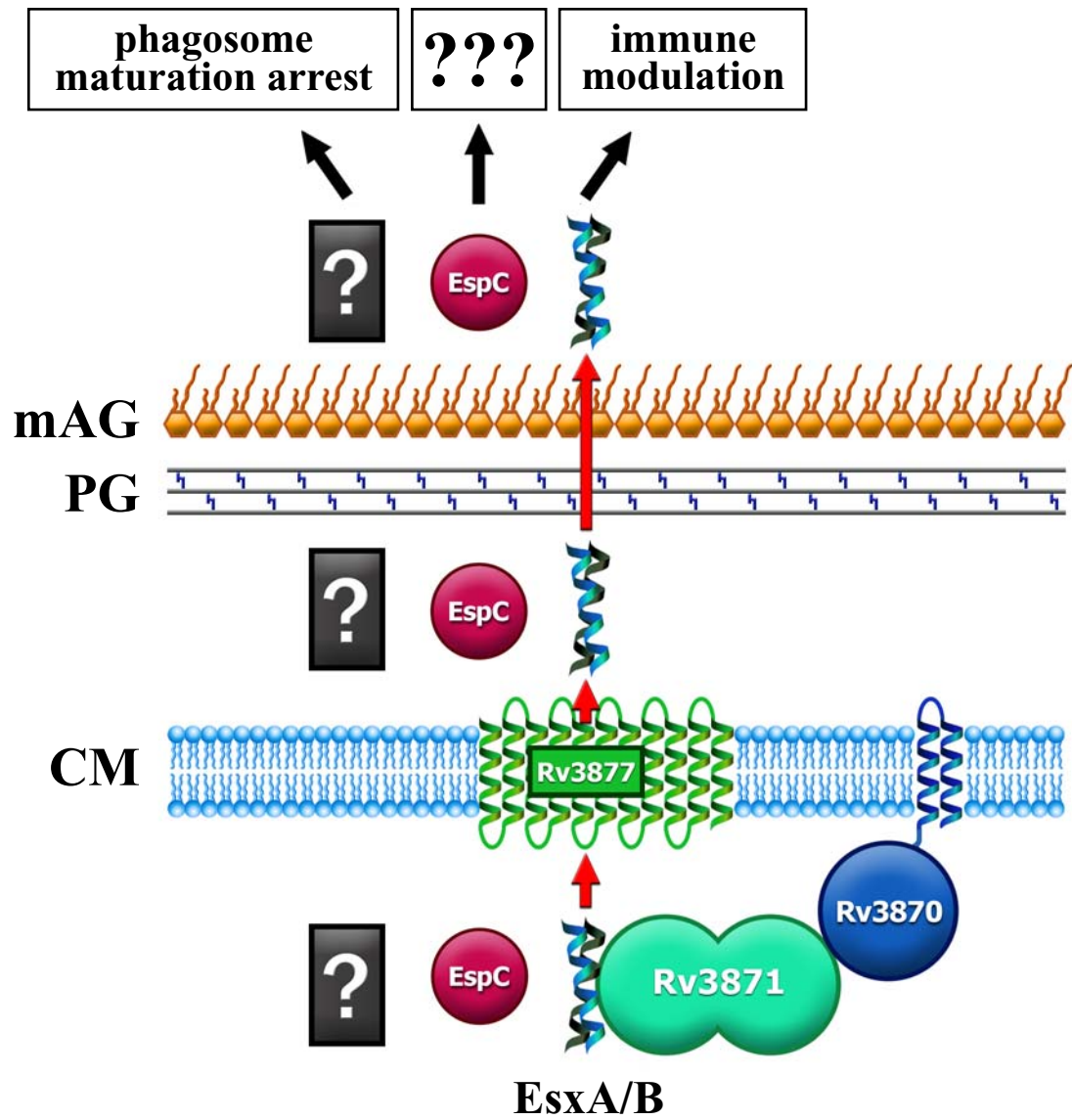
Figure 3. EspC forms a high MW complex with other secreted proteins.

Secreted EspC exists in a high molecular weight complex that results from

homomultimerization and interactions with other proteins secreted by Esx, SecYEG, and

TAT export pathways. In contrast, EspC does not interact with ESAT-6 or CFP-10, the

two most abundantly secreted proteins in *M. tuberculosis*. PG = peptidoglycan. mAG =

mycolyl-arabinogalactan.

Fig. 3

Figure 4. A model for targeting sphingomyelinase activity to host membranes.

We propose that Rv0888, a putative sphingomyelinase, is targeted to phagosomal

membranes via interaction with the EspC protein complex. Production of ceramide on

the lumenal leaflet of the phagosomal membrane could affect multiple host signaling

pathways. PM = phagosomal membrane.

Fig. 4

References

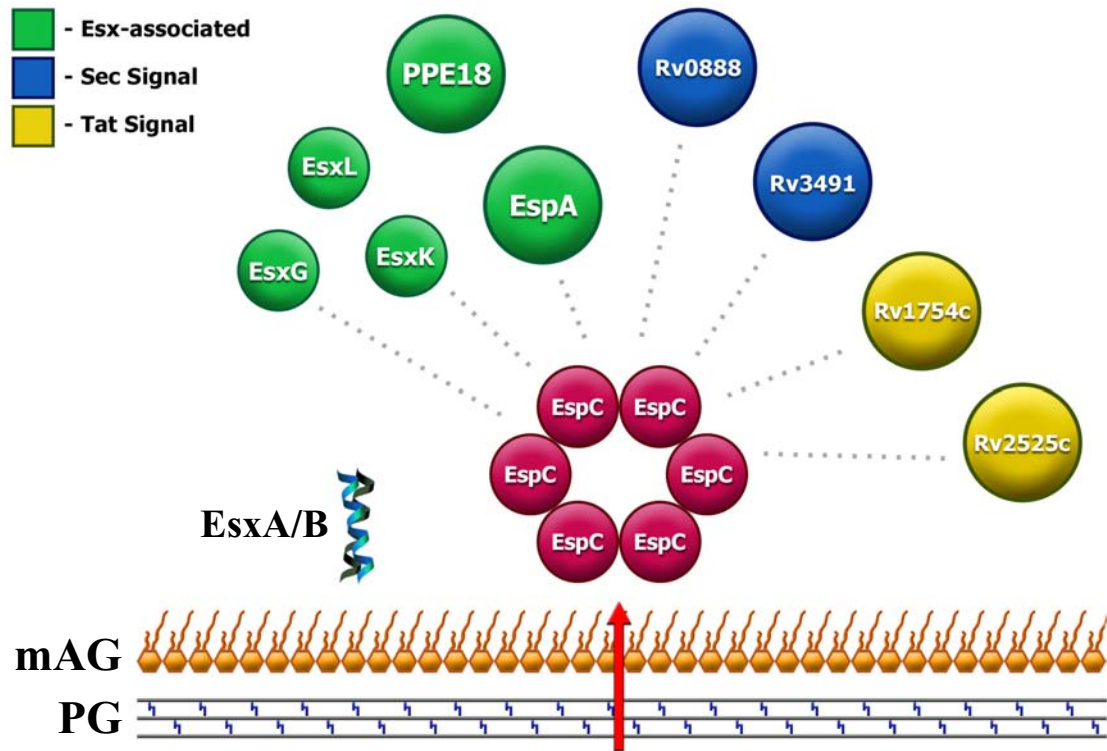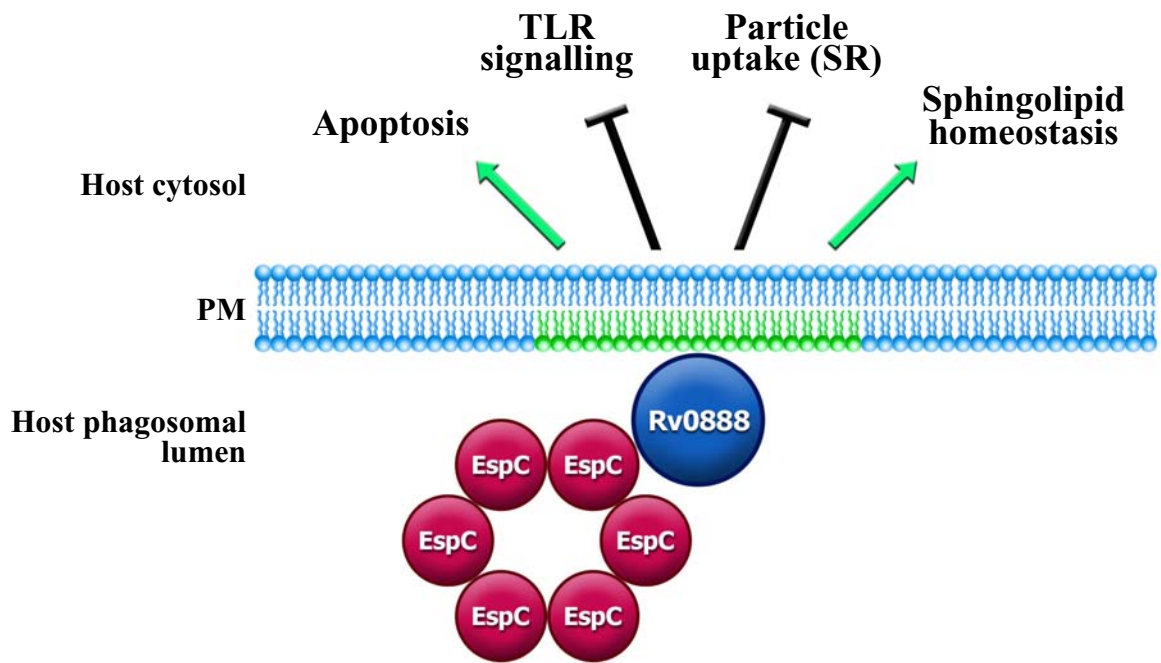Abdallah, A. M., T. Verboom, F. Hannes, M. Safi, M. Strong, D. Eisenberg, R. J. Musters, C. M. Vandenbroucke-Grauls, B. J. Appelmelk, J. Luirink and W. Bitter (2006). A specific secretion system mediates PPE41 transport in pathogenic mycobacteria. Mol Microbiol *62*, 667-79.

Aderem, A. and D. M. Underhill (1999). Mechanisms of phagocytosis in macrophages. Annu Rev Immunol *17*, 593-623.

Alto, N. M., F. Shao, C. S. Lazar, R. L. Brost, G. Chua, S. Mattoo, S. A. McMahon, P. Ghosh, T. R. Hughes, C. Boone and J. E. Dixon (2006). Identification of a bacterial type III effector family with G protein mimicry functions. Cell *124*, 133-45.

Andersen, A. B., L. Ljungqvist, K. Haslov and M. W. Bentzon (1991). MPB 64 possesses 'tuberculosis-complex'-specific B- and T-cell epitopes. Scand J Immunol *34*, 365-72.

Arbibe, L., D. W. Kim, E. Batsche, T. Pedron, B. Mateescu, C. Muchardt, C. Parsot and P. J. Sansonetti (2007). An injected bacterial effector targets chromatin access for transcription factor NF-kappaB to alter transcription of host genes involved in immune responses. Nat Immunol *8*, 47-56.

Armstrong, J. A. and P. D. Hart (1971). Response of cultured macrophages to

Mycobacterium tuberculosis, with observations on fusion of lysosomes with phagosomes.

J Exp Med *134*, 713-40.

Behr, M. A., M. A. Wilson, W. P. Gill, H. Salamon, G. K. Schoolnik, S. Rane and P. M.

Small (1999). Comparative genomics of BCG vaccines by whole-genome DNA

microarray. Science *284*, 1520-3.

Berthet, F. X., M. Lagranderie, P. Gounon, C. Laurent-Winter, D. Ensergueix, P.

Chavarot, F. Thouron, E. Maranghi, V. Pelicic, D. Portnoi, G. Marchal and B. Gicquel

(1998). Attenuation of virulence by disruption of the Mycobacterium tuberculosis erp

gene. Science *282*, 759-62.

Berthet, F. X., P. B. Rasmussen, I. Rosenkrands, P. Andersen and B. Gicquel (1998). A

Mycobacterium tuberculosis operon encoding ESAT-6 and a novel low-molecular-mass

culture filtrate protein (CFP-10). Microbiology *144 (Pt 11)*, 3195-203.

Braunstein, M., B. J. Espinosa, J. Chan, J. T. Belisle and W. R. Jacobs, Jr. (2003). SecA2

functions in the secretion of superoxide dismutase A and in the virulence of

Mycobacterium tuberculosis. Mol Microbiol *48*, 453-64.

Burts, M. L., W. A. Williams, K. DeBord and D. M. Missiakas (2005). EsxA and EsxB are secreted by an ESAT-6-like system that is required for the pathogenesis of Staphylococcus aureus infections. Proc Natl Acad Sci U S A *102*, 1169-74.

Cavalli, V., F. Vilbois, M. Corti, M. J. Marcote, K. Tamura, M. Karin, S. Arkinstall and J. Gruenberg (2001). The stress-induced MAP kinase p38 regulates endocytic trafficking via the GDI:Rab5 complex. Mol Cell *7*, 421-32.

Chatterjee, S. (1999). Neutral sphingomyelinase: past, present and future. Chem Phys Lipids *102*, 79-96.

Chua, J., I. Vergne, S. Master and V. Deretic (2004). A tale of two lipids: Mycobacterium tuberculosis phagosome maturation arrest. Curr Opin Microbiol *7*, 71-7.

Clarke, C. J., C. F. Snook, M. Tani, N. Matmati, N. Marchesini and Y. A. Hannun (2006). The extended family of neutral sphingomyelinases. Biochemistry *45*, 11247-56.

Clemens, D. L. and M. A. Horwitz (1995). Characterization of the Mycobacterium tuberculosis phagosome and evidence that phagosomal maturation is inhibited. J Exp Med *181*, 257-70.

Clemens, D. L. and M. A. Horwitz (1996). The Mycobacterium tuberculosis phagosome interacts with early endosomes and is accessible to exogenously administered transferrin. J Exp Med *184*, 1349-55.

Cole, S. T., R. Brosch, J. Parkhill, T. Garnier, C. Churcher, D. Harris, S. V. Gordon, K. Eiglmeier, S. Gas, C. E. Barry, 3rd, F. Tekaia, K. Badcock, D. Basham, D. Brown, T. Chillingworth, R. Connor, R. Davies, K. Devlin, T. Feltwell, S. Gentles, N. Hamlin, S. Holroyd, T. Hornsby, K. Jagels, B. G. Barrell and et al. (1998). Deciphering the biology of Mycobacterium tuberculosis from the complete genome sequence. Nature *393*, 537-44.

Cole, S. T., R. Brosch, J. Parkhill, T. Garnier, C. Churcher, D. Harris, S. V. Gordon, K. Eiglmeier, S. Gas, C. E. Barry, 3rd, F. Tekaia, K. Badcock, D. Basham, D. Brown, T. Chillingworth, R. Connor, R. Davies, K. Devlin, T. Feltwell, S. Gentles, N. Hamlin, S. Holroyd, T. Hornsby, K. Jagels, A. Krogh, J. McLean, S. Moule, L. Murphy, K. Oliver, J. Osborne, M. A. Quail, M. A. Rajandream, J. Rogers, S. Rutter, K. Seeger, J. Skelton, R. Squares, S. Squares, J. E. Sulston, K. Taylor, S. Whitehead and B. G. Barrell (1998). Deciphering the biology of Mycobacterium tuberculosis from the complete genome sequence. Nature *393*, 537-44.

Converse, S. E. and J. S. Cox (2005). A protein secretion pathway critical for Mycobacterium tuberculosis virulence is conserved and functional in Mycobacterium smegmatis. J Bacteriol *187*, 1238-45.

Converse, S. E., J. D. Mougous, M. D. Leavell, J. A. Leary, C. R. Bertozzi and J. S. Cox (2003). MmpL8 is required for sulfolipid-1 biosynthesis and Mycobacterium tuberculosis virulence. Proc Natl Acad Sci U S A *100*, 6121-6.

Cowley, S., M. Ko, N. Pick, R. Chow, K. J. Downing, B. G. Gordhan, J. C. Betts, V. Mizrahi, D. A. Smith, R. W. Stokes and Y. Av-Gay (2004). The Mycobacterium tuberculosis protein serine/threonine kinase PknG is linked to cellular glutamate/glutamine levels and is important for growth in vivo. Mol Microbiol *52*, 1691-702.

Cox, J. S., B. Chen, M. McNeil and W. R. Jacobs, Jr. (1999). Complex lipid determines tissue-specific replication of Mycobacterium tuberculosis in mice. Nature *402*, 79-83.

Darwin, K. H., S. Ehrt, J. C. Gutierrez-Ramos, N. Weich and C. F. Nathan (2003). The proteasome of Mycobacterium tuberculosis is required for resistance to nitric oxide. Science *302*, 1963-6.

Deretic, V. and R. A. Fratti (1999). Mycobacterium tuberculosis phagosome. Mol Microbiol *31*, 1603-9.

Deretic, V., S. Singh, S. Master, J. Harris, E. Roberts, G. Kyei, A. Davis, S. de Haro, J. Naylor, H. H. Lee and I. Vergne (2006). Mycobacterium tuberculosis inhibition of

phagolysosome biogenesis and autophagy as a host defence mechanism. Cell Microbiol *8*, 719-27.

Deretic, V., L. E. Via, R. A. Fratti and D. Deretic (1997). Mycobacterial phagosome maturation, rab proteins, and intracellular trafficking. Electrophoresis *18*, 2542-7.

Desvaux, M., A. Khan, A. Scott-Tucker, R. R. Chaudhuri, M. J. Pallen and I. R. Henderson (2005). Genomic analysis of the protein secretion systems in Clostridium acetobutylicum ATCC 824. Biochim Biophys Acta *1745*, 223-53.

Dlakic, M. (2000). Functionally unrelated signalling proteins contain a fold similar to Mg2+-dependent endonucleases. Trends Biochem Sci *25*, 272-3.

Dobos, K. M., K. H. Khoo, K. M. Swiderek, P. J. Brennan and J. T. Belisle (1996). Definition of the full extent of glycosylation of the 45-kilodalton glycoprotein of Mycobacterium tuberculosis. J Bacteriol *178*, 2498-506.

Dobos, K. M., K. Swiderek, K. H. Khoo, P. J. Brennan and J. T. Belisle (1995). Evidence for glycosylation sites on the 45-kilodalton glycoprotein of Mycobacterium tuberculosis. Infect Immun *63*, 2846-53.

Domenech, P., M. B. Reed and C. E. Barry, 3rd (2005). Contribution of the Mycobacterium tuberculosis MmpL protein family to virulence and drug resistance. Infect Immun *73*, 3492-501.

Dye, C., S. Scheele, P. Dolin, V. Pathania and M. C. Raviglione (1999). Consensus statement. Global burden of tuberculosis: estimated incidence, prevalence, and mortality by country. WHO Global Surveillance and Monitoring Project. Jama *282*, 677-86.

Fisher, M. A., B. B. Plikaytis and T. M. Shinnick (2002). Microarray analysis of the Mycobacterium tuberculosis transcriptional response to the acidic conditions found in phagosomes. J Bacteriol *184*, 4025-32.

Flint, J. L., J. C. Kowalski, P. K. Karnati and K. M. Derbyshire (2004). The RD1 virulence locus of Mycobacterium tuberculosis regulates DNA transfer in Mycobacterium smegmatis. Proc Natl Acad Sci U S A *101*, 12598-603.

Flynn, J. L. and J. Chan (2003). Immune evasion by Mycobacterium tuberculosis: living with the enemy. Curr Opin Immunol *15*, 450-5.

Fortune, S. M., A. Jaeger, D. A. Sarracino, M. R. Chase, C. M. Sassetti, D. R. Sherman, B. R. Bloom and E. J. Rubin (2005). Mutually dependent secretion of proteins required for mycobacterial virulence. Proc Natl Acad Sci U S A *102*, 10676-81.

Fratti, R. A., J. M. Backer, J. Gruenberg, S. Corvera and V. Deretic (2001). Role of phosphatidylinositol 3-kinase and Rab5 effectors in phagosomal biogenesis and mycobacterial phagosome maturation arrest. J Cell Biol *154*, 631-44.

Fratti, R. A., J. Chua, I. Vergne and V. Deretic (2003). Mycobacterium tuberculosis glycosylated phosphatidylinositol causes phagosome maturation arrest. Proc Natl Acad Sci U S A *100*, 5437-42.

Gao, L. Y., S. Guo, B. McLaughlin, H. Morisaki, J. N. Engel and E. J. Brown (2004). A mycobacterial virulence gene cluster extending RD1 is required for cytolysis, bacterial spreading and ESAT-6 secretion. Mol Microbiol *53*, 1677-93.

Gey Van Pittius, N. C., J. Gamieldien, W. Hide, G. D. Brown, R. J. Siezen and A. D. Beyers (2001). The ESAT-6 gene cluster of Mycobacterium tuberculosis and other high G+C Gram-positive bacteria. Genome Biol *2*, RESEARCH0044.

Glickman, M. S., J. S. Cox and W. R. Jacobs, Jr. (2000). A novel mycolic acid cyclopropane synthetase is required for cording, persistence, and virulence of Mycobacterium tuberculosis. Mol Cell *5*, 717-27.

Gomes, M. S., S. Paul, A. L. Moreira, R. Appelberg, M. Rabinovitch and G. Kaplan (1999). Survival of Mycobacterium avium and Mycobacterium tuberculosis in acidified vacuoles of murine macrophages. Infect Immun *67*, 3199-206.

Goren, M. B., P. D'Arcy Hart, M. R. Young and J. A. Armstrong (1976). Prevention of phagosome-lysosome fusion in cultured macrophages by sulfatides of Mycobacterium tuberculosis. Proc Natl Acad Sci U S A *73*, 2510-4.

Goren, M. B., A. E. Vatter and J. Fiscus (1987). Polyanionic agents as inhibitors of phagosome-lysosome fusion in cultured macrophages: evolution of an alternative interpretation. J Leukoc Biol *41*, 111-21.

Guarente, L. and M. Ptashne (1981). Fusion of Escherichia coli lacZ to the cytochrome c gene of Saccharomyces cerevisiae. Proc Natl Acad Sci U S A *78*, 2199-203.

Guinn, K. M., M. J. Hickey, S. K. Mathur, K. L. Zakel, J. E. Grotzke, D. M. Lewinsohn, S. Smith and D. R. Sherman (2004). Individual RD1-region genes are required for export of ESAT-6/CFP-10 and for virulence of Mycobacterium tuberculosis. Mol Microbiol *51*, 359-70.

Herrmann, J. L., P. O'Gaora, A. Gallagher, J. E. Thole and D. B. Young (1996). Bacterial glycoproteins: a link between glycosylation and proteolytic cleavage of a 19 kDa antigen from Mycobacterium tuberculosis. Embo J *15*, 3547-54.

Hsu, T., S. M. Hingley-Wilson, B. Chen, M. Chen, A. Z. Dai, P. M. Morin, C. B. Marks, J. Padiyar, C. Goulding, M. Gingery, D. Eisenberg, R. G. Russell, S. C. Derrick, F. M.

Collins, S. L. Morris, C. H. King and W. R. Jacobs, Jr. (2003). The primary mechanism of attenuation of bacillus Calmette-Guerin is a loss of secreted lytic function required for invasion of lung interstitial tissue. Proc Natl Acad Sci U S A *100*, 12420-5.

Iyer, L. M., K. S. Makarova, E. V. Koonin and L. Aravind (2004). Comparative genomics of the FtsK-HerA superfamily of pumping ATPases: implications for the origins of chromosome segregation, cell division and viral capsid packaging. Nucleic Acids Res *32*, 5260-79.

Johansen, K. A., R. E. Gill and M. L. Vasil (1996). Biochemical and molecular analysis of phospholipase C and phospholipase D activity in mycobacteria. Infect Immun *64*, 3259-66.

Kelley, L. A., R. M. MacCallum and M. J. Sternberg (2000). Enhanced genome annotation using structural profiles in the program 3D-PSSM. J Mol Biol *299*, 499-520.

Kramer, R. W., N. L. Slagowski, N. A. Eze, K. S. Giddings, M. F. Morrison, K. A. Siggers, M. N. Starnbach and C. F. Lesser (2007). Yeast Functional Genomic Screens Lead to Identification of a Role for a Bacterial Effector in Innate Immunity Regulation. PLoS Pathog *3*, e21.

Kurtz, S., K. P. McKinnon, M. S. Runge, J. P. Ting and M. Braunstein (2006). The SecA2 secretion factor of Mycobacterium tuberculosis promotes growth in macrophages and inhibits the host immune response. Infect Immun *74*, 6855-64.

Lambert, C., N. Leonard, X. De Bolle and E. Depiereux (2002). ESyPred3D: Prediction of proteins 3D structures. Bioinformatics *18*, 1250-6.

Laqueyrerie, A., P. Militzer, F. Romain, K. Eiglmeier, S. Cole and G. Marchal (1995). Cloning, sequencing, and expression of the apa gene coding for the Mycobacterium tuberculosis 45/47-kilodalton secreted antigen complex. Infect Immun *63*, 4003-10.

Lee, V. T. and O. Schneewind (2001). Protein secretion and the pathogenesis of bacterial infections. Genes Dev *15*, 1725-52.

Lewis, K. N., R. Liao, K. M. Guinn, M. J. Hickey, S. Smith, M. A. Behr and D. R. Sherman (2003). Deletion of RD1 from Mycobacterium tuberculosis mimics bacille Calmette-Guerin attenuation. J Infect Dis *187*, 117-23.

Li, H., H. Xu, Y. Zhou, J. Zhang, C. Long, S. Li, S. Chen, J. M. Zhou and F. Shao (2007). The phosphothreonine lyase activity of a bacterial type III effector family. Science *315*, 1000-3.

Lightbody, K. L., P. S. Renshaw, M. L. Collins, R. L. Wright, D. M. Hunt, S. V. Gordon, R. G. Hewinson, R. S. Buxton, R. A. Williamson and M. D. Carr (2004). Characterisation of complex formation between members of the Mycobacterium tuberculosis complex CFP-10/ESAT-6 protein family: towards an understanding of the rules governing complex formation and thereby functional flexibility. FEMS Microbiol Lett *238*, 255-62.

Luan, Y. and H. R. Griffiths (2006). Ceramides reduce CD36 cell surface expression and oxidised LDL uptake by monocytes and macrophages. Arch Biochem Biophys *450*, 89-99.

MacGurn, J. A., S. Raghavan, S. A. Stanley and J. S. Cox (2005). A non-RD1 gene cluster is required for Snm secretion in Mycobacterium tuberculosis. Mol Microbiol *57*, 1653-63.

Mahairas, G. G., P. J. Sabo, M. J. Hickey, D. C. Singh and C. K. Stover (1996). Molecular analysis of genetic differences between Mycobacterium bovis BCG and virulent M. bovis. J Bacteriol *178*, 1274-82.

Majlessi, L., P. Brodin, R. Brosch, M. J. Rojas, H. Khun, M. Huerre, S. T. Cole and C. Leclerc (2005). Influence of ESAT-6 Secretion System 1 (RD1) of Mycobacterium tuberculosis on the Interaction between Mycobacteria and the Host Immune System. J Immunol *174*, 3570-9.

Malik, Z. A., C. R. Thompson, S. Hashimi, B. Porter, S. S. Iyer and D. J. Kusner (2003). Cutting edge: Mycobacterium tuberculosis blocks Ca2+ signaling and phagosome maturation in human macrophages via specific inhibition of sphingosine kinase. J Immunol *170*, 2811-5.

Matsuo, H., J. Chevallier, N. Mayran, I. Le Blanc, C. Ferguson, J. Faure, N. S. Blanc, S. Matile, J. Dubochet, R. Sadoul, R. G. Parton, F. Vilbois and J. Gruenberg (2004). Role of LBPA and Alix in multivesicular liposome formation and endosome organization. Science *303*, 531-4.

McCaffery, J. M. and M. G. Farquhar (1995). Localization of GTPases by indirect immunofluorescence and immunoelectron microscopy. Methods Enzymol *257*, 259-79.

Mills, I. G., A. T. Jones and M. J. Clague (1999). Regulation of endosome fusion. Mol Membr Biol *16*, 73-9.

Mueller, P. and J. Pieters (2006). Modulation of macrophage antimicrobial mechanisms by pathogenic mycobacteria. Immunobiology *211*, 549-56.

Nagai, H., J. C. Kagan, X. Zhu, R. A. Kahn and C. R. Roy (2002). A bacterial guanine nucleotide exchange factor activates ARF on Legionella phagosomes. Science *295*, 679-82.

Ng, V. H., J. S. Cox, A. O. Sousa, J. D. MacMicking and J. D. McKinney (2004). Role of KatG catalase-peroxidase in mycobacterial pathogenesis: countering the phagocyte oxidative burst. Mol Microbiol *52*, 1291-302.

Oettinger, T. and A. B. Andersen (1994). Cloning and B-cell-epitope mapping of MPT64 from Mycobacterium tuberculosis H37Rv. Infect Immun *62*, 2058-64.

Okkels, L. M. and P. Andersen (2004). Protein-protein interactions of proteins from the ESAT-6 family of Mycobacterium tuberculosis. J Bacteriol *186*, 2487-91.

Okkels, L. M., E. C. Muller, M. Schmid, I. Rosenkrands, S. H. Kaufmann, P. Andersen and P. R. Jungblut (2004). CFP10 discriminates between nonacetylated and acetylated ESAT-6 of Mycobacterium tuberculosis by differential interaction. Proteomics *4*, 2954-60.

O'Sullivan M, P., S. O'Leary, D. M. Kelly and J. Keane (2007). A caspase-independent pathway mediates macrophage cell death in response to M. tuberculosis infection. Infect Immun.

Pallen, M. J. (2002). The ESAT-6/WXG100 superfamily -- and a new Gram-positive secretion system? Trends Microbiol *10*, 209-12.

Pappin, D. J., P. Hojrup and A. J. Bleasby (1993). Rapid identification of proteins by peptide-mass fingerprinting. Curr Biol *3*, 327-32.

Pethe, K., D. L. Swenson, S. Alonso, J. Anderson, C. Wang and D. G. Russell (2004). Isolation of Mycobacterium tuberculosis mutants defective in the arrest of phagosome maturation. Proc Natl Acad Sci U S A *101*, 13642-7.

Pettersson, J., A. Holmstrom, J. Hill, S. Leary, E. Frithz-Lindsten, A. von Euler-Matell, E. Carlsson, R. Titball, A. Forsberg and H. Wolf-Watz (1999). The V-antigen of Yersinia is surface exposed before target cell contact and involved in virulence protein translocation. Mol Microbiol *32*, 961-76.

Pym, A. S., P. Brodin, R. Brosch, M. Huerre and S. T. Cole (2002). Loss of RD1 contributed to the attenuation of the live tuberculosis vaccines Mycobacterium bovis BCG and Mycobacterium microti. Mol Microbiol *46*, 709-17.

Ramachandra, L., E. Noss, W. H. Boom and C. V. Harding (2001). Processing of Mycobacterium tuberculosis antigen 85B involves intraphagosomal formation of peptide-major histocompatibility complex II complexes and is inhibited by live bacilli that decrease phagosome maturation. J Exp Med *194*, 1421-32.

Rao, V., N. Fujiwara, S. A. Porcelli and M. S. Glickman (2005). Mycobacterium tuberculosis controls host innate immune activation through cyclopropane modification of a glycolipid effector molecule. J Exp Med *201*, 535-43.

Renshaw, P. S., K. L. Lightbody, V. Veverka, F. W. Muskett, G. Kelly, T. A. Frenkiel, S. V. Gordon, R. G. Hewinson, B. Burke, J. Norman, R. A. Williamson and M. D. Carr (2005). Structure and function of the complex formed by the tuberculosis virulence factors CFP-10 and ESAT-6. Embo J *24*, 2491-8.

Renshaw, P. S., P. Panagiotidou, A. Whelan, S. V. Gordon, R. G. Hewinson, R. A. Williamson and M. D. Carr (2002). Conclusive evidence that the major T-cell antigens of the Mycobacterium tuberculosis complex ESAT-6 and CFP-10 form a tight, 1:1 complex and characterization of the structural properties of ESAT-6, CFP-10, and the ESAT-6*CFP-10 complex. Implications for pathogenesis and virulence. J Biol Chem *277*, 21598-603.

Rodriguez, G. M., M. I. Voskuil, B. Gold, G. K. Schoolnik and I. Smith (2002). ideR, An essential gene in mycobacterium tuberculosis: role of IdeR in iron-dependent gene expression, iron metabolism, and oxidative stress response. Infect Immun *70*, 3371-81.

Rousseau, C., O. C. Turner, E. Rush, Y. Bordat, T. D. Sirakova, P. E. Kolattukudy, S. Ritter, I. M. Orme, B. Gicquel and M. Jackson (2003). Sulfolipid deficiency does not

affect the virulence of Mycobacterium tuberculosis H37Rv in mice and guinea pigs. Infect Immun *71*, 4684-90.

Rousseau, C., N. Winter, E. Pivert, Y. Bordat, O. Neyrolles, P. Ave, M. Huerre, B. Gicquel and M. Jackson (2004). Production of phthiocerol dimycocerosates protects Mycobacterium tuberculosis from the cidal activity of reactive nitrogen intermediates produced by macrophages and modulates the early immune response to infection. Cell Microbiol *6*, 277-87.

Russell, D. G. (2001). Mycobacterium tuberculosis: here today, and here tomorrow. Nat Rev Mol Cell Biol *2*, 569-77.

Saint-Joanis, B., C. Demangel, M. Jackson, P. Brodin, L. Marsollier, H. Boshoff and S. T. Cole (2006). Inactivation of Rv2525c, a substrate of the twin arginine translocation (Tat) system of Mycobacterium tuberculosis, increases beta-lactam susceptibility and virulence. J Bacteriol *188*, 6669-79.

Sassetti, C. M., D. H. Boyd and E. J. Rubin (2003). Genes required for mycobacterial growth defined by high density mutagenesis. Mol Microbiol *48*, 77-84.

Sassetti, C. M. and E. J. Rubin (2003). Genetic requirements for mycobacterial survival during infection. Proc Natl Acad Sci U S A *100*, 12989-94.

Schaible, U. E., S. Sturgill-Koszycki, P. H. Schlesinger and D. G. Russell (1998). Cytokine activation leads to acidification and increases maturation of Mycobacterium avium-containing phagosomes in murine macrophages. J Immunol *160*, 1290-6.

Schwarz, G. (2005). Molybdenum cofactor biosynthesis and deficiency. Cell Mol Life Sci *62*, 2792-810.

Shohdy, N., J. A. Efe, S. D. Emr and H. A. Shuman (2005). Pathogen effector protein screening in yeast identifies Legionella factors that interfere with membrane trafficking. Proc Natl Acad Sci U S A *102*, 4866-71.

Singh, C. R., R. A. Moulton, L. Y. Armitige, A. Bidani, M. Snuggs, S. Dhandayuthapani, R. L. Hunter and C. Jagannath (2006). Processing and Presentation of a Mycobacterial Antigen 85B Epitope by Murine Macrophages Is Dependent on the Phagosomal Acquisition of Vacuolar Proton ATPase and In Situ Activation of Cathepsin D. J Immunol *177*, 3250-9.

Skeiky, Y. A. and J. C. Sadoff (2006). Advances in tuberculosis vaccine strategies. Nat Rev Microbiol *4*, 469-76.

Stanley, S. A., S. Raghavan, W. W. Hwang and J. S. Cox (2003). Acute infection and macrophage subversion by Mycobacterium tuberculosis require a specialized secretion system. Proc Natl Acad Sci U S A *100*, 13001-6.

Stewart, G. R., J. Patel, B. D. Robertson, A. Rae and D. B. Young (2005). Mycobacterial mutants with defective control of phagosomal acidification. PLoS Pathog *1*, 269-78.

Strong, M., M. R. Sawaya, S. Wang, M. Phillips, D. Cascio and D. Eisenberg (2006). Toward the structural genomics of complexes: crystal structure of a PE/PPE protein complex from Mycobacterium tuberculosis. Proc Natl Acad Sci U S A *103*, 8060-5.

Sturgill-Koszycki, S., P. H. Schlesinger, P. Chakraborty, P. L. Haddix, H. L. Collins, A. K. Fok, R. D. Allen, S. L. Gluck, J. Heuser and D. G. Russell (1994). Lack of acidification in Mycobacterium phagosomes produced by exclusion of the vesicular proton-ATPase. Science *263*, 678-81.

Tan, T., W. L. Lee, D. C. Alexander, S. Grinstein and J. Liu (2006). The ESAT-6/CFP-10 secretion system of Mycobacterium marinum modulates phagosome maturation. Cell Microbiol *8*, 1417-1429.

Ullrich, H. J., W. L. Beatty and D. G. Russell (2000). Interaction of Mycobacterium avium-containing phagosomes with the antigen presentation pathway. J Immunol *165*, 6073-80.

VanderVen, B. C., J. D. Harder, D. C. Crick and J. T. Belisle (2005). Export-mediated assembly of mycobacterial glycoproteins parallels eukaryotic pathways. Science *309*, 941-3.

Via, L. E., D. Deretic, R. J. Ulmer, N. S. Hibler, L. A. Huber and V. Deretic (1997). Arrest of mycobacterial phagosome maturation is caused by a block in vesicle fusion between stages controlled by rab5 and rab7. J Biol Chem *272*, 13326-31.

Vogel, J. P. and R. R. Isberg (1999). Cell biology of Legionella pneumophila. Curr Opin Microbiol *2*, 30-4.

Volkman, H. E., H. Clay, D. Beery, J. C. Chang, D. R. Sherman and L. Ramakrishnan (2004). Tuberculous granuloma formation is enhanced by a mycobacterium virulence determinant. PLoS Biol *2*, e367.

Walburger, A., A. Koul, G. Ferrari, L. Nguyen, C. Prescianotto-Baschong, K. Huygen, B. Klebl, C. Thompson, G. Bacher and J. Pieters (2004). Protein kinase G from pathogenic mycobacteria promotes survival within macrophages. Science *304*, 1800-4.

Walton, K. A., B. G. Gugiu, M. Thomas, R. J. Basseri, D. R. Eliav, R. G. Salomon and J. A. Berliner (2006). A role for neutral sphingomyelinase activation in the inhibition of LPS action by phospholipid oxidation products. J Lipid Res *47*, 1967-74.

Wards, B. J., G. W. de Lisle and D. M. Collins (2000). An esat6 knockout mutant of Mycobacterium bovis produced by homologous recombination will contribute to the development of a live tuberculosis vaccine. Tuber Lung Dis *80*, 185-9.

Waters, W. R., B. J. Nonnecke, M. V. Palmer, S. Robbe-Austermann, J. P. Bannantine, J. R. Stabel, D. L. Whipple, J. B. Payeur, D. M. Estes, J. E. Pitzer and F. C. Minion (2004). Use of recombinant ESAT-6:CFP-10 fusion protein for differentiation of infections of cattle by Mycobacterium bovis and by M. avium subsp. avium and M. avium subsp. paratuberculosis. Clin Diagn Lab Immunol *11*, 729-35.

Woodman, P. G. (2000). Biogenesis of the sorting endosome: the role of Rab5. Traffic *1*, 695-701.

Xu, S., A. Cooper, S. Sturgill-Koszycki, T. van Heyningen, D. Chatterjee, I. Orme, P. Allen and D. G. Russell (1994). Intracellular trafficking in Mycobacterium tuberculosis and Mycobacterium avium-infected macrophages. J Immunol *153*, 2568-78.
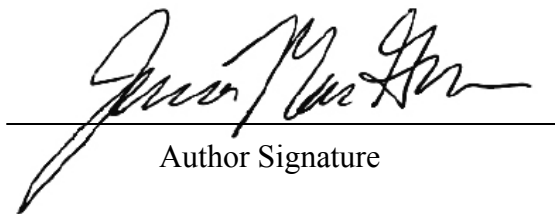
Zimmerli, S., S. Edwards and J. D. Ernst (1996). Selective receptor blockade during phagocytosis does not alter the survival and growth of Mycobacterium tuberculosis in human macrophages. Am J Respir Cell Mol Biol *15*, 760-70.

Publishing Agreement

It is the policy of the University to encourage the distribution of all theses and dissertations. Copies of all UCSF theses and dissertations will be routed to the library via the Graduate Division. The library will make all theses and dissertations accessible to the public and will preserve these to the best of their abilities, in perpetuity.

Please sign the following statement:

I hereby grant permission to the Graduate Division of the University of California, San Francisco to release copies of my thesis or dissertation to the Campus Library to provide access and preservation, in whole or in part, in perpetuity.

<table>
<tr><td></td><td>March 16, 2007</td></tr>
<tr><td>Author Signature</td><td>Date</td></tr>
</table>

174